



Published in final edited form as:

Chem Soc Rev. 2016 October 7; 45(19): 5232–5263. doi:10.1039/c6cs00026f.

## Metal-containing and Related Polymers for Biomedical Applications

Yi Yan<sup>a,b,\*</sup>, Jiuyang Zhang<sup>a,†</sup>, Lixia Ren<sup>c</sup>, and Chuanbing Tang<sup>a,\*</sup>

<sup>a</sup>Department of Chemistry and Biochemistry, University of South Carolina, Columbia, SC 29208, United States

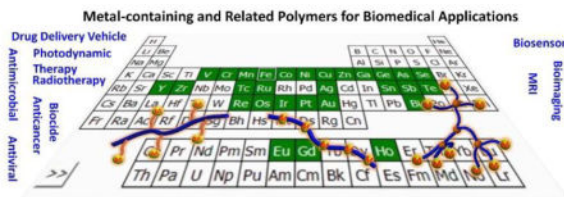
<sup>b</sup>Department of Applied Chemistry, School of Science, Northwestern Polytechnical University, Xi'an, Shannxi, 710129, China

<sup>c</sup>School of Material Science and Engineering, Tianjin University, Tianjin 300072, China

### Abstract

A survey of the most recent progress in the biomedical applications of metal-containing polymers is given. Due to the unique optical, electrochemical, and magnetic properties, at least 30 different metal elements, most of them transition metals, are introduced into polymeric frameworks for interactions with biology-relevant substrates via various means. Inspired by the advance of metal-containing small molecular drugs and promoted by the great progress in polymer chemistry, metal-containing polymers have gained momentum during recent decades. According to their different applications, this review summarizes the following biomedical applications: 1) metal-containing polymers as drug delivery vehicles; 2) metal-containing polymeric drugs and biocides, including antimicrobial and antiviral agents, anticancer drugs, photodynamic therapy agents, radiotherapy and biocide; 3) metal-containing polymers as biosensors, and 4) metal-containing polymers in bioimaging.

### Graphical Abstract



## 1. Introduction

Metal-containing polymers, also named organometallic polymers or metallopolymers, are one of major classes of polymers discovered in the 20<sup>th</sup> century.<sup>1–3</sup> They stand out independent because of a unique combination of organic and inorganic components in one macromolecular system.<sup>4–12</sup> Thus a full benefit could be achieved by simultaneously

\*Corresponding authors: tang4@mailbox.sc.edu; yanyi@nwpu.edu.cn.

†These authors equally contributed.

entertaining the mechanical and processing properties of polymeric frameworks and the electronic, catalytic, magnetic and radioactive properties of metal building blocks.<sup>13–20</sup> With the advent of polymer science in the 1950s, metals were subsequently introduced into polymers within the hands of organic and polymer scientists.<sup>21–26</sup> As a statistical example, Fig. 1 lists the evolution of publications containing “organometallic polymers” over the last two and half decades, searched *via* SciFinder (Fig. 1). There has been a steady growth of significant research in this field. Over the years metal-containing polymers have aggregated to enjoy a conglomeration of applications that span diverse fields, such as sensing, catalysis, media storage, electrolysis, electro-optical devices.<sup>27–34</sup> Research of metal-containing polymers in the biomedical field is emerging.<sup>35, 36</sup> The research is primarily inspired by the progress in polymer chemistry and medicinal chemistry of organometallic compounds that have been found vast utilities including anti-cancer, anti-bacterial, anti-fungal, and anti-virus treatments.<sup>37–40</sup> The ability of cisplatin for killing cancer cells, the first approved organometallic drug, is arguably the most exciting biomedical discovery in the field.<sup>41, 42</sup> Many other organometallic compounds have been reported for entering different stages of clinical trials.<sup>43, 44</sup>

The early pioneer work has served as a springboard to push metal-containing polymers for applications in the biomedical context.<sup>36, 45–49</sup> The key to the success is to understand their structural, compositional and chemical variation and to correlate fundamentals already discovered in small organometallic compounds in the environment of a macromolecular system. Generally, these metal centers exist in either sandwich, half-sandwich,  $\pi$ -ligand, CO-coordination, carbene, or supramolecular interactions.<sup>50–52</sup> The essential of metals in biological media typically relies on electron transfer between metals and biological substrates, either by a radical or an ionic pathway.<sup>53</sup> The metal building blocks are either hydrophobic or hydrophilic. The incorporation into a polymeric framework affords them more tunable physical properties in conjunction with diversity of organic chemistry of macromolecules, thus facilitating their biological functions. Robust organic chemistry and controlled polymerization techniques allow precision installation of metal centers into desirable locations of macromolecules, which in return devote their artificially tunable architectures to catering rational design.<sup>54–57</sup>

There are about 30 different metals used in polymeric systems (Fig. 2). Given the nature of polymers and metals usually bridged by covalent or supramolecular bonds, most of them are transition metals. Among them, Pt is probably the mostly studied, while iron, cobalt, silver and ruthenium are also widely explored. Beyond Pt, metals in Groups IV and V have attracted most attention in the scientific research communities. Based on their biological functions of metal-containing polymers, this review is organized into four sections including (1) polymers as drug delivery system; (2) polymers as drug and biocide; (3) polymers for biosensing; and (4) polymers for bioimaging. In the first section, most drug delivery systems utilize the redox chemistry or dynamic covalent bond chemistry of metals. The second section is the major focus of this review. The metal drugs/biocides are classified into antimicrobial/antiviral, anticancer, photodynamic therapy, radiotherapy and biocides. The biosensing application in the third section is centred on the redox properties of metals; while the bioimaging in the last section is composed of fluorescent imaging and magnetic

resonance imaging. Meanwhile, biomedical applications of polymers containing some non-metallic elements (Ge, As, Se) are also covered in this review.

To the best of our knowledge, there has been a missing summary on the biomedical applications of metal-containing polymers. This comprehensive review is a timely contribution to the emerging field. Different aspects of biomedical applications are embedded in numerous excellent reviews or book chapters on metal-containing polymers: such as “Metallopolymers: New Multifunctional Materials” by Manners,<sup>2</sup> “Recent developments in the Supramolecular Chemistry of Terpyridine-metal Complexes” by Schubert et al.,<sup>58</sup> “Macromolecules Containing Metal and Metal-Like Elements” by Abd-El-Aziz,<sup>59</sup> “Polymers with Platinum Drugs and Other Macromolecular Metal Complexes for Cancer Treatment” by Stenzel et al.,<sup>37</sup> to name just a few.

## 2. Metal-containing and related polymers as drug delivery vehicles

Metal-containing polymers are excellent candidates for drug delivery due to their redox and charged state. With fully reversible redox chemistry, ferrocene-containing polymers are promising candidates and widely studied for smart drug delivery.<sup>60–63</sup> Using a layer-by-layer strategy of polyanionic and polycationic poly(ferrocenylsilane) (PFS), Vancso et al. constructed a hybrid polymer capsule with controlled permeability.<sup>64</sup> The permeability and swellability of such capsule can be adjusted by the chemical oxidation of ferrocene. Using PFS with *N*-dimethylethyl ammonium and *N*-dimethyldecyl ammonium substituents, they also built redox-responsive micelles, which can be used to load and release drugs like paclitaxel.<sup>65</sup> Importantly, this polymer showed low cell toxicity below the concentration of 10 mg/mL.

Similarly, liposomes with controlled permeability can be prepared from a ferrocene-modified phospholipid.<sup>66</sup> Zhang et al. synthesized a ferrocene-containing block copolymer consisting of hydrophilic poly(ethylene oxide) (PEO) and hydrophobic poly(2-(methacryloyloxy) ethyl ferrocene-carboxylate) (PMAEFc), as shown in Fig. 3.<sup>67</sup> By using the hydrophilic Rhodamine B as an imitative drug, this system demonstrated efficient controlled release upon the oxidation of H<sub>2</sub>O<sub>2</sub>, which played a more important role in the specific physiological environment of tumors than in normal tissues.

Another strategy to construct smart delivery system from ferrocene is to utilize host-guest chemistry between cyclodextrin and ferrocene. For example, Yuan et al. reported a redox-responsive vesicle by using poly(styrene)- $\beta$ -cyclodextrin (PS- $\beta$ -CD) and poly(ethylene oxide)-ferrocene (PEO-Fc) as building blocks.<sup>68</sup> Upon oxidation, the host-guest interaction was destroyed, thus the vesicle was disassembled, which can be used to deliver drugs with controlled release. In a similar study, Ritter et al. prepared a redox-responsive supramolecular graft polymer using the host-guest interaction between ferrocene-containing acrylic copolymer (PDMA-stat-Fc) and  $\beta$ -CD-terminated polydiethylacrylamide (PDEA).<sup>69</sup>

To deliver drugs toward intracellular targets, the Zuber group reported a smart cytosolic protein delivery system by using a nickel-containing polymer.<sup>70</sup> As shown in Fig. 4, they used a supramolecular system that facilitated the assembly of pyridylthiourea-grafted

polyethylenimine (pPEI) with affinity-purified His-tagged proteins pre-organized onto a nickel-immobilized polymeric guide. The guide was prepared by functionalization of an ornithine polymer with nitrilotriacetic acid groups, which were excellent binding sites for His-tagged proteins. The delivery efficiency was high by evaluation in living U87 glioblastoma cells with an easily detectable fluorescent protein and single-chain antibodies. Transduction of the protease caspase 3 induced apoptosis in two cancer cell lines, demonstrating that this new protein delivery method could be used to interfere with cellular functions.

Another interesting smart delivery system is selenium-containing polymers. Selenium is an important element in human body. Selenoproteins, a combination of selenium and protein, have the ability to prevent cellular damage from free radicals.<sup>71, 72</sup> A lot of selenium-containing biomolecules have been prepared as antioxidants against free radicals to treat some chronic diseases, such as cancer and heart disease.<sup>73</sup> These studies indicate potential bioactivities of selenium-containing materials. Although selenium-containing small molecules have been broadly studied, study on selenium-containing polymers is rare in the past decades.<sup>71</sup> Since 2008, Zhang, Xu, and coworkers have extensively investigated selenium-containing polymers.<sup>71</sup> Various architectures of selenium-containing polymers were designed by their group, including main-chain selenium-containing polymers, side-chain analogues and dendrimers. Based on the unique chemical and biological properties of selenium element, these polymeric materials have been applied as advanced biomaterials.

In 2010, they reported a selenium-containing main-chain block copolymer based on diselenide.<sup>72</sup> Considering the bigger radius of selenium atom and the weaker electronegativity of selenium compared with sulphur, energy of selenium-selenium bonds (Se-Se) (172 kJ/mol) is much lower than that of S-S bonds (240 kJ/mol). The low energy of Se-Se makes it easier to break the bonds under mild oxidation conditions. As shown in Fig. 5, diselenide-containing main-chain polymers (PEG-PUSESe-PEG) were prepared *via* coupling with diselenide-containing diols. The PEG-PUSESe-PEG polymers showed good solubility in common solvents.

Due to the amphiphilic nature of block copolymers, PEG-PUSESe-PEG formed micelles in water with a critical micellar concentration of  $3.1 \times 10^{-4}$  mg/mL. The micelles were stable under ambient conditions. The diselenide was encapsulated in the core of micelles. These micelles can be disassembled by the oxidation under very mild conditions, such as in 0.01% (v/v) H<sub>2</sub>O<sub>2</sub> solution. This study indicated that diselenide-containing block copolymers are excellent candidates for redox-responsive drug delivery vehicles.

Xu and coworkers found that micelles from PEG-PUSESe-PEG can be disrupted as diselenide is also sensitive to  $\gamma$ -radiation.<sup>74</sup> They prepared doxorubicin-loaded PEG-PUSESe-PEG micelles in aqueous solution based on the hydrophobic interaction. Under  $\gamma$ -radiation (Dose: 50 J/kg), the micelles were disrupted, and further  $\gamma$ -radiation dose (500 J/kg) led to the release of doxorubicin drugs. The dose of  $\gamma$ -radiation was quite similar to the amount that was received by patients during a single radiotherapy treatment. They demonstrated that such  $\gamma$ -radiation sensitive materials have great potential as advanced drug delivery materials in the combination of radiotherapy and chemotherapy.

Besides  $\gamma$ -radiation and  $\text{H}_2\text{O}_2$  oxidation, PEG-PUSeSe-PEG micelles are also sensitive to singlet oxygen, which can be produced in solution by porphyrin derivatives when irradiated with red light.<sup>75</sup> As shown in Fig. 6, diselenide was oxidized by singlet oxygen, and the micelles were disaggregated. As a result, the doxorubicin drug was effectively released.

They also successfully synthesized monoselenide-containing main-chain block copolymers and used them as new vehicles for drugs.<sup>76</sup> Hydrophobic selenide can be easily tuned into hydrophilic selenoxide or selenone groups *via* chemical oxidation. Thus, redox responsive polymeric materials can be prepared based on selenide-containing polymers.

In a similar synthetic route to PEG-PUSeSe-PEG, PEG-PUSe-PEG was also prepared.<sup>76</sup> The amphiphilic nature of PEG-PUSe-PEG led to the formation of spherical micelles with the ability to load doxorubicin. The drug could be conveniently released *via* the oxidation of hydrophobic selenide into hydrophilic selenoxide and selenone by 0.1% (v/v)  $\text{H}_2\text{O}_2$ .

Recently, Xu et al. found that the monoselenide-containing polymers had the ability to coordinate with platinum ions ( $\text{Pt}^{2+}$ ).<sup>77</sup> PEG-PUSeSe-PEG was first coordinated with  $\text{Pt}^{2+}$ , and doxorubicin was encapsulated to form stable micelles. Such micelles were disassembled under glutathione (GSH) due to the strong affinity between GSH and platinum ions. As a result, doxorubicin was released into the medium *via* such coordination reactions. They demonstrated that this novel system could have great potential in drug delivery applications considering GSH as the most abundant thiol species in cancer cells.

Besides main-chain polymers, selenide-containing side-chain polymers have been also investigated by the groups of Zhang and Xu.<sup>78</sup> They reported two kinds of selenide-containing side-chain polymers: (1) covalent side-chain selenium-containing polymers; (2) non-covalent side-chain selenium-containing polymers. Generally, the covalent side-chain selenium-containing polymers were synthesized *via* esterification with selenide-containing alcohols.<sup>78</sup> These polymers can also form micelles in aqueous solution. The covalent side-chain selenium-containing polymers have similar chemical properties to the main-chain ones. *Via* the oxidation of selenide compound by diluted  $\text{H}_2\text{O}_2$  solution, the micelles could be disrupted and then release drugs. Interestingly, instead of further oxidization to selenone, the PEG-*b*-PAA-Se would be only oxidized into selenoxide. Such selenoxide-containing polymers were reduced back to selenide-containing polymeric micelles by mild reducing agents, such as Vitamin C. The reversible redox process could be performed several cycles. The redox responsive materials are excellent materials for drug delivery.

The non-covalent side-chain selenium-containing polymers were prepared *via* electrostatic interactions between a selenium-containing cationic ammonium surfactant (SeQTA) and an anionic polyacrylic acid (PEG-*b*-PAA), as shown in Fig. 7.<sup>79</sup> Such side-chain selenium-containing PEG-*b*-PAA-SeQTA complex showed similar redox properties to PEG-*b*-PAA-Se polymers, which could also release drugs under oxidation and reduction.

Compared with selenium-containing polymers, tellurium-containing polymers are far less explored though tellurium has very similar physical and chemical behaviors to selenium.<sup>80, 81</sup> Tellurium-containing compounds have been identified as mimics of glutathione peroxidase (GPx), which has the ability to protect cells from oxidative stress.

Furthermore, tellurium-containing molecules are usually less toxic to human than selenium-containing compounds.<sup>81, 82</sup>

Considering the quite similar properties between tellurium and selenium, techniques and applications used in selenium-containing polymers might be also suitable for tellurium-containing polymers. In 2014, Xu et al. reported the utilization of tellurium-containing polymers as a new possible coordination-responsive drug delivery system.<sup>81</sup> The polymer, PEG-PUTe-PEG, which has a similar structure to selenium-containing polymer (PEG-PUse-PEG), was prepared *via* a similar synthetic technique. PEG-PUTe-PEG formed micelles in aqueous solution due to its amphiphilic nature. Critical micellar concentration (CMC) of the polymer is  $1.4 \times 10^{-3}$  g/L (about  $3.7 \times 10^{-8}$  M). As an analogue of PEG-PUse-PEG, PEG-PUTe-PEG also showed the excellent ability to associate with cisplatin, which can be confirmed by <sup>127</sup>Te NMR. Such coordination interaction could be disrupted when certain amount of glutathione (GSH) was added. Due to the strong affinity between GSH and platinum ions, cisplatin was effectively released in the medium. The overall mechanism is shown in Fig. 8.

Similar to selenium-containing polymers, tellurium-containing polymers are also sensitive to oxidation and  $\gamma$ -radiation.<sup>83, 84</sup> Such properties provide opportunities to utilize tellurium-containing polymers as advanced redox-responsive and light-responsive materials. Compared with selenium-containing polymers, the tellurium-containing polymer is highly sensitive to oxidation, which is ascribed to the oxidation-sensitive nature of tellurium element.<sup>84</sup> Upon oxidation under very mild conditions ( $100 \mu\text{M H}_2\text{O}_2$ ) or  $\gamma$ -radiation, PEG-PUTe-PEG was oxidized into PEG-PUTeO-PEG (telluride-containing), and the micelles started to change their morphology. Further oxidation led to the decomposition of the micelles. Such tellurium-containing polymers provided an ultra-sensitive redox-responsive platform that uniquely took advantage of the sensitive nature of tellurium element. Besides the linear polymers, branched tellurium-containing polymers were also reported.<sup>83</sup> The branched polymer was synthesized *via* Williamson ether synthesis between PEG-Te and tris(bromomethyl)benzene. The aggregation of this branched polymer was also redox sensitive to a low concentration of  $\text{H}_2\text{O}_2$  ( $100 \mu\text{M}$ ).

### 3. Metal-containing polymeric drugs and biocides

Considering the diverse redox properties, cytotoxicity and their special interaction with DNA/RNA, metal-containing polymers are promising drugs with broad applications, ranging from antibacterial agents to anticancer drugs. The most well-known example is the cisplatin-containing anticancer drugs, some of them have been already approved by FDA and used in clinics. We mainly summarize the metal-containing polymeric drugs or prodrugs according to their different applications.

#### 3.1 Antimicrobial and antiviral agents

Infections by bacteria and fungal are leading to a global crisis, which is even worse in developing countries. A lot of drugs with promising antibacterial and antifungal properties were developed during the last century. Due to their charged nature and interesting

bioactivities, most metal-containing polymers, especially the transition metal-containing polymers, showed interesting antimicrobial and antiviral properties.

Zirconium-containing polymers were found to have an antiviral activity. Carraher et al. reported that a polymer from bis(cyclopentadienyl)zirconium dichloride and diethylstilbestrol (Fig. 9) was active against vaccinia virus, preventing more than 35% of treated cells from infection at a high concentration of 0.15 g/mL.<sup>85</sup> Through condensation with different drug precursors, Carraher et al. also reported titanium-containing polymers (Fig. 9) with potential anticancer and antibacterial properties.<sup>86, 87</sup>

The Islam group reported the antibacterial activity of vanadium-containing metallopolymers.<sup>88</sup> These polymers, including Na<sub>3</sub>[V<sub>2</sub>O<sub>2</sub>(O<sub>2</sub>)<sub>4</sub>(carboxylate)]-PA [PA = poly(acrylate)] (PAV) and Na<sub>2</sub>[VO(O<sub>2</sub>)<sub>2</sub>(carboxylate)]-PMA [PMA = Poly(methacrylate)] (PMAV), were synthesized by a reaction of V<sub>2</sub>O<sub>5</sub> with H<sub>2</sub>O<sub>2</sub> and sodium salts of respective macromolecular ligands at pH ≈ 6. The antibacterial activity was screened against Gram-negative *Escherichia coli* (*E. coli*) and Gram-positive *Staphylococcus aureus* (*S. aureus*). Significantly, PMAV treatment resulted in 66.8% inhibition of *S. aureus* at a low concentration of 20 μg/mL.

Chromium-containing polymers also show interesting biomedical applications due to their biological, pharmacological, and clinical importance. The Nartop group synthesized Schiff base-functionalized polystyrene, which could form complexes with Cr(III) complexes,<sup>89</sup> as shown in Fig. 10. All of these polymers showed moderate or high antibacterial activities against different bacteria, such as *S. aureus*, *Shigella dysenteriae* type 10, *Listeria monocytogenes* 4b, *E. coli*, *Salmonella typhi* H, *Staphylococcus epidermis*, *Brucella abortus*, *Micrococcus luteus*, *Bacillus cereus* sp., *Pseudomonas putida* sp., and antifungal activity against *Candida albicans*.

A series of biocompatible cobalt-containing polymers with interesting anticandidal applications were reported by the Hashmi group.<sup>90</sup> These polymers were synthesized from sunflower fatty amide diol, adipic acid and cobalt chloride through a microwave reaction. They showed significant antifungal activity against *Candida* both in liquid and solid media. Preliminary mechanism study showed that the activity was originated from the inhibition of plasma membrane. Using the similar strategy to the construction of cobalt-sunflower oil based polymers, another sunflower oil based nickel-zinc bimetallic polymer was reported by the same group (Fig. 11).<sup>91</sup> This polymer showed interesting antifungal properties by using *Candida* species as model organisms. The concentration of this polymer plays an important role on the growth and sensitivity of the *Candida* species. Its study on the mechanism showed that the antifungal activity of this polymer arose from the targeting H<sup>+</sup>-ATPase mediated H<sup>+</sup>-pumping, which led to intracellular acidification and cell death.

Polymeric Schiff bases are widely used to prepare transition metal-containing polymers through coordination interactions. Main-chain polymeric Schiff bases were prepared through a condensation reaction.<sup>74</sup> Then, the target metal-containing polymer can be prepared in quantitative yields by interacting with equimolar amount of transition metal salts (Mn(II), Co(II), Ni(II), Cu(II) and Zn(II)). Compared with the polymeric Schiff bases, Parveen et al.

found that all of these metal-containing polymeric compounds showed enhanced antibacterial activity against *E. coli*, *B. subtilis*, *S. aureus*, *P. aeruginosa* and *S. typhi*, and antifungal activity against *T. longifusus*, *C. albicans*, *M. canis*, *F. solani* and *C. glaberata*. In another study, they designed new polymeric Schiff bases and corresponding metallopolymers, which showed similar antibacterial and antifungal activities. They attributed the enhanced activity to the coordination interaction with metal ions.<sup>92, 93</sup>

Germanium and its derivatives have been utilized for dietary supplements, immunity enhancement and antimicrobial materials.<sup>94–96</sup> Based on their unique properties, germanium-containing polymers were also investigated. In 2014, Mohamed and coworkers reported the modification of functionalized polyethylene glycol (PEG) by germanium dioxide to produce a germanium nonionic surfactant (Fig. 12).<sup>97</sup> The surfactant spontaneously formed micelles in aqueous solution with a critical concentration of 0.3 ~ 0.5 mM. *Via* standard disk-diffusion assay, the surfactant showed good ability to inhibit the growth of Gram-positive, Gram-negative bacteria and fungi. The diameter of inhibition zones on disk achieved 20 ~ 40 mm with 1 mg of surfactant for different bacteria and fungi.

Organotins are among the most widely used organometallic materials with different functionalities. They are broadly used as biocidal materials.<sup>98, 99</sup> Tin-containing polymethylacrylate are well-known for delivering substance to micro-organisms at certain rates.<sup>98</sup> Trialkyltin-containing polymeric materials have been used as surface coating materials against marine organisms that foul ship bottoms.<sup>100</sup> Tributyltin-containing polymers usually give the best antifouling effects due to the readily hydrolysis from carboxylate group.<sup>98</sup> As a result, a lot of effective coating materials based on tin-containing polymethacrylates were produced. Such polymeric materials successively released tin complexes in order to inhibit the growth of certain organism in a long period.

Due to the great advantages of organotin molecules, tin-containing polymers are also prepared as antimicrobial materials. Through condensation polymerization, tin-containing polyamines (dibutyltin pyrimidine polyamines, Fig. 13) were prepared and showed effective inhibition towards various strains of bacteria, including *E. coli*, *S. cerevisiae*, *S. aureus* and so on.<sup>101</sup> Using a similar technique, organotin can also form esters with some commercial antibiotics. For example, Zhao and Carraher reported the polycondensation reactions between organotin and commercial available antibiotic ciprofloxacin.<sup>102</sup> The resultant tin-containing polymers had the ability to kill different kinds of virus, including *reovirus ST3*, *vaccinia WR*, *herpes simplex virus (HSV)-1*, and *varicella zoster virus (VZV)*. Furthermore, the polymers can also inhibit Balb 3T3 cancer cells, which indicated their potential as anticancer drugs. Additionally, these polymers have great ability to kill various kinds of bacteria and yeasts. With different alkyl groups in organotin molecules, they showed different effects against cancer cells. The best polymer was based on divinyltin-ciprofloxacin. All of these results demonstrated that organotin-containing polymers are candidates as new biomedical materials.

Metallocene-containing polymers are also very promising candidates for antibacterial drugs. Cobaltocenium has many advantages over its analogue, ferrocene, such as better stability and ion-dependent solubility. Metzler-Nolte and coworkers reported a series of



cobaltocenium bioconjugates prepared *via* solid phase peptide synthesis (SPPS).<sup>103</sup> It was found that the presence of a positively charged cobaltocenium did not significantly influence hydrogen bonds in peptide structures. Taking advantage of the higher redox potential and chemical stability of cobaltocenium, they reported the first example of directed nuclear delivery of cobaltocenium, by conjugation to the SV-40 T antigen nuclear localization signal (NLS; primary sequence HPro-Lys-Lys-Lys-Arg-Lys-Val-OH) peptide. They also found that these bioconjugates showed potential antibacterial activity against *E. coli*, *Pseudomonas aeruginosa* and *S. aureus*, although very limited.<sup>104</sup>

The Manners group investigated main-chain cobaltocenium-containing polymers *via* anionic ring-opening polymerization.<sup>105–107</sup> They first reported the association between main-chain cobaltocenium-containing polymers and DNA due to ionic interactions, which could be potentially utilized for DNA or gene delivery.<sup>108</sup>

Recently, we reported the synthesis of side-chain cobaltocenium-containing polymers and their applications as advanced materials.<sup>109–121</sup> In 2014, we reported the utilization of side-chain cobaltocenium-containing polymers as novel antimicrobial materials to kill methicillin-resistant *Staphylococcus aureus* (MRSA).<sup>122</sup> MRSA is resistant to most of currently commercial  $\beta$ -lactam antibiotics. We found that cobaltocenium-containing polymers could be effective against various strains of MRSA. Due to the unique ionic interaction between carboxylic anions and cationic cobaltocenium moieties, these cobaltocenium-containing polymers have the ability to rejuvenate traditional antibiotics against MRSA *via* the binding with  $\beta$ -lactamase.  $\beta$ -Lactamase produced by MRSA is an enzyme that can deactivate antibiotics *via* hydrolysis of the  $\beta$ -lactam rings in antibiotics. As shown in Fig. 14, through association with carboxylic anions in antibiotics, the bioconjugates of cobaltocenium-containing polymers could protect antibiotics from the hydrolysis by  $\beta$ -lactamase. Such conjugation was stable in aqueous solution and confirmed by <sup>1</sup>H NMR study. Furthermore, the antibiotics can be released effectively when the bioconjugates arrived at the negative charged bacterial cell membranes or cell walls. Additionally, these side-chain cobaltocenium-containing polymers themselves also have the ability to kill various strains of bacteria, including MRSA at relatively low concentrations (1–10  $\mu$ M) *via* disruption of cell membranes. According to *in vivo* and *in vitro* tests, these metallopolymers exhibited an extremely low cytotoxicity to red blood cells and high selectivity against bacterial cells. These studies indicated the great potential of cobaltocenium-containing polymers as advanced antimicrobial materials.

With such antimicrobial activities and binding affinity with antibiotics, we also introduced these cationic cobaltocenium moieties into polymeric networks to form cobaltocenium-containing hydrogels.<sup>123</sup> The gels were prepared *via* free radical polymerization of methacrylate cobaltocenium monomers and dimethacrylate functionalized PEO crosslinkers. Based on the unique anion-dependent solubility of cobaltocenium moieties,<sup>117, 124</sup> these gels showed a transition between organogels and hydrogels. Such a transition could be easily achieved by using tetrabutylammonium salts (Fig. 15). Gels with PF<sub>6</sub><sup>-</sup> anions were compatible with a few organic solvents. However, Cl<sup>-</sup>-paired cobaltocenium-containing gels (PCoCl-Gel) were highly hydrophilic. The gels showed quite different mechanical properties and water uptake ability with different anions. Additionally, considering the binding affinity

between anionic antibiotics and cationic cobaltocenium moieties,<sup>125</sup> Cl<sup>-</sup>-paired cobaltocenium-containing gels have high efficiency to absorb  $\beta$ -lactam antibiotics, which can be applied to treat antibiotic-contaminated water. Contamination of antibiotics has become a critical issue in the world due to the fact that  $\beta$ -lactam antibiotics have greatly enhanced the evolution of bacterial resistance.<sup>126</sup> Cl<sup>-</sup>-paired cobaltocenium-containing gels showed a better ability to remove  $\beta$ -lactam antibiotics (1.5 g/L gel could clean antibiotics waste at a concentration of 3 ~ 10 mg/L), compared with other adsorption techniques.<sup>127, 128</sup> Furthermore, PCoCl-Gel could also inhibit the growth of different strains of bacteria due to the antimicrobial activities of cobaltocenium moieties,<sup>125</sup> Gram-negative *E-coli*, Gram-positive *S. aureus* and MRSA under different concentrations (~20 mg/mL). These versatile cobaltocenium-containing hydrogels are new materials for broad applications, especially in the areas of biomedicines and environmental treatment.

The Abd-El-Aziz group developed antimicrobial agents based on the cationic  $\eta^6$ -arene- $\eta^5$ -cyclopentadienyliron(II) (Cp-Fe<sup>II</sup>-arene) complex (Fig. 16).<sup>129</sup> These antimicrobial organometallic dendrimers showed tunable activity against multidrug-resistant Gram-positive bacteria, such as MRSA and vancomycin-resistant *Enterococcus faecium*, with the minimum inhibitory concentration (MIC) in the low micromolar range. Interestingly, these dendrimers were non-cytotoxic to epidermal cell lines and to mammalian red blood cells. Mechanistically, they found two mechanisms for the enhanced antimicrobial activity, which include interactions with cell membranes and induction of oxidative stress on bacteria.

### 3.2 Anticancer drugs

Due to their special interaction with biological substrates and unique chemical properties such as Fenton chemistry and reactive oxygen species, metal-containing polymers show promising applications as anticancer drugs.<sup>47</sup>

It is known that ferrocene shows low acute toxicity, while its oxidized state, ferrocenium, can generate reactive oxygen species (ROS) and hydroxyl radical (so called Fenton chemistry)<sup>130</sup> in a physiological environment, which shows specific toxicity to tumor cells. Neuse et al. carried out a series of studies on the anti-cancer activity of ferrocene-containing polymers.<sup>131</sup> They grafted hydrophobic ferrocene to a water-soluble carrier polyaspartamide (Fig. 17). *In vitro* antiproliferative activity of these ferrocene-containing polymers was tested against HeLa cancer line, and showed the similar activities to cisplatin polymers.<sup>132</sup>

To further enhance therapeutic effectiveness, Neuse et al. introduced the concept of drug co-conjugation with polymer carriers, which led to reduction in the doses and side effects caused by the high dose of pure drug. For example, they grafted both ferrocene and methotrexate (MTX) to the polyaspartamide carriers.<sup>133</sup> In another study, they successfully grafted the relative cheap MTX analogue, folic acid, to polyaspartamide carriers, with a content of ca. 15%.<sup>134</sup> They even grafted aminoquinolines and ferrocene to polyaspartamide, a potential cancer chemotherapy agent with drug adjuvant.<sup>135</sup> Mukaya et al. synthesized macromolecular co-conjugates of bisphosphonate and ferrocene.<sup>136</sup> Their study on the drug release at different pH conditions revealed that both ferrocene complex and bisphosphonate were released with increasing release rates upon the decrease of pH.

Besides polyaspartamide, Neuse et al. also developed a polyamidoamine-based carrier. The introduction of oligo(ethylene oxide) greatly increased the hydrophilicity and water solubility of ferrocene-containing polymers (Fig. 18).<sup>137–144</sup> They used cell lines derived from cultured human cancers, such as HeLa, LNCaP, and Caco-2 to evaluate preliminary biological effects. Interestingly, the polyaspartamide-based conjugates revealed an unexpectedly uniform performance spectrum against the three test lines, which gave IC<sub>50</sub> around 2–10 μg Fe/mL. After a careful survey of the structure-effect relationship, they concluded that the ferrocene-containing polymers were readily conveyed into endoplasmic space and exerted a powerful antiproliferative imprint upon the affected cells. They also found that the ferrocene-containing polymers, which possess tertiary amine groups, were exceptionally promising and displayed similar activities to cisplatin.

The Mirza group synthesized a series of ferrocene-containing main-chain poly(azomethine)esters and studied their biological activities (Fig. 19).<sup>145</sup> In biological studies it was found that the fluorinated material was antibacterial with activity comparable to antibiotics that was used as control. Significant antibacterial, cytotoxic and antitumor activities indicated their potential use as antibiotics and anticancer agents. All polymers were found highly potent antioxidant and more importantly to protect DNA. These polymers can be studied further for pharmacological activities as potential drug candidates. In another study, they screened these polymers for antibacterial, brine shrimp cytotoxic, free radical induced oxidative DNA damage and DPPH free radical scavenging activity. Among all, PFeF showed inhibition of *S. aureus*, *Micrococcus luteus*, *Bordetella bronchiseptica* and *Salmonella typhimurium*. In brine shrimp cytotoxicity assay PFeF and PFePr exhibited LD<sub>50</sub> < 1 ppm, a highly cytotoxic behavior. A Schiff base monomer (SB) significantly inhibited the tumor (36.02%) and revealed a higher radical scavenging activity (IC<sub>50</sub> 13.65 ppm) than polymers.<sup>146</sup> In general, all polymers (PAMEs) had good antioxidant and DNA protecting behavior. Molecular docking and QSAR studies were carried out to investigate the interactions between polymers and double stranded DNA. The studies showed good correlation of binding strength and activity of polymers. The high value of binding constant implied that respective drugs strongly bound to DNA.

Zhang et al. prepared shell cross-linked (SCL) thermoresponsive polymer micelles by cross-linking poly(*N*-isopropylacrylamide-*co*-aminoethyl methacrylate)-*b*-polymethyl methacrylate with 1,1'-ferrocenedicarboxylic acid.<sup>147</sup> Such ferrocene-containing hybrid polymeric micelles exhibited antitumor activity, with cytotoxicity toward HeLa cells with IC<sub>50</sub> as low as 0.2 g/L.

Bearing similar chemical properties to iron-containing polymers, ruthenium-containing polymers are also used as potential biosensors, anti-cancer drugs. Although ruthenocene-containing polymers were successfully synthesized by the Tang group, these polymers did not show cytotoxicity towards cancer cells.<sup>148</sup> The ruthenium complexes commonly used for the biomedical applications are ruthenium-ligand coordination complexes or half-ruthenocenes.<sup>149</sup>

Valente et al. carried out a anti-cancer study of ruthenium-cyclopentadienyl derivatives (Fig. 20).<sup>149</sup> They synthesized *D*-glucose end-capped polylactide ruthenocenium

cyclopentadienyl complex (compound **1** in Fig. 20). Biological tests against human MCF7 and MDAMB231 breast and A2780 ovarian adenocarcinoma reveal that these complexes were potential anti-cancer drugs with IC<sub>50</sub> values in the micromolar range.<sup>150</sup>

Besides the side-chain topology, main-chain ruthenium-containing polymers were also prepared for biomedical application. By using the coordination interaction between bis(terpyridine) derivatives and Ru<sup>2+</sup> or Fe<sup>2+</sup> ions, Higuchi et al. constructed a series of metallo-supramolecular polymers (compound **2** in Fig. 20).<sup>151</sup> Owing to the electrostatic interaction between the metal cations of polymers and the phosphate anions of DNA, these polymers showed high binding ability to different DNAs, such as calf thymus DNA,<sup>152</sup> herring sperm DNA, [poly(dA-dT)]<sub>2</sub>, and [poly(dG-dC)]<sub>2</sub>. Meanwhile, these polymers displayed highly statistical significance to human non-small cell lung cancer lines (NCI-H460).

Dendritic ruthenium-containing polymers are also widely explored for biological applications, especially owing to the “enhanced permeability and retention” (EPR) effect, which allows large molecules to selectively enter cancer cells. Smith et al. developed a series of multinuclear arene ruthenium-containing poly(propyleneimine) (PEI) dendrimers (compound **3** in Fig. 20). Anti-cancer study against the A2780 human ovarian cancer cell line indicated that these ruthenium-containing dendrimers showed moderate anti-proliferative activity. Importantly, there was a clear trend between the size of molecules and cytotoxicity: the larger the size, the more toxic the molecule.<sup>153</sup> In another study, they prepared chelating neutral (N, O) and cationic (N, N) ruthenium arene dendrimers based on a PEI scaffold. The cytotoxicity was evaluated over A2780 (cisplatin sensitive) and A2780cisR (cisplatin resistant) human ovarian carcinoma cancer cell lines. The results showed that the antiproliferative activity was almost similar in both cell lines, indicating that these polymers have different anticancer mechanisms to that of cisplatin.<sup>154</sup>

Some ruthenium metallacages were also used in the construction of ruthenium-containing polymers for potential biological applications. The Therrien group prepared a series of water soluble ruthenium macromolecules through the host-guest interaction between arene ruthenium metallaprisms and pyrenyl-functionalized dendrimers (compounds **4** and **5** in Fig. 20). These host-guest systems showed enhanced cytotoxicity than pyrenyl-containing polymers and metallaprism itself, which might be attributed to the increased water solubility. It is notable that the host-guest systems showed similar cytotoxicity for both the cisplatin-sensitive A2780 and cisplatin-resistant A2780cisR cancer cell lines, indicating that they behaved in a different mechanism from the reference drug, cisplatin.<sup>155, 156</sup> They further designed another host-guest system by using a water soluble guest, which allowed to compare the biological activity of both dendrimers and the host-guest system.<sup>157</sup> Biological test towards human ovarian cancer cells showed that the host-guest system was considerably more cytotoxic than the individual hosts and guests. Meanwhile, this system was quite stable in biological media.

Cobalt-containing compounds and polymers are widely used as anticancer, antifungal, and antibacterial agents. Natarajan et al. synthesized a water soluble cobalt-containing coordination polymer through the coordination between Co(NO<sub>3</sub>)<sub>2</sub> and a new ligand (Fig.

21).<sup>158</sup> This coordination polymer was found to form stable complex with calf thymus DNA (CT-DNA) and bovine serum albumin (BSA) through intercalation. Interestingly, they found this cobalt-containing polymer has strong radical scavenging potency against different radicals, such as hydroxyl radicals, 2,2-diphenyl-1-picrylhydrazyl radicals, nitric oxide and superoxide anion radicals. Moreover, the water soluble complex exhibited good cytotoxic activity against HeLa, HEp-2, Hep G2 and A431 cancer cell lines without significantly affecting the normal NIH 3T3 cells. Especially, it exhibited excellent cytotoxic specificity against Hep G2 cells with anticancer activity of ca. three times higher than that of cisplatin.

The Arunachalam group also reported a series of side-chain cobalt-containing polymer by using some cobalt-pyridine complexes (Fig. 22).<sup>159</sup> Similar to the cobalt-containing coordination polymer, these side-chain polymers can form stable binding complexes with different DNAs. All these polymers showed good anticancer activities: the stronger the binding between polymers and DNAs, the higher the inhibition value. Recently, they found that the side-chain polymer formed by the simple bipyridine ligand showed better antibacterial and antifungal activities against some human pathogenic microorganisms, such as *S. aureus*, *Bacillus subtilis*, *E. coli*, *Pseudomonas auregenosa* and *Candida albicans*.<sup>160</sup>

Copper-containing polymers also exhibited potential anticancer and antibacterial properties. The Arunachalam group reported the cytotoxic property of a Cu-containing polymer against human lung cancer cells.<sup>161</sup> The Cu-containing polymer was synthesized from copper ion and 2,2'-bipyridyl ligand and branched polyethyleneimine. It was found that most of the NCI-H460 human lung cancer cells were killed through apoptosis and/or necrosis after treatment with the Cu-containing polymers.

Similarly, they prepared another Cu-containing polymers by using 1, 10-phenanthroline and *L*-arginine as ligands.<sup>162</sup> These polymers can form stable complexes with DNA/RNA through intercalation and electrostatic interaction, which is dependent on the degree of coordination. These polymers showed cytotoxicity towards MCF-7 mammary carcinoma cells through apoptosis. Meanwhile, these polymers also exhibited antimicrobial activities to some pathogens.

Germanium-containing polymers are also utilized as anticancer materials. In 1982, Norihiro filed a patent about using organogermanium oligomers as anticancer agents (Fig. 23).<sup>163</sup> The oligomer effectively inhibited growth of cancer cells, while this phenomenon was not observed for germanium monomers.

Although elements in Group VA only make up less than 0.2% of the weight of earth crust, they are critically important in both daily life and industry. Nitrogen and phosphorus are the most necessary elements for nutrients in the world. As a result, tremendous amount of reports have been published about nitrogen or phosphorus-containing polymers.<sup>164–166</sup> Compared with nitrogen and phosphorus, arsenic, antimony and bismuth-containing polymers are less explored, although the biological activities of these elements have been well known for a long time.<sup>102</sup> Arsenic, antimony and bismuth have quite similar chemical properties. For example, halide compounds of these elements are extremely easy to react with alcohol or amine to form esters or amides.<sup>102</sup> Various kinds of arsenic, antimony and

bismuth-containing polyethers or polyamines have been synthesized *via* the esterification or amidation between dihalide compounds and dialcohol or diamine. Additionally, these dihalide compounds also have the ability to react with diacid to form polyesters. Considering the biological activities of arsenic, antimony and bismuth, these polymers can be applied as new anticancer drugs and antimicrobial materials.<sup>102</sup> Fig. 24 shows structures of currently reported biopolymers containing arsenic, antimony and bismuth.

During the past two decades, the Carraher group has extensively studied the synthesis and biological activities of arsenic, antimony and bismuth-containing polyethers or polyamines. They discovered many kinds of drugs and biomaterials based on the above mentioned three types of reactions. In 2014, they found that thiodiglycolic acid could react with arsenic, antimony and bismuth dihalide compounds to form polyesters (Fig. 24) with good yield in less than one minute under room temperature.<sup>167</sup> The resultant polymers have molecular weights ranging from 80 kDa to 200 kDa. These polymers showed excellent activities against different tumor cell lines and low toxicity towards normal human cells. The arsenic polyesters had outstanding inhibition against the human pancreas adenocarcinoma pancreatic cancer cell line (AsPC-1) with  $IC_{50}$  at 0.055  $\mu\text{g}/\text{mL}$ , which was much lower than cisplatin ( $IC_{50}$ : 1400  $\mu\text{g}/\text{mL}$ ). Due to the metastasization prior to detection of the disease, treatment of pancreatic cancer is rarely successful. Arsenic and bismuth-containing polymers also effectively inhibited the growth of the PC-3 human prostate cancer cell line with a low  $IC_{50}$  at 0.064  $\mu\text{g}/\text{mL}$  and 12  $\mu\text{g}/\text{mL}$ , respectively. Furthermore, the antimony polymers were also capable to show activities on both the MDA-MB-231 ( $IC_{50}$ : 0.77  $\mu\text{g}/\text{mL}$ ) and MCF-7 human pleural effusion breast cancer cells ( $IC_{50}$ : 3.1  $\mu\text{g}/\text{mL}$ ). These polymers showed better or comparable performance in contrast with cisplatin.

With a similar technique, the Carraher group reported another drug, glycyrrhetic acid, which could be coupled with arsenic, antimony and bismuth dihalides *via* esterification and ether formation in less than 15 seconds.<sup>168</sup> The structures of polymers are shown in Fig. 24. The yields to form these polymers were in the range of 10% ~ 50%, depending on the compounds used and reaction conditions. The molecular weight of these polymers was around 200 kDa, quite similar to polymers with thiodiglycolic acid. Similarly, these polymers showed activities against different cell lines, including AsPC-1, human pancreas epithelioid duct carcinoma cell line (PANC-1), normal embryonic human lung fibroblast cells (WI-38 cells), and mouse embryo-fibroblast (NIH-3T3) cell line. These results are summarized in Table 1. These polyesters showed good inhibition against different cell lines, though less effective than cisplatin.

The work by the Carraher group focused on the main-chain metal-containing polymers, which were usually obtained from polycondensation. The molecular weight and polydispersity were difficult to control. In 2014, the Le group reported the utilization of side-chain arsenic-containing polymers as new anticancer drugs.<sup>169</sup> They first synthesized prodrugs of poly(ethylene oxide)-*b*-poly[*a*-(6-mecaptohexyl amino)carboxylate-*e*-caprolactone] (PEO-*b*-PCCL). The PEO-*b*-PCCL was then functionalized with thiol groups, which could bind with phenylarsenic oxide *via* As-S bonds (Fig. 25). Using inductively coupled plasma mass spectrometry (ICP-MS) characterization, 65% of thiol groups were found to conjugate with phenylarsine oxide (PAO).

The critical micelle concentration of PEO-*b*-P(CCLC<sub>6</sub>-S-PAO) was determined to be 0.07 mg/mL. In a *vitro* study, the release of conjugated PAO in the polymeric micellar carrier was prolonged, compared with free PEO-*b*-P(CCLC<sub>6</sub>-S-PAO). However, the rate could be accelerated in the presence of glutathione due to the higher binding affinity between glutathione and PAO. Both PEO-*b*-P(CCLC<sub>6</sub>-S-PAO) and PEO-*b*-P(CCLC<sub>6</sub>-SH) showed effects against MDA-MB-435 cancer cells. The results indicated that the IC<sub>50</sub> of PEO-*b*-P(CCLC<sub>6</sub>-S-PAO) was not significantly different from that of free PAO. These results demonstrated that PEO-*b*-P(CCLC<sub>6</sub>-SH) was a promising carrier for successful arsenic delivery for cancer therapy.

Carraher et al. found that Zr-containing polymers have the ability to suppress the growth of a series of tumor cell lines originating from breast, colon, prostate, and lung cancers at concentrations generally lower than those required for inhibition of cell growth by cisplatin.<sup>170</sup>

Some precious metal-containing polymers were found to show interesting anticancer activities. Silver-, gold-polyacrylic acid complexes were studied by Ostrovskaya et al. They found that the silver-containing polymer was highly effective against Lewis lung carcinoma, and can inhibit almost 90% of the tumor growth, and extend the average lifespan of the mice by 46% in comparison with the control group. While in the case of Acatol adenocarcinoma, the growth was inhibited by 55%. Interestingly, the Au-containing polymer efficiently inhibited the growth of both tumors by at least 80%, which was recommended for thorough preclinical study.<sup>171</sup>

Platinum-containing complexes (some structures are shown in Fig. 26) are widely used in anticancer study, some of them are even used in clinic.<sup>37</sup> Cisplatin, as the first platinum drug, is one of commercially available anticancer drugs, which shows broad-spectrum anticancer effects, including ovarian cancer, prostate cancer, testicular cancer, lung cancer, nasopharyngeal carcinoma, esophageal cancer, malignant lymphoma, head and neck squamous cell carcinoma, thyroid carcinoma and osteogenic sarcoma.<sup>172</sup>

However, most of these drugs are associated with significant side effects, rising drug resistance and low hydrolytic stability.<sup>173</sup> To combat these problems, drug delivery carriers have been developed to increase the protection of drugs and increase efficacy. Generally, there are mainly two approaches to design platinum drug-polymer conjugates: 1) physical encapsulation in a polymer substrate; 2) attachment to a polymer backbone *via* covalent bonding.

Neuse, Rensburg and coworkers carried a systematic study to prepare water-soluble platinum drug-containing polymers. Most of the polymer backbones they used are based on polyaspartamide, as shown in Fig. 27. These conjugates initially showed full solubility in water, and tended to undergo an ageing process on storage. However, in frozen aqueous solution, they were stable enough for extended periods of time.<sup>174, 175</sup> They also used the main-chain strategy *via* aliphatic polyamide carriers with ethylenediamine segments. However, in such design, the platinum drugs were shielded in the PEO segments and prevented the efficient intracellular release of drugs.<sup>176, 177</sup> As a result, the IC<sub>50</sub> (determined

by using HeLa cells) for the main-chain polymer was as high as 120  $\mu\text{g}/\text{mL}$ , while the value for the side chain counterpart was as low as 14  $\mu\text{g}/\text{mL}$ . By using LNCaP human metastatic prostate adenocarcinoma cell line, they also found that both monoamine-coordinated platinum-containing polymers and cis-diamine-coordinated platinum-containing polymers showed good antiproliferative activity.<sup>178</sup> In addition to the direct cytotoxic properties, the platinum drugs have been reported to generate ROS, which is also responsible for the anticancer properties.<sup>179</sup> Rensburg et al. studied the effect of cisplatin and water soluble platinum-containing polymers on the production of ROS. The results demonstrated that different from cisplatin, these Pt-containing polymers were unable to generate ROS by granulocytes and monocytes/macrophages, which made them potential clinical anticancer agents.<sup>180</sup>

Kataoka and Yokoyama et al. introduced cisplatin to polymer micelles for drug delivery.<sup>181</sup> They found that Pt-containing micelles allowed prolonged circulation of Pt and specific accumulation in the tumors.<sup>182</sup> They also successfully introduced oxaliplatin to block copolymer micelles.<sup>183</sup> These Pt-containing micelles were stable enough for 240 h, and showed sustained release within 96 h. Such micelles showed considerable *in vitro* cytotoxicity against murine colon adenocarcinoma 26 (C-26) cells, which was lower than oxaliplatin, but increased with the exposure time as a result of the release of platinum complexes from micelles. The long-term delivery and release of platinum drug can be also realized by using in situ-formed hydrogel. Ding et al. designed a conjugate by covalently linking Pt(IV) complex to the hydrophobic end of two methoxyl poly(ethylene glycol)-*b*-poly(*D,L*-lactide) (mPEG-PLA) copolymer chains (Fig. 28).<sup>184</sup> Such conjugates can form micelles and gels in water depending on the concentration. *In vitro* release experiments of Pt(IV)-conjugated thermogel showed that the platinum release lasted as long as two months. Interestingly, most of the released Pt(IV) drugs were mainly in the form of micelles and micellar aggregates from the gel depot. More importantly, the micellar Pt drug showed enhanced *in vitro* cytotoxicity against cancer cells due to the effective accumulation into cells *via* endocytosis.

The Jing and Huang group designed a series of platinum drug-containing polymers.<sup>185</sup> They prepared a biodegradable block copolymer poly(ethylene glycol)-*b*-poly(*L*-lactide-*co*-2-methyl-2-carboxyl-propylene carbonate) as a carrier for oxaliplatin analogue, as shown in Fig. 29. This polymer self-assembled into micelles, which can release platinum drug under an acidic condition. *In vitro* evaluation showed that the micelles exhibited the same or higher cytotoxicity against SKOV-3, HeLa, and EC-109 cancer cells, compared with oxaliplatin. It was attributed to the effective internalization of micelles by cells *via* endocytosis and the sensitivity of SKOV-3 cells to platinum drugs. By using a similar strategy, they also successfully prepared a polymer carrier for oxaliplatin analogue. Such polymer-drug conjugate approach can remarkably enhance the uptake of substances by cancer cells and partially overcome the drug resistance in ovarian cancer cells.<sup>186</sup> Through co-assembly of oxaliplatin- and gemcitabine-containing block copolymers, they found that the hybrid micelles showed much lower systemic toxicity and enhanced efficacy against the xenograft cancer model than either of them alone or even Gem/Pt combinations.<sup>187</sup> In a similar study, they also co-assembled cisplatin and all-trans-retinoic acid-containing block copolymers,<sup>188</sup> and daunorubicin and oxaliplatin-containing block copolymers.<sup>189</sup> This method achieved



enhanced drug efficacy and safety. To increase the loading efficiency of platinum drug, they used thiolene chemistry to prepare 1,2-bidentate carboxyl group-containing biodegradable block copolymers, which can be used to chelate with the active anticancer species (DACH-Pt) of oxaliplatin. *In vitro* study showed that this Pt-containing polymer exhibited enhanced cytotoxicity against SKOV-3 and MCF-7 cancer cells. However, the presence of sulfur was a major cause of drug resistance to platinum drugs.<sup>190</sup>

By using a strategy of combination chemotherapy,<sup>191</sup> Huang et al. achieved co-delivery of multiple drugs using a polymer-(tandem drugs) conjugate system. Different combinations of drugs were used, such as two drugs (demethylcantharidin (DMC) and cisplatin),<sup>192</sup> and three drugs (cisplatin, azidyl radical and DMC).<sup>193</sup> Interestingly, when the polymer-(multifunctional single-drug) conjugate was internalized by cisplatin-resistant cells (A549R), all drugs can be sequentially released from the polymer chain within reactivated endosomes/lysosomes under a UVA irradiation to kill cancer cells and overcome cisplatin resistance. To achieve specific targets, they also co-assembled oxaliplatin- and folic acid-containing block copolymers. Antitumor activity evaluation with mice bearing H22 liver cancers showed that the micelles with folic acid moieties exhibited greater antitumor efficacy than those without folic acid or oxaliplatin.<sup>194</sup> Enhanced drug toxicity can be also achieved by conjugation of the platinum drugs to polymers with guanidine-containing zwitterionic groups. Stenzel et al. demonstrated that the drug did not need to be cleaved from the polymer in order to be active, and the key was to create carriers with sufficient solubility.<sup>195</sup> In a recent study, they found that conjugation of albumin with polymer-drug conjugates can enhance the anticancer activity.<sup>196</sup>

The Qiao group prepared cross-linked polymer vesicles by using ring-opening metathesis polymerization (ROMP) and thiolene chemistry (Fig. 30).<sup>197</sup> This system allowed a steady release, due to the combined diffusion and chemically controlled de-complexation processes. In a recent report, they designed degradable cross-linked polymer vesicles for the efficient delivery of cisplatin.<sup>198</sup> To avoid the presence of sulfur, 2,2'-(propane-2,2-diyl bis(oxy))diethanamine was used. This chemical design provided a faster drug release under acidic conditions (pH = 5.5) due to the presence of an acid-degradable linker. The anticancer activity of cisplatin loaded into the cross-linked vesicle was improved in comparison with free cisplatin. A similar strategy was also reported via crosslinking a polymer micellar core. The cisplatin-loaded micelles were very stable for an extended period of time. *In vitro* studies demonstrated that the cross-linked micelles rapidly internalized and delivered cisplatin into human A2780 ovarian carcinoma cells.<sup>199</sup>

Hyperbranched polymers were also used in Pt-containing anticancer drugs. The Burt group reported the use of hyperbranched aliphatic polyesters as a platform to load cisplatin.<sup>200</sup> The cisplatin-loaded hyperbranched polymers were stable for at least 5 days and exhibited a slow release profile over 7 days.

Coordination polymers were also designed for drug delivery. The Lin group reported nanoscale coordination polymers (NCPs) from Tb<sup>3+</sup> ions and *c,c,t*-(diamminedichlorodisuccinato) Pt(IV) complex (Fig. 31).<sup>201</sup> Then the resultant NCPs were coated with a shell of amorphous silica, which allowed enhanced water dispersibility and

biocompatibility. Furthermore, the release of platinum drug can be tuned by varying the thickness of silica shell. In order to enhance the cellular uptake of NCPs *in vitro*, a RGD sequence was grafted onto the surface of silica shell. Their results showed that the RGD-targeted NCPs had an IC<sub>50</sub> value of 9.7  $\mu\text{M}$ , while the cisplatin standard had an IC<sub>50</sub> value of 13.0  $\mu\text{M}$ . Recently, they achieved enhanced antitumor activities by using zinc bisphosphonate NCPs that carried ca. 48% cisplatin prodrug and 45% oxaliplatin prodrug.<sup>202</sup> In all tumour xenograft models evaluated, including CT26 colon cancer, H460 lung cancer and AsPC-1 pancreatic cancer, pegylated NCPs showed superior potency and efficacy, compared with free drugs.

More importantly, several platinum-containing polymers were successfully used in chemotherapeutics. One example is AP5346 developed by Access Pharmaceuticals (Fig. 32).<sup>203</sup> Chemically, AP5346 is a polymer-linked diaminocyclohexyl platinum complex. Sood et al. reported the synthesis of AP5346. Generally, they started from the copolymerization of *N*-(2-hydroxypropyl)methacrylamide (HPMA) and MA-GG-ONp, followed by the conversion of -NO<sub>2</sub> group to amidomalonate and coordination with DACHPtCl<sub>2</sub>. They also reported an improved method to synthesize AP5346, which was more cost-effective and scalable. They also carried out the phase I and pharmacokinetic trial of AP5346.<sup>204</sup> Twenty-six patients were treated at seven dose levels from 40 mg Pt/m<sup>2</sup> to 1280 mg Pt/m<sup>2</sup> for 3 weeks. The pharmacokinetics of AP5346 indicated a prolonged half-life, and evidence of antitumor activity at the dose level of 640 mg Pt/m<sup>2</sup>. Now, AP5346 is in phase II clinical trial.

Another example is AP5280, also developed by Access Pharmaceuticals. Preliminary study showed that AP5280 showed an encouraging *in vitro* and *in vivo* activity against solid tumors.<sup>205</sup> In the phase I trial, the result showed that AP5280 can be administered safely as a 1-h i.v. infusion and produced prolonged plasma exposure, compared with any of free Pt-containing drugs.<sup>206</sup>

### 3.3 Photodynamic therapy (PDT) agents

Photodynamic therapy (PDT) is a promising light-activated treatment that is used clinically to destroy locally diseased tissues.<sup>207–209</sup> When exposed to light, a photosensitizer transfers its excitation energy to ground-state triplet oxygen and generates highly reactive singlet oxygen and other cytotoxic reactive oxygen species, inducing oxidative damage to cells that causes localized cell death and ultimately tissue apoptosis or necrosis (Fig. 33).<sup>210</sup> In comparison with other treatments such as chemotherapy, a major advantage of PDT is that, in the absence of light, the photosensitizer is biologically benign.

Zinc-porphyrin/phthalocyanine (Pc) complexes have been extensively studied for PDT and as imaging agents because of their optical properties and long triplet excited state lifetime. Sarantopoulou et al. used Zn-Pc-containing zero generation polyamidoamine (G0-PAMAM) as a sensitizer to treat symptomatic and asymptomatic human carotid tissues.<sup>211</sup> Compared to the deposition on atheromatous tissues with different aggregation features between G0 and G0/ZnPc nanoparticles, the deposition of nanodrug carriers on healthy tissues resulted in an inverse impact. The results indicated the importance of PAMAM dendrimer carriers as a novel and promising PDT platform for atherosclerosis therapies.

The Wong group reported the synthesis of a few amphiphilic Ru(II) and Zn(II) porphyrins using different linkers. In order to find out optimal linker properties in these Ru(II)-porphyrin conjugates, they investigated luminescence, subcellular localization, cellular uptake, and photo-cytotoxic and (dark) cytotoxic properties.<sup>212</sup> All conjugates had IC<sub>50</sub> values in the low micromolar range, which decreased by at least 10 times upon irradiation of cell cultures with visible light.<sup>213</sup>

Ruthenium porphyrin derivatives are also very important and widely studied due to their ability to produce reactive oxygen species that can be used in PDT of cancer (Fig. 34).<sup>214</sup> Therrien et al. prepared a series of ruthenium porphyrin complexes and tested their application as photosensitizing chemotherapeutic agents. Biological test and cellular uptake experiments demonstrated that the ruthenium complexes can facilitate uptake and result in highly active photosensitizing under a light irradiation dose of only 5 J/cm<sup>2</sup>. Meanwhile, the ruthenium porphyrin compounds accumulated in the cytoplasm and intracellular organelles different from the lysosomes and nuclei of human melanoma cells.<sup>215</sup> To obtain longer excited-state lifetime and achieve better PDT efficiency, halogenated tetraaryl porphyrins were used. For example, Swavey et al. synthesized a ruthenium-bipyridine fluorinated porphyrin, which can bind DNA very strongly according to the DNA titration with calf thymus (CT). When irradiated with a 60 W tungsten lamp, this complex preferentially led to apoptosis of the melanoma cells over the normal skin cells.<sup>216</sup>

Meanwhile, making use of the ability of Ir(III) complex to sensitize singlet oxygen formation (<sup>1</sup>O<sub>2</sub>), the Yang group achieved a three-in-one platform for optical imaging, T<sub>1</sub>-weighted magnetic resonance imaging (MRI), and PDT (Fig. 35).<sup>217</sup> The Ir-Gd coordination polymer nanoparticles (CPPs) showed good stability in simulated biological media and low cytotoxicity toward a model line of HeLa cancer cells. Due to co-presence of phosphorescent properties of the iridium complex and magnetic properties of the metallic Gd(III) ions, the Ir-Gd CPPs could be simultaneously used as an optical probe and MR contrast agent. Moreover, <sup>1</sup>O<sub>2</sub> was generated effectively upon irradiation with a visible light, which can be used for the PDT of cancer cells.

In combination with cisplatin and poly(ethylene glycol)-*b*-poly(*L*-aspartic acid) (PEG-PLA), the Jang group prepared polymer-metal complex micelles that can be used as both drug carrier and PDT agent (Fig. 36).<sup>218</sup> The polymer-metal complex micelles were formed by coordination interaction between cisplatin with ZnPc and PEG-PLA. These micelles were very stable in phosphate buffer solution (PBS) without NaCl, while it can slowly release cisplatin in a physiological PBS solution at 37 °C. Meanwhile, upon laser irradiation, these micelles can also generate singlet oxygen for PDT.

The zinc porphyrin complex can be also introduced to organosilica framework through condensation. Interestingly, the two-photon imaging capacity was preserved in the resultant nanoparticles.<sup>219</sup> These particles were nontoxic towards MCF-7 breast cancer cells, which allowed the uptake of these particles. Upon laser irradiation, it was clear that the nanoparticles were successfully endocytosed by cancer cells, as shown by two-photon fluorescence imaging (TPEF) at 750 and 800 nm.

However, most of the phthalocyanine complexes were hydrophobic and easily formed aggregates, which resulted in serious self-quenching. To solve this problem, the Kataoka group developed a zinc-phthalocyanine typed sensitizer by incorporation of dendrimer phthalocyanine (DPc) into polyion complex micelles.<sup>220</sup> Their results demonstrated that the micelles showed significant enhancement in *in vitro* photo-cytotoxicity for about 10 times (Fig. 37).

Meanwhile, the use of disulfide crosslinking in the micellar core can prevent unfavourable photochemical reactions with serum proteins without compromising photochemical reactions involving oxygen molecules, leading to remarkably enhanced PDT.<sup>221, 222</sup>

To avoid the use of UV-visible light in conventional PDT and increase the penetration in tissues, Heitz et al. reported a two-photon (TP) sensitizer, zinc diketopyrrolopyrrole-porphyrin conjugates, which could be excited under near infrared (NIR) light.<sup>223</sup> Their preliminary TP-PDT experiments on HeLa cells showed that 90% cells were killed after irradiation at 910 nm for 300 scans.

Besides the modification of exterior functional groups, different core structures were also studied for enhanced TP-PDT efficiency. For example, the Maillard group synthesized a series of conjugated zinc porphyrin oligomers by incorporation of various neutral  $\pi$ -conjugated cores, ethynyl, butadiyne, diethynylbenzene, and electron-donor triphenylamine (Fig. 38).<sup>224</sup> The singlet oxygen quantum yields of these porphyrin oligomers were around 45%-75%. In comparison with the lower TPA cross-section for the monomer (50 GM), these oligomers showed higher values above 1300 GM, which made these oligomers promising candidates for TP-PDT. Meanwhile, they also introduced  $\alpha$ -mannose units on each chromophore for targeting tumor cells with over-expressing lectin-type membrane receptors.

### 3.4 Radiotherapy

Radiotherapy is a medical treatment of diseases (especially cancer) with the exposure to a radioactive substance. Ionizing radiation can damage DNAs of cancerous tissues, leading to cellular death. Almost all the radionuclides used are early transition metal ions.

Due to its energetic  $\beta$  emission ( $E_{\max} = 2.28$  MeV) and moderate half-life time, Yttrium-90 (<sup>90</sup>Y) is a clinically acceptable  $\beta$ -emitting radionuclide. <sup>90</sup>Y-containing metallopolymer are widely used for imaging and radionuclide therapy. Hnatowich and coworkers used a DNA analogue, morpholinos (MORFs), labelled with either 1,4,7,10-tetraazacyclododecane-*N,N'*,*N''*,*N'''*-tetraacetic acid (DOTA) or mercaptoacetyltriglycine (MAG<sub>3</sub>) to form radionuclide metallopolymer with <sup>90</sup>Y for therapeutic applications. By comparing the *in vitro* stability and biodistribution in normal mice, it was found that <sup>90</sup>Y-labeled MORF showed increased instability relative to that of <sup>111</sup>In.<sup>225</sup> When radiolabelled with MAG<sub>3</sub>, <sup>188</sup>Re showed *in vitro* and *in vivo* instability compared to <sup>99m</sup>Tc, while all labels were still largely intact after 48 h in saline or serum.

Similarly, Hruby et al. used a thermoresponsive poly(*N*-isopropylacrylamide) conjugated with *L*-tyrosinamide or diethylenetriaminepentaacetic acid (DTPA) to chelate <sup>125</sup>I and <sup>90</sup>Y for local radiotherapy.<sup>226</sup> These polymers were readily soluble in water at room temperature,

which allowed facile isotope labelling and administration *via* injection, and they precipitated slightly below the body temperature so they should persist at the site of injection.

Polymeric microspheres prepared by a solvent evaporation technique are also widely used in radiotherapy. Basically, polymers are dissolved in a suitable volatile solvent and dispersed in a continuous medium using a stabilizing agent. Controlled evaporation of solvent results in the formation of solid microspheres. This method was used for the preparation of polylactic acid microspheres containing  $^{166}\text{Ho}$ ,  $^{90}\text{Y}$ ,  $^{186}\text{Re}$  as radioisotopes.<sup>227</sup> Radioactive  $^{166}\text{Ho}$ -loaded polylactic acid microspheres were prepared by Mumper et al.<sup>228</sup>  $^{166}\text{Ho}$ -acetylacetonate (HoAcAc) and polylactic acid were dissolved in chloroform, and the solution was added to polyvinyl alcohol solution. These microspheres were recently tested for the treatment of hepatic malignancies in rabbits.<sup>229</sup> Biodistribution and histological analysis confirmed that radioactive microspheres were heterogeneously distributed over the liver and accumulated preferentially in the tumor area. It was demonstrated that  $^{166}\text{Ho}$  polylactic acid microspheres were the promising system for liver tumor treatment.

In 1992, Mumper et al. investigated poly-*L*-lactic acid (PLA) microspheres containing neutron activated  $^{166}\text{Ho}$  as potential agents for radionuclide synovectomy.<sup>230</sup> *In vivo* retention studies were conducted by administering irradiated  $^{166}\text{Ho}$  polylactic acid microspheres into the joint space of normal rabbits (n ¼ 6). Biodistribution data for  $^{166}\text{Ho}$  was acquired by killing the rabbits at 44 h or 120 h after administration of polylactic acid microspheres. It appeared that the majority of  $^{166}\text{Ho}$  leaching occurred from the joint in the first 44 h after administration. However, no  $^{166}\text{Ho}$  activity was observed in the feces or lymph nodes after 120 h.

Because of its rapid data collection and low exposure of radiation to patient during a scanning procedure,  $^{99\text{m}}\text{Tc}$  is an ideal radioisotope for scintigraphic imaging. Cabral et al. reported a  $^{99\text{m}}\text{Tc}$ -based cancer imaging agent by treating PAMAM-G4-FITC dendrimer with a  $^{99\text{m}}\text{Tc}(\text{CO})_3$  complex. *In vivo* Biodistribution of  $^{99\text{m}}\text{Tc}(\text{CO})_3$ -dendrimer-FITC was carried out with C57BL/6 mice and melanoma-bearing mice.<sup>231</sup> For both cases, accumulation was observed in hepatic, renal and bladder. Scintigraphic imaging showed high uptake in liver and kidney for melanoma-bearing mice. Radiolabelling of dendrimer was stable for at least 24 h with a yield of approx. 90%.

Other technetium salts can be also used to prepare  $^{99\text{m}}\text{Tc}$ -containing polymers. For example, Veronese, Mazzi et al. reported a simple  $^{99\text{m}}\text{Tc}$ -labelling procedure through in-situ coordination between PN2S modified polyethylene glycol and  $^{99\text{m}}\text{TcO}_4^-$  (Fig. 39).<sup>232</sup> Such  $^{99\text{m}}\text{Tc}$ -containing amphiphilic polymers can self-assemble into micelles in aqueous solution, while  $[\text{}^{99\text{m}}\text{TcO}]^{3+}$  species was coordinated at the same time. Such prepared  $^{99\text{m}}\text{Tc}$ -containing polymers exhibited high stability both *in vitro* and *in vivo*.

Peñuelas et al. developed an oral administrated  $^{99\text{m}}\text{Tc}$ -based imaging agent by using poly(anhydride)-cyclodextrin (NP-CD) nanoparticles.<sup>233</sup> As proved by single photon emission computed tomography (SPECT), when orally administered, NP-CD remained in the gut with no evidence of translocation or distribution to other organs of the body of animals. In addition, CD-NP moved more slowly inside the gut than conventional NP,

probably due to their physicochemical structure that allowed stronger interactions with the gut mucosa.

Blood pool imaging is also assisted with  $^{99m}\text{Tc}$ -labeled synthetic polymers, which could be helpful for cardiovascular imaging, capillary leak imaging, and gastrointestinal bleeding studies. Weisslede et al. used a DTPA-terminated poly-*L*-lysine labelled with  $^{99m}\text{Tc}$  for phase I clinical trial with human (Fig. 40).<sup>234</sup> Laboratory values, ECG findings, and hemodynamic parameters were not observed significant abnormalities.

Conjugation of mannose molecules to  $^{99m}\text{Tc}$ -labeled macromolecules like polylysine, albumin, dextrans, and gold nanoparticles led to compounds that could be trapped in the sentinel node with minimal spread to non-target organs. The most promising compound was the mannosylated  $^{99m}\text{Tc}$ -DTPA-dextran ( $^{99m}\text{Tc}$ -Tilmanocept) reported by Vera et al., which was recently approved by FDA for sentinel lymph node detection (SLND) in melanoma and breast cancer. Santos et al. reported a multifunctional imaging agent for sentinel lymph node based on the modification of dextran with radionuclide ( $^{99m}\text{Tc}$  or  $^{68}\text{Ga}$ ) and a near-infrared (NIR) reporter (Fig. 41).<sup>235</sup> The probes allowed a clear visualization of the popliteal node by SPECT or positron emission tomography (PET), as well as real-time optically guided excision. Such multifunctional nanoplatforms displayed a popliteal extraction efficiency >90%, highlighting their potential to be further explored as dual imaging agents.

Polyamidoamine (PAMAM) dendrimer (G5-Ac), partially acetylated G5, was reacted with biotin and 2-(p-isothiocyanatobenzyl)-6-methyl-diethylenetriaminepentaacetic acid (1B4M-DTPA) to produce a complex Bt-G5-Ac-1B4M, followed by subsequent conjugation with avidin, yielding a conjugate Av-G5-Ac-1B4M.  $^{99m}\text{Tc}$  was then used as the radiolabel to both conjugates. An *in vitro* study showed that Av-G5-Ac-1B4M- $^{99m}\text{Tc}$  had much higher cellular uptake in HeLa cells than Bt-G5-Ac-1B4M- $^{99m}\text{Tc}$ . In addition, biodistribution and micro-SPECT imaging was observed only for the former.<sup>236</sup>

*N*-(2-hydroxypropyl) methacrylamide (HPMA) copolymers carrying doubly cyclized Arg-Gly-Asp motifs (HPMA copolymer-RGD4C conjugate) were also used to form water soluble complex with  $^{99m}\text{Tc}$ .<sup>237</sup> According to the scintigraphic images of prostate tumor-bearing SCID mice obtained 24 h post-i.v. injection, there was greater tumor localization of HPMA copolymer-RGD4C conjugate than the control, HPMA copolymer-RGE4C conjugate. More importantly, HPMA copolymer-RGD4C conjugates sustained tumor retention over 72 h with reasonably efficient clearance from the background organs. These results suggested that specific tumor angiogenesis targeting was possible with HPMA copolymer-RGD4C conjugates.

Besides synthetic polymers, DNA analogue morpholinos (MORFs) were used to label with  $^{99m}\text{Tc}$ . It was found that the stability of  $^{99m}\text{Tc}$ -MORF was greater than 85% over 24 h in 37°C serum with minimal protein binding.<sup>238</sup>

Several other reports indicated different ways of preparing and binding *N,S*-containing bifunctional chelators to peptides involving amide coupling between the peptide molecule and metal complexes/ligands.<sup>239</sup>

$^{188}\text{Re}$  (Rhenium) is another easily obtained and frequently used radionuclide. Different polymers were used to load  $^{188}\text{Re}$  for radionuclide therapy. For example, Kim et al. studied the anti-tumor activity of  $^{188}\text{Re}$  labelled transferrin-polyethylenimine (Tf-PEI) conjugate through intratumoral injection.<sup>240</sup> Typically, they used the branched cationic PEI as a platform and Tf for site-specific drug delivery. When treating the Ramos lymphoma (human Burkitt's lymphoma) xenografted tumors, this  $^{188}\text{Re}$ -containing polymer showed increased retention time inside the tumor and caused extensive tumor necrosis.

### 3.5 Biocide

Metallopolymers, prepared from group IVB metallocene dichlorides and plant growth hormone gibberellic acid (GA3 or GA),<sup>241</sup> were used to help the restoration of Everglades and to improve the germination of seeds including seeds producing food. Generally, GA3 has three reactive sites, two alcohol groups and one acid functional group. The products were crosslinked, and a representative structure is given in Fig. 42. It was found that ppm amounts of both polymers and GA3 could decrease the germination time and increase the germination rate of sawgrass, which was one of the essential features in the Everglades. While in the case of cattail seeds, the germination rate decreased with longer germination time.<sup>242</sup> Carraher et al. also found that the Group IVB-GA3 containing polymer can increase the germination of (Jagger) wheat seed to 2–3 times and (Little Marvel) peas to 8 times.<sup>243</sup>

They also found potential applications on the leaf formation for metallopolymers prepared from indole-3-butyric acid (auxins, IBA for short) and titanocene dichloride. Compared with IBA, this metallopolymer showed enhanced leaf formation and greater proportion of roots in rooting experiments using *Albo Lacinatus*.<sup>244, 245</sup>

## 4. Metal-containing polymers as biosensors

Another biomedical application for ferrocene-containing polymers lies in the field of biosensors.<sup>246, 247</sup> Due to the fully reversible redox process of ferrocene, ferrocene-containing polymers are widely used as redox-active mediators. In this case both the ferrocene-containing polymers and their hybrids with different functional materials are used. For example, Gao et al. cross-linked a ferrocene-containing polymer with glucose oxidase as an efficient glucose sensor using poly(ethylene glycol) diglycidyl ether and bovine serum albumin (BSA).<sup>248</sup>

The Xiao group explored biosensing properties of a series of ferrocene-containing highly branched polyurethane. They found that the supramolecular recognition between the hyper-branched polymer and glucose or ATP anion (adenosine-5' triphosphate,  $\text{ATP}^{2-}$ ) changed the electron transfer during the redox process of ferrocene, making it a promising candidate for biosensing.<sup>249, 250</sup> To avoid the leeching of the mediator from the electrode and to get better sensitivity and linearity, Singh et al. designed a copolymer through the direct electrochemical polymerization of pyrrole and ferrocenecarboxylate modified pyrrole on indium-tin-oxide (ITO) substrate. By incorporating glucose oxidase into the copolymer film, this film showed fast detection of glucose within 3 s and with linearity up to 16.8 mM.<sup>251</sup>

Besides glucose sensing, different sensors can be constructed by incorporating corresponding enzymes into a polymeric framework of ferrocene. For example, Erden et al. reported a uric acid biosensor based on ferrocene-containing poly(vinylferrocene), carboxylated multiwalled carbon nanotubes and gelatin modified electrodes. The Uricase enzyme was immobilized covalently through *N*-ethyl-*N'*-(3-dimethylaminopropyl) carbodiimide (EDC) and *N*-hydroxyl succinimide (NHS) chemistry. Under optimal conditions this system showed detection limit as low as  $2.3 \times 10^{-8}$  M and a dynamic linear range of uric acid from  $2.0 \times 10^{-7}$  M to  $7.1 \times 10^{-4}$  M. By determining the uric acid in human serum they also demonstrated that this uric acid biosensor showed good selectivity and sensitivity.<sup>252</sup> By combining Pt nanoparticles and hyperbranched ferrocene-containing polymers, Armada et al. developed a dihydronicotinamide adenine dinucleotide (NADH) sensor. The detection limit for NADH was as low as  $4.78 \mu\text{M}$ .<sup>253</sup> Based on this result, they developed a novel amperometric alcohol biosensor by using alcohol dehydrogenase (ADH). The devices showed more affinity for methanol than for ethanol with a wide linear range to 30 mM and sensitivities of 0.957 and  $0.756 \mu\text{AmM}^{-1}\text{cm}^{-2}$ .

As shown in Fig. 43, Liu et al. developed a label-free immunosensing strategy for detection of tumor necrosis factor-alpha antigen (TNF- $\alpha$ ) *via* surface-initiated atom transfer radical polymerization (SI-ATRP) of ferrocenylmethyl methacrylate (FMMA) and glycidyl methacrylate (GMA), and TNF- $\alpha$  antibody on a gold substrate.<sup>254</sup> Due to the redox property of ferrocene as an electron-transfer mediator, this design provided a platform for sensitive detection of TNF- $\alpha$  with a low detection limit of  $3.9 \text{ pg/mL}$ .

Leech et al. prepared osmium (Os)-containing polymers with osmium complexes attached *via* a "covalent binding approach". Reversible redox property was observed for these polymers (Fig. 44), which were further evaluated as mediators in biosensors and biofuel cells.<sup>255</sup> They integrated these polymers with glucose oxidase and multiwalled carbon nanotube together. The electrode displayed current densities of glucose oxidation as high as  $560 \mu\text{Acm}^{-2}$  for PBS containing 100 mM glucose at 0.45 V vs. Ag/AgCl.

Antiochia et al. developed a rapid amperometric biosensor for fructose in food analysis based on the osmium-polymer hydrogel (Fig. 44).<sup>256</sup> By immobilising fructose dehydrogenase (FDH) and the Os-containing hydrogel into carbon nanotube paste electrode, the electrode showed a detection limit for fructose of  $1 \mu\text{M}$  and a large linear range between 0.1 and 5 mM. More importantly, 80% of its initial sensitivity was maintained even after 4 months.

Gao et al. reported a glucose biosensor using ruthenium-containing polymer-mediated enzymatic oxidation of glucose (Fig. 45).<sup>257</sup> Ruthenium-containing polymer and glucose oxidase were co-assembled on a glassy carbon electrode by crosslinking with glutaraldehyde. This electrode displayed excellent catalytic activity toward the oxidation of glucose with a sensitivity of  $24.3 \mu\text{AmM}^{-1}\text{cm}^{-2}$  and linearity up to 10 mM. Due to the relatively low operating potential of  $-0.15$  V (vs. Ag/AgCl), the interferences in blood were effectively alleviated.



## 5. Metal-containing polymers in bioimaging

Another promising application for metal-containing polymers is bioimaging, which can be divided into fluorescence imaging and magnetic resonance imaging (MRI), according to different metals that are used. Due to the highly luminescence efficiency and paramagnetic property, most of the metals used in this area are Ir, Pt, Ga, In, Mn, and Gd.

### 5.1 Fluorescence imaging

Different from organic dyes and chromophores with poor solubility in water and easy photobleaching, metal-containing polymers are promising fluorescence imaging agents because of their excellent water solubility and stable luminescence. Due to their high photoluminescence efficiency, Iridium(III) complexes and polymers are regarded as one of the most excellent phosphorescent materials and widely used in bio-imaging.<sup>258–261</sup> Li and coworkers prepared Ir-containing polymers that exhibited bioimaging properties (Fig. 46). They integrated an Ir(III) complex into thermoresponsive PNIPAM. The change of phosphorescence was due to the interaction between  $\beta$ - or  $\gamma$ -aminothiol group and the aldehyde group in the Ir(III) complex. Thus it would be used as a sensor for cysteine (Cys)/homocysteine (Hcy).<sup>262</sup> By crosslinking Ir(III)-containing polymers, they also synthesized a quasi-solid sensing system. Living-cell imaging confirmed that the bioprobe was membrane permeable and capable of detecting Cys in living cells.

By embedding the fluorophore Ir(III) complex and photochrome diarylethene derivatives into polyacrylamide nanoparticles, Yang et al. successfully prepared a photo-switchable luminescent probe for bioimaging applications.<sup>263</sup>

The excellent phosphorescence property of Ir(III) complexes can be also integrated with other imaging system, such as MRI will be described in detail in section 5.2), to achieve multiple imaging. Yang and coworkers prepared magneto-phosphorescent d-fCPPs by using Ir(III) and Gd(III) ions as metallic nodes.<sup>264</sup> These water soluble CPPs showed intense red phosphorescence, moderate longitudinal relaxivity ( $r_1$ ) and low cytotoxicity.

Excellent bioimaging agents for hypoxia were reported with Pt-containing polymers. Huang, Li and coworkers synthesized a platinum(II) porphyrin and fluorine-based conjugated polymer that was used as a fluorescent/phosphorescent dual-emissive system (Fig. 47).<sup>265</sup> This polymer self-assembled into ultrasmall conjugated polymer dots in PBS solution. This system displayed excellent luminescence response to  $O_2$  content because of the presence of  $O_2$ -sensitive groups. *In vivo* oxygen sensing experiments were carried out by luminescence imaging of tumor hypoxia in nude mice.

The utilization of metal-containing complexes in group IIIA as catalysts, solar cells, and biomedicines has been broadly investigated.<sup>266–268</sup> However, incorporation of these metals into polymers has received less attention due to the difficulties in chemistry. Recently, Nichols and coworkers found that isotope of gallium,  $^{68}\text{Ga}$  radionuclide, could be used for bioimaging.<sup>269</sup> Dextran polymers were first modified with DTPA and tetrazine groups.  $^{68}\text{Ga}$  was then incorporated into polymers through chelation with DTPA groups. The tetrazine had excellent ability to react with trans-cyclooctene antibodies (Fig. 48) *via* Diels-alder

reactions. Through such interaction,  $^{68}\text{Ga}$  could be located on tumor cells as advanced probes for cancer cells.

Using a similar technique, Rajesh and coworkers reported  $^{111}\text{In}$ -containing polymers for bioimaging *in vivo*.<sup>270</sup> The  $^{111}\text{In}$  was chelated with polyethylene glycol-*b*-polyphosphoramidate (PEG-*b*-PPA) by DTPA. The labelled polymers were able to bind with DNA to form hybrid nanoparticles as vehicles. Quantitative imaging analysis was achieved, and *in vivo* trafficking kinetics for PEG-*b*-PPA/DNA nanoparticles was revealed *via* this technique.

## 5.2 Magnetic resonance imaging (MRI)

Due to the noninvasive nature, minimal radiation, and the ability for real-time 3D imaging, MRI has received wide attention in fundamental research and clinical diagnosis.<sup>271</sup> Generally, the MRI signal is dictated by the longitudinal ( $T_1$ ) and transverse ( $T_2$ ) relaxation times of hydrogen nuclei, which are abundant in various tissues. Different magnetic materials are used, especially Gd and Mn, to accelerate the relaxation of protons and enhance the MRI signal. Manganese compounds show interesting magnetic properties, which can be used as potential MRI agents. Pan et al. prepared polymer micelles by co-self-assembly of an amphiphilic diblock copolymer polystyrene-*b*-poly(acrylic acid) (PS<sub>8</sub>-*b*-PAA<sub>400</sub>) with a polyoxyethylene sorbitan monooleate, in which the acidic carboxylate groups can be used to load single molecule magnets Mn<sub>12</sub>-acetate  $[[\text{Mn}^{\text{III/IV}}_{12}\text{O}_{12}(\text{CH}_3\text{CO}_2)_{16}(\text{H}_2\text{O})_4]$  (Fig. 49).<sup>272</sup> *In vitro* MRI studies revealed that these particles offered higher  $T_1$  relaxivity in comparison to bare Mn<sub>12</sub>-acetate. Preliminary *in vivo* study with a rat model using intravenous (IV) dose showed that this system was promising for biological imaging in living subjects.

Paramagnetic metals chelate Gd(III)-DTPA, Gd(III)-DOTA, and their derivatives have been found to increase the relaxation rate of surrounding water protons, and thus are used as contrast agents for MRI.<sup>273</sup> However, these agents cannot effectively discriminate diseased tissues from normal tissues due to their low molecular weight. Macromolecular Gd(III) complexes could be developed to enhance image contrast enhancement by conjugating Gd(III) chelates to biopolymers, including poly(amino acids), polysaccharides, dendrimers, proteins, etc.

The Lu group carried out systematic research on the Gd-based MRI agents. They prepared a polymer-Gd(III) chelate conjugate that contained a degradable disulfide spacer to facilitate the excretion of Gd complexes.<sup>274</sup> They chose anionic poly(*L*-glutamic acid) (PGA) and cystamine as a macromolecular carrier for Gd(III) chelates and a cleavable spacer respectively (Fig. 50). Because of the reaction between cystamine and cysteine, an endogenous plasma thiol, the Gd(III) DOTA chelate derivative was readily released from the polymer conjugate. Significant MRI blood pool contrast enhancement was produced in nude mice with OVCAR-3 human ovarian carcinoma xenographs. The pharmacokinetic MRI results indicated that the complex was released by the endogenous thiols and excreted through renal filtration, as the Gd(III) complex mainly accumulated in the urinary bladder.

To further optimize the physicochemical and pharmacokinetic properties of Gd-containing polymers, the Lu group further introduced the nontoxic, nonantigenic and biocompatible poly(ethylene glycol).<sup>275</sup> Their results indicated that enhancement in the heart and blood vessels MRI were achieved by using the Gd-containing polymer as compared to a low molecular weight control agent, Gd-(DTPA-BMA).

Besides the side-chain strategy, Lu et al. also reported main-chain biodegradable polydisulfide-based macromolecular Gd(III) complexes, which showed improvement in both *in vivo* retention time and MRI contrast enhancement.<sup>276</sup> However, the molecular weight of this main-chain polymer was not high enough. They prepared Gd-containing poly(*L*-glutamic acid) with different molecular weight. As shown in Fig. 51, the conjugate with molecular weight 28 kDa rapidly cleared from the circulation and had a relatively lower tumor accumulation. The conjugates with higher molecular weight showed a more prolonged blood circulation and higher tumor accumulation.<sup>271</sup> Similar results were obtained by using dendrimers with different generations.<sup>277</sup>

Using dynamic contrast-enhanced MRI (DCE-MRI), Lu et al. discovered that a biodegradable polydisulfide-based Gd(III)-containing polymer was assessed the antiangiogenic efficacy of Avastin in the animal tumor model, which was based on vascular parameters in tumor periphery.<sup>278</sup> By introducing targeting groups or photo sensitizer molecules, they also achieved detection of angiogenesis biomarker  $\alpha_v\beta_3$  integrin<sup>4</sup> and MRI-guided PDT for site-specific cancer treatment<sup>279</sup>.

Similarly, Li et al. prepared a series of biocompatible MRI contrast agents by using poly(*L*-glutamic acid) as a substrate. The resulting copolymers can form spherical micelles in aqueous solution at pH 7.4, where the size of micelles can be tuned by pH. DTPA-Gd chelated to the shell layer of micelles exhibited significantly higher spin-lattice relaxivity ( $r_1$ ) than a small-molecular-weight MRI contrast agent, indicating that water molecules could readily access the Gd ions in the micelles.<sup>280, 281</sup>

To achieve specific targeting, Na et al. developed a cancer-recognizable MRI contrast agent (CR-CAs) by using amphiphilic block copolymers, which consisted of methoxy poly(ethylene glycol)-*b*-poly(*L*-histidine) (PEG-*p*(*L*-His)) and methoxy poly(ethylene glycol)-*b*-poly(*L*-lactic acid)-diethylenetriaminopentaacetic acid dianhydride-gadolinium chelate (PEG-*p*(*L*-LA)-DTPA-Gd).<sup>282</sup> Under the physiological pH (pH = 7.4), the CR-CAs self-assembled into spherical micelles with a size of ca. 40 nm. However, the CR-CAs were disassembled in an acidic tumoral environment (pH 6.5), because of the protonation of *p*(*L*-His) blocks, leading to positively charged water-soluble polymers. In the tumor region the CR-CAs exhibited highly effective  $T_1$  MR contrast enhancement.

Besides linear polymers, dendrimers have been widely used as substrates for MRI.<sup>283, 284</sup> Much of the early work using dendrimers as contrast agents focused on PAMAM, as investigated by Wiener et al.<sup>285</sup> G2 and G6 PAMAM dendrimers were conjugated with DTPA to create polymers with 11 and 170 surface DTPA groups, respectively. *In vivo* analysis showed that these dendrimers increased half-life from 24 min for Gd(III)DTPA to 40 and 200 min for the G2 and G6 analogues, respectively. Bryant et al. studied the

relationship between  $r_1$  and generation numbers of PAMAM–DOTA scaffolds and determined that  $r_1$  increased up to G7, but then plateaued, which was ascribed to slow water exchange.<sup>286</sup> To further increase the size of the dendrimer, Tsourkas et al. synthesized dendrimer nanoclusters (DNCs) through crosslinking fifth generation PAMAM dendrimers with NHS-PEG-NHS.<sup>287</sup> The size of the DNCs was ca. 75–150 nm. As a result, the relaxivity per DNC was as high as ca.  $3.6 \times 10^6 \text{ mM}^{-1}\text{s}^{-1}$ .

Raymond et al. developed hydroxypyridonate (HOPO)-based chelates, such as the heterotripodal Gd-TREN-bisHOPO-TAM-Me, which showed promise due to the high relaxivity while maintaining high stability and selectivity, regardless of functionalization on the TAM moiety.<sup>288</sup> As shown in Fig. 52, they further conjugated amine-functionalized TREN-bis(1,2-HOPO)-TAM-ethylamine and TREN-bis-(1-Me-3,2-HOPO)-TAM-ethylamine ligands with biocompatible esteramide(EA)- and poly-*L*-lysine (PLL)-based dendrimers, which are capable of binding up to eight gadolinium complexes. These conjugates had  $T_1$  relaxivity of up to  $38.14 \pm 0.02 \text{ mM}^{-1}\text{s}^{-1}$  per gadolinium at 37 °C, corresponding to relaxivity of up to  $228 \text{ mM}^{-1}\text{s}^{-1}$  per dendrimer molecule.<sup>289, 290</sup>

Interestingly, it was found that ligands also play an important role in the water exchange rate. Merbach et al. conjugated G5-G9 PAMAM with ethylenepropylenetriamine pentaacetic acid (EPTPA), it was observed that relaxivity increased from G5 to G7. However, this trend was reversed for the G9 structure.<sup>291</sup> It was found that the higher relaxivity came from the induced scaffold rigidity due to the protonation of the tertiary amines of PAMAM. The effect of scaffold rigidity on relaxivity enhancement was also studied by other groups.<sup>292–294</sup> For example, Kobayashi et al. synthesized a series of dendrimer-based MRI agents with rigid linkers, from which they achieved a relaxivity of  $29 \text{ mM}^{-1}\text{s}^{-1}$  for G5 analogue. Meanwhile Meijer et al. found a reduction of relaxivity by using a flexible linker.<sup>294</sup>

MRI can be also coupled with other imaging tools, or even a drug delivery vehicle, to obtain multi-modal imaging and targeted chemotherapy and diagnosis. As shown in Fig. 53, Chang et al. fabricated a multifunctional platform for simultaneous MRI and targeted therapeutics.<sup>295</sup> This platform was self-assembled from a hydrophobic poly(*D,L*-lactide-coglycolide)(PLGA) core and a hydrophilic paramagnetic-folate-coated PEGylated lipid shell. In such system, the Gd-containing shell served as MRI agent due to its higher spin-lattice relaxivity, while the PLGA core can be used to load and release hydrophobic anticancer drug.

Ghandehari et al. used *N*-(2-hydroxypropyl)methacrylamide (HPMA) as a platform to load both MRI agent and anticancer drug through covalent bonds. Coupled with low toxicity, high stability and relaxivity, these conjugates showed the potential for monitoring the *in vivo* fate of HPMA-based drug delivery systems by MRI techniques.<sup>296</sup> Liu et al. constructed functional unimolecular micelles,<sup>260</sup> which were prepared from a G4 hyperbranched polyester by ring-opening polymerization of 3-caprolactone, ATRP of oligo(ethylene glycol) monomethyl ether methacrylate and 3-azidopropyl methacrylate (AzPMA), and subsequent click reaction with alkynyl-functionalized cancer cell-targeting moieties, alkynyl-folate, and  $T_1$ -type MRI contrast agents. These micelles were capable of encapsulating paclitaxel with a loading content of 6.67 w/w%. These micelles exhibited controlled release of up to 80%

drug over a time period of ca. 120 h. *In vitro* MRI experiments demonstrated considerably enhanced  $T_1$  relaxivity ( $18.14 \text{ mM}^{-1}\text{s}^{-1}$ ) for unimolecular micelles compared to  $3.12 \text{ mM}^{-1}\text{s}^{-1}$  for that of the small molecule counterpart, alkynyl-DOTA-Gd. *In vivo* MR imaging in rats revealed prominent positive contrast enhancement, good accumulation of unimolecular micelles within rat liver and kidney, and relatively long duration of blood circulation.

Woods et al. reported a Eu-containing polycationic polymer as an MRI contrast agent. Due to its quantitative binding to DNA, this polymer was used as a reporter for gene therapy (Fig. 54).<sup>297</sup> Significantly, the MR contrast signal from the agent itself diminished as a result of this binding event. This polymer could provide a platform for imaging and gene delivery into cells and tissues, enabling the monitoring of gene delivery in real time.

For imaging the delivery of therapeutic nucleic acids at different biological scales, Reineke et al. developed polymer beacons based on the oligoethyleneamines (Fig. 55), which can bind and compact nucleic acids into nanoparticles, and coordinate with lanthanide (Ln) ions (both luminescent europium ( $\text{Eu}^{3+}$ ) and paramagnetic gadolinium ( $\text{Gd}^{3+}$ )).<sup>298</sup> The Ln-containing polymers allowed the visualization of the delivery vehicle *via* microscopy and MRI at different scales.

Recently, Tsien et al. developed a dendrimer-based chelating agent with both a contrast agent and a fluorescent probe.<sup>299, 300</sup> They conjugated a G5 PAMAM dendrimer with activatable cell penetrating peptides (ACPPs) masked by PEG. The PEG chain can be cleaved from the ACPPs by proteases, and the cell penetrating peptides can then adhere to and be taken up by surrounding cells. Because the proteases MMP-2 and MMP-9 were associated with tumor growth and metastasis, the conjugates afforded tumor-specific target. Then the conjugates were further labeled with Cy5 fluorescing agent and DOTA, which could be used to load Gd(III). When administered *via* tail-vein injections into mice with HT-1080 tumors 48 h prior to scanning, it was observed that the ACPP-dendrimer constructs increased  $r_1$  and signal intensity by 32% and 21%, respectively. Meanwhile, for HT-1080 tumors injected intramuscularly, it was observed that following ACPP-dendrimer administration, the Cy5 ligand showed brightest fluorescence at the tumor edges. As a result, these constructs had potential for aiding in the complete surgical removal of tumor tissues.

## 5. Conclusions and perspectives

Metals, with various unique functionalities, have the ability to bring new and powerful tools into polymer science. Nowadays metal-containing polymers are becoming increasingly important in the areas of interdisciplinary research. This review majorly focuses on biomedical applications. Metal-containing polymers have been successfully and broadly applied as advanced biomaterials in drug delivery, new drugs, radiotherapy, biosensors and bioimaging.

Metals and their derivatives are validly proved as effective drugs for various diseases and bacteria. Starting the 20<sup>th</sup> century, metals have been gradually incorporated into polymers, leading to metal-polymer conjugates or metallopolymers, which have been investigated as

new biomedical materials with many advantages over traditional polymers. Various drug delivery materials based on metallopolymers have been successfully designed and evaluated in *in vivo* and *in vitro* studies. These new metallopolymer-based drug delivery systems are usually 'smart', with remarkable response toward different stimuli, including thermal, light, oxidation/reduction and pH. Such characters are introduced by metals in the polymers, significantly distinct from regular organic polymers. Metallopolymers have been identified as effective antimicrobial agents for various strains of bacteria, including drug-resistant ones. Metallopolymers can be also utilized as anticancer drugs against different tumors with low toxicity towards mammalian cells. Furthermore, the unique redox properties of metal-containing complexes make metallopolymers as biosensors, such as glucose sensors and food analytical tools. Magnetic response and radioactivity of metal elements in metallopolymers have been utilized to establish new radiotherapies for various cancers and to construct magnetic imaging devices. Although not covered in this review, metallopolymers with dynamic bonds could serve as responsive materials for many biomedical applications.<sup>21–23</sup>

Though a flourishing future of metal-containing polymers in the biomedical field could be envisioned, there are several major obstructions that limit the development of metallopolymers as biomaterials. Firstly, the limited variation of metals has slowed down the discovery of new biomaterials containing metals. Among all metal elements, only about 30 of them have been reported as metal-containing biopolymers. Most of them are from VIII, IB and VA group elements. There are great opportunities to discover powerful tools to overcome biological issues. Secondly, the difficulties in the synthesis of metallopolymers hinder the versatility of metallopolymers. Currently, most of the metallopolymers for biomedical applications are based on coordination polymers, which usually lack the precise control over polymer architectures, molecular weight and molecular weight distribution. Radical and ionic polymerizations are typical controlled techniques for polymers with controlled properties. However, the synthesis of metallopolymers *via* controlled radical or ionic polymerizations are far less investigated. Metals in polymerization systems remarkably increase the complexity of polymerization processes. Thirdly, the toxicity of metals severely limits the applications of metal-containing materials in human bodies. Some of metals have been well known for their toxicities in the biological systems. How to avoid toxic metals in the environment is a critical challenge lying in the construction of metal-containing biomaterials.

## Acknowledgments

The support from National Institute of Health (1R01AI120987 to C.T.) and National Science Foundation (CHE-1151479 to C.T.) is acknowledged. Yi Yan thanks the funding support from "the Fundamental Research Funds for the Central Universities" (3102015QD0024 and 3102015BJ(IIMYZ27) and Open Project of State Key Laboratory of Supramolecular Structure and Materials (sklssm201625).

## Notes and references

1. Whittell GR, Hager MD, Schubert US, Manners I. *Nat Mater*. 2011; 10:176–188. [PubMed: 21336298]
2. Whittell GR, Manners I. *Adv Mater*. 2007; 19:3439–3468.

3. Qian JS, Zhang M, Manners I, Winnik MA. *Trends Biotechnol.* 2010; 28:84–92. [PubMed: 19962775]
4. Ke T, Jeong EK, Wang X, Feng Y, Parker DL, Lu ZR. *Int J Nanomed.* 2007; 2:191.
5. Bellas V, Rehahn M. *Angew Chem Int Ed.* 2007; 46:5082–5104.
6. Rehahn M. *Acta Polym.* 1998; 49:201–224.
7. Burnworth M, Knapton D, Rowan SJ, Weder C. *J Inorg Organomet Polym Mater.* 2007; 17:91–103.
8. Weder C. *J Inorg Organomet Polym Mater.* 2006; 16:101–113.
9. Dutton JL, Ragogna PJ. *Coord Chem Rev.* 2011; 255:1414–1425.
10. Jäkle F. *Chem Rev.* 2010; 110:3985–4022. [PubMed: 20536123]
11. Resendes R, Nelson JM, Fischer A, Jäkle F, Bartole A, Lough AJ, Manners I. *J Am Chem Soc.* 2001; 123:2116–2126. [PubMed: 11456856]
12. Grubbs RB. *Polym Rev.* 2007; 47:197–215.
13. Kulbaba K, Manners I. *Macromol Rapid Commun.* 2001; 22:711–724.
14. Wong WY, Ho CL. *Coord Chem Rev.* 2006; 250:2627–2690.
15. Schacher FH, Rupar PA, Manners I. *Angew Chem Int Ed.* 2012; 51:7898–7921.
16. Abd-El-Aziz AS. *Macromol Rapid Commun.* 2002; 23:995–1031.
17. Heilmann JB, Scheibitz M, Qin Y, Sundararaman A, Jäkle F, Kretz T, Bolte M, Lerner HW, Holthausen MC, Wagner M. *Angew Chem Int Ed.* 2006; 45:920–925.
18. Wang L, Chen YP, Miller KP, Cash BM, Jones S, Glenn S, Benicewicz BC, Decho AW. *Chem Commun.* 2014; 50:12030–12033.
19. Wang L, Cole M, Li J, Zheng Y, Chen YP, Miller KP, Decho AW, Benicewicz BC. *Polym Chem.* 2015; 6:248–255.
20. Li Y, Krentz TM, Wang L, Benicewicz BC, Schadler LS. *ACS Appl Mater Inter.* 2014; 6:6005–6021.
21. Wojtecki RJ, Meador MA, Rowan SJ. *Nat Mater.* 2011; 10:14–27. [PubMed: 21157495]
22. Burnworth M, Tang LM, Kumpfer JR, Duncan AJ, Beyer FL, Fiore GL, Rowan SJ, Weder C. *Nature.* 2011; 472:334–U230. [PubMed: 21512571]
23. Shanmuganathan K, Capadona JR, Rowan SJ, Weder C. *Prog Polym Sci.* 2010; 35:212–222.
24. Sui XF, Feng XL, Hempenius MA, Vancso GJ. *J Mater Chem B.* 2013; 1:1658–1672.
25. Grubbs RB. *Nat Mater.* 2007; 6:553–555. [PubMed: 17667978]
26. Massey J, Power KN, Manners I, Winnik MA. *J Am Chem Soc.* 1998; 120:9533–9540.
27. Chan WK. *Coord Chem Rev.* 2007; 251:2104–2118.
28. Abd-El-Aziz AS, Todd EK. *Coord Chem Rev.* 2003; 246:3–52.
29. Happ B, Winter A, Hager MD, Schubert US. *Chem Soc Rev.* 2012; 41:2222–2255. [PubMed: 22080248]
30. Wang XS, McHale R. *Macromol Rapid Commun.* 2010; 31:331–350. [PubMed: 21590911]
31. Pittman CU. *J Inorg Organomet Polym Mater.* 2005; 15:33–55.
32. Astruc D. *Acc Chem Res.* 1997; 30:383–391.
33. Chadha P, Ragogna PJ. *Chem Commun.* 2011; 47:5301–5303.
34. Hudson ZM, Qian JS, Boott CE, Winnik MA, Manners I. *ACS Macro Lett.* 2015; 4:187–191.
35. Cohen SM. *Curr Opin Chem Biol.* 2007; 11:115–120. [PubMed: 17276132]
36. Neuse EW. *Macromol Symp.* 1994; 80:111–128.
37. Callari M, Aldrich-Wright JR, de Souza PL, Stenzel MH. *Prog Polym Sci.* 2014; 39:1614–1643.
38. Wang Z, Niu G, Chen XY. *Pharm Res.* 2014; 31:1358–1376. [PubMed: 23765400]
39. Pomogailo, AD.; Kestel'man, VN. *Metallopolymer Nanocomposites.* Springer Science & Business Media; 2006.
40. Gielen, M.; Tiekink, ER. *Metallotherapeutic Drugs and Metal-Based Diagnostic Agents: The Use of Metals In Medicine.* John Wiley & Sons; 2005.
41. Durant, JR. *Cisplatin: A Clinical Overview.* Academic Press; New York: 1980.
42. Rosenberg B, Van Camp L, Krigas T. *Nature.* 1965; 205:698–699. [PubMed: 14287410]

43. Hartinger CG, Dyson PJ. *Chem Soc Rev.* 2009; 38:391–401. [PubMed: 19169456]
44. Martins P, Marques M, Coito L, Pombeiro AJL, Viana Baptista P, Fernandes AR. *Anti-Cancer Agent Med.* 2014; 14:1199–1212.
45. Ringsdorf H. *J Polym Sci: Polym Symp.* 1975; 51:135–153.
46. Jaouen, G.; Metzler-Nolte, N. *Medicinal Organometallic Chemistry.* Springer; 2010.
47. Gasser G, Ott I, Metzler-Nolte N. *J Med Chem.* 2010; 54:3–25. [PubMed: 21077686]
48. Miller KP, Wang L, Benicewicz BC, Decho AW. *Chem Soc Rev.* 2015; 44:7787–7807. [PubMed: 26190826]
49. Miller KP, Wang L, Chen Y-P, Pellechia PJ, Benicewicz BC, Decho AW. *Front Microbiology.* 2015; 6
50. Hardy CG, Zhang J, Yan Y, Ren L, Tang C. *Prog Polym Sci.* 2014; 39:1742–1796.
51. Lanigan N, Wang XS. *Chem Commun.* 2013; 49:8133–8144.
52. Wang XS, Cao K, Liu YB, Tsang B, Liew S. *J Am Chem Soc.* 2013; 135:3399–3402. [PubMed: 23425192]
53. Quirante J, Dubar F, Gonzalez A, Lopez C, Cascante M, Cortes R, Forfar I, Pradines B, Biot C. *J Organomet Chem.* 2011; 696:1011–1017.
54. Matyjaszewski K, Xia J. *Chem Rev.* 2001; 101:2921–2990. [PubMed: 11749397]
55. Hawker CJ, Bosman AW, Harth E. *Chem Rev.* 2001; 101:3661–3688. [PubMed: 11740918]
56. Chiefari J, Chong Y, Ercole F, Krstina J, Jeffery J, Le TP, Mayadunne RT, Meijs GF, Moad CL, Moad G. *Macromolecules.* 1998; 31:5559–5562.
57. Bielawski CW, Grubbs RH. *Prog Polym Sci.* 2007; 32:1–29.
58. Hofmeier H, Schubert US. *Chem Soc Rev.* 2004; 33:373–399. [PubMed: 15280970]
59. Carraher, C.; Siegmund-Louda, D. *Macromolecules Containing Metal and Metal-Like Elements: Biomedical Applications.* Wiley; Hoboken, NJ: 2004.
60. Manners, I. *Synthetic Metal-Containing Polymers.* Wiley-VCH Verlag GmbH & Co. KGaA; Weinheim: 2006.
61. Kong J, Schmalz T, Motz G, Müller AH. *Macromolecules.* 2011; 44:1280–1291.
62. Staff RH, Gallei M, Mazurowski M, Rehahn M, Berger R, Landfester K, Crespy D. *ACS Nano.* 2012; 6:9042–9049. [PubMed: 23020219]
63. Sui XF, Hempenius MA, Vancso GJ. *J Am Chem Soc.* 2012; 134:4023–4025. [PubMed: 22353019]
64. Ma Y, Dong W-F, Hempenius MA, Möhwald H, Julius Vancso G. *Nat Mater.* 2006; 5:724–729. [PubMed: 16921362]
65. Janczewski D, Song J, Csanyi E, Kiss L, Blazso P, Katona RL, Deli MA, Gros G, Xu J, Vancso GJ. *J Mater Chem.* 2012; 22:6429–6435.
66. Correia-Ledo D, Arnold AA, Mauzeroll J. *J Am Chem Soc.* 2010; 132:15120–15123. [PubMed: 20932007]
67. Liu L, Rui L, Gao Y, Zhang W. *Polym Chem.* 2015; 6:1817–1829.
68. Yan Q, Yuan J, Cai Z, Xin Y, Kang Y, Yin Y. *J Am Chem Soc.* 2010; 132:9268–9270. [PubMed: 20565093]
69. Szillat F, Schmidt BVKJ, Hubert A, Barner-Kowollik C, Ritter H. *Macromol Rapid Commun.* 2014; 35:1293–1300. [PubMed: 24753002]
70. Postupalenko V, Desplancq D, Orlov I, Arntz Y, Spehner D, Mely Y, Klaholz BP, Schultz P, Weiss E, Zuber G. *Angew Chem Int Ed.* 2015; 54:10583–10586.
71. Xu HP, Cao W, Zhang X. *Acc Chem Res.* 2013; 46:1647–1658. [PubMed: 23581522]
72. Ma N, Li Y, Xu HP, Wang ZQ, Zhang X. *J Am Chem Soc.* 2010; 132:442–443. [PubMed: 20020681]
73. Huang X, Liu XM, Luo QA, Liu JQ, Shen JC. *Chem Soc Rev.* 2011; 40:1171–1184. [PubMed: 21125082]
74. Nishat N, Khan S, Rasool R, Parveen S. *J Inorg Organomet Polym Mater.* 2011; 21:673–681.
75. Han P, Li SC, Cao W, Li Y, Sun ZW, Wang ZQ, Xu HP. *J Mater Chem B.* 2013; 1:740–743.



76. Ma N, Li Y, Ren HF, Xu HP, Li ZB, Zhang X. *Polym Chem.* 2010; 1:1609–1614.
77. Cao W, Li Y, Yi Y, Ji SB, Zeng LW, Sun ZW, Xu HP. *Chem Sci.* 2012; 3:3403–3408.
78. Ren HF, Wu YT, Ma N, Xu HP, Zhang X. *Soft Matter.* 2012; 8:1460–1466.
79. Han P, Ma N, Ren HF, Xu HP, Li ZB, Wang ZQ, Zhang X. *Langmuir.* 2010; 26:14414–14418. [PubMed: 20722431]
80. Mao SZ, Dong ZY, Liu JQ, Li XQ, Liu XM, Luo GM, Shen JC. *J Am Chem Soc.* 2005; 127:11588–11589. [PubMed: 16104720]
81. Cao W, Gu YW, Meineck M, Li TY, Xu HP. *J Am Chem Soc.* 2014; 136:5132–5137. [PubMed: 24605909]
82. Thomas J, Dong ZY, Dehaen W, Smet M. *Macromol Rapid Commun.* 2012; 33:2127–2132. [PubMed: 22996964]
83. Fang RC, Xu HP, Cao W, Yang LL, Zhang X. *Polym Chem.* 2015; 6:2817–2821.
84. Cao W, Gu YW, Li TY, Xu HP. *Chem Commun.* 2015; 51:7069–7071.
85. Roner M, Shahi K, Barot G, Battin A, Carraher C Jr. *J Inorg Organomet Polym Mater.* 2009; 19:410–414.
86. Carraher CE Jr, Lanz L. *Polym Mater Sci Eng.* 2002; 87:243.
87. Peterson J, Carraher CE Jr, Salamone A, Francis A. *Polym Mater Sci Eng.* 1999; 81:149.
88. Kalita D, Sarmah S, Das SP, Baishya D, Patowary A, Baruah S, Islam NS. *React Funct Polym.* 2008; 68:876–890.
89. Selvi C, Nartop D. *Spectrochim Acta A.* 2012; 95:165–171.
90. Singh T, Khan NU, Shreaz S, Hashmi AA. *Polym Eng Sci.* 2013; 53:2650–2658.
91. Singh T, Shreaz S, Hashmi AA. *Int J Polym Mater.* 2013; 62:653–662.
92. Nishat N, Khan S, Rasool R, Parveen S. *J Inorg Organomet Polym Mater.* 2012; 22:455–463.
93. Hasnain S, Zulfeqar M, Nishat N. *J Coord Chem.* 2011; 64:952–964.
94. Dorman HJD, Deans SG. *J Appl Microbiol.* 2000; 88:308–316. [PubMed: 10736000]
95. Miliuskas G, Venskutonis PR, van Beek TA. *Food Chem.* 2004; 85:231–237.
96. Nielsen FH. *J Trace Elem Exp Med.* 1998; 11:251–274.
97. Zaki MF, Tawfik SM. *J Oleo Sci.* 2014; 63:921–931. [PubMed: 25132086]
98. Carraher, CE., Jr; Pittman, CU. *Macromolecules Containing Metal and Metal-Like Elements.* John Wiley & Sons, Inc; 2004. p. 1-18.
99. KERK, GJMvd. *Organotin Compounds: New Chemistry and Applications.* Vol. 157. American Chemical Society; 1976. p. 1-25.
100. Chambers LD, Stokes KR, Walsh FC, Wood RJK. *Surf Coat Technol.* 2006; 201:3642–3652.
101. Battin AJ, Carraher CE Jr. *Abstr Papers Am Chem Soc.* 2005; 229:U1145–U1145.
102. Abd-El-Aziz, AS.; Carraher, CE., Jr; Pittman, CU.; Zeldin, M. *Inorganic and Organometallic Macromolecules-Design and Applications.* Springer Science+Business Media, LLC; USA: 2007.
103. Gross A, Habig D, Metzler-Nolte N. *ChemBioChem.* 2013; 14:2472–2479. [PubMed: 24218362]
104. Chantson JT, Vittoria Verga Falzacappa M, Crovella S, Metzler-Nolte N. *ChemMedChem.* 2006; 1:1268–1274. [PubMed: 17004283]
105. Mayer UF, Gilroy JB, O'Hare D, Manners I. *J Am Chem Soc.* 2009; 131:10382–10383. [PubMed: 19586050]
106. Mayer UF, Charmant JP, Rae J, Manners I. *Organometallics.* 2008; 27:1524–1533.
107. Gilroy JB, Patra SK, Mitchels JM, Winnik MA, Manners I. *Angew Chem Int Ed.* 2011; 50:5851–5855.
108. Qiu H, Gilroy JB, Manners I. *Chem Commun.* 2013; 49:42–44.
109. Yan Y, Zhang J, Qiao Y, Tang C. *Macromol Rapid Commun.* 2014; 35:254–259. [PubMed: 24023049]
110. Zhang J, Ren L, Hardy CG, Tang C. *Macromolecules.* 2012; 45:6857–6863.
111. Zhang J, Yan Y, Chance MW, Chen J, Hayat J, Ma S, Tang C. *Angew Chem Int Ed.* 2013; 52:13387–13391.
112. Ren L, Zhang J, Bai X, Hardy CG, Shimizu KD, Tang C. *Chem Sci.* 2012; 3:580–583.

113. Ren L, Hardy CG, Tang C. *J Am Chem Soc.* 2010; 132:8874–8875. [PubMed: 20540580]
114. Yan Y, Deaton TM, Zhang J, He H, Hayat J, Pageni P, Matyjaszewski K, Tang C. *Macromolecules.* 2015; 48:1644–1650.
115. Yan Y, Zhang J, Tang C. *Controlled Radical Polymerization: Materials*, American Chemical Society. 2015; 1188:15–27.
116. Zhang J, Yan Y, Chen J, Chance WM, Hayat J, Gai Z, Tang C. *Chem Mater.* 2014; 26:3185–3190.
117. Zhang J, Pellechia PJ, Hayat J, Hardy CG, Tang C. *Macromolecules.* 2013; 46:1618–1624.
118. Ren L, Zhang J, Hardy CG, Doxie D, Fleming B, Tang C. *Macromolecules.* 2012; 45:2267–2275.
119. Ren L, Zhang J, Hardy CG, Ma S, Tang C. *Macromol Rapid Commun.* 2012; 33:510–516. [PubMed: 22252886]
120. Ren L, Hardy CG, Tang S, Doxie DB, Hamidi N, Tang C. *Macromolecules.* 2010; 43:9304–9310.
121. Yan Y, Zhang J, Wilbon P, Qiao Y, Tang C. *Macromol Rapid Commun.* 2014; 35:1840–1845. [PubMed: 25250694]
122. Zhang J, Chen YP, Miller KP, Ganewatta MS, Bam M, Yan Y, Nagarkatti M, Decho AW, Tang C. *J Am Chem Soc.* 2014; 136:4873–4876. [PubMed: 24628053]
123. Zhang J, Yan J, Pageni P, Yan Y, Wirth A, Chen Y, Qiao Y, Wang Q, Decho AW, Tang C. *Sci Rep.* 2015; 5:11914. [PubMed: 26202475]
124. Zhang J, Yan Y, Chance MW, Chen JH, Hayat J, Ma SG, Tang C. *Angew Chem Int Ed.* 2013; 52:13387–13391.
125. Zhang J, Chen Y, Miller KP, Ganewatta MS, Bam M, Yan Y, Nagarkatti M, Decho AW, Tang C. *J Am Chem Soc.* 2014; 136:4873–4876. [PubMed: 24628053]
126. Engler AC, Wiradharma N, Ong ZY, Coady DJ, Hedrick JL, Yang YY. *Nano Today.* 2012; 7:201–222.
127. Homem V, Santos L. *J Environ Manage.* 2011; 92:2304–2347. [PubMed: 21680081]
128. Adams C, Wang Y, Loftin K, Meyer M. *J Environ Eng.* 2002; 128:253–260.
129. Abd-El-Aziz AS, Agatemor C, Etkin N, Overy DP, Lanteigne M, McQuillan K, Kerr RG. *Biomacromolecules.* 2015; 16:3694–3703. [PubMed: 26452022]
130. Osella D, Ferrali M, Zanello P, Laschi F, Fontani M, Nervi C, Cavigiolio G. *Inorg Chim Acta.* 2000; 306:42–48.
131. Neuse E. *J Inorg Organomet Polym Mater.* 2005; 15:3–31.
132. Neuse EW. *Polym Adv Technol.* 1998; 9:786–793.
133. Mufula A, Aderibigbe BA, Neuse E, Mukaya H. *J Inorg Organomet Polym Mater.* 2012; 22:423–428.
134. Mufula A, Neuse E. *J Inorg Organomet Polym Mater.* 2012; 22:134–148.
135. Aderibigbe B, Jacques K, Neuse E. *J Inorg Organomet Polym Mater.* 2011; 21:336–345.
136. Carlotti, S.; Peruch, F. *Anionic Polymerization*. Hadjichristidis, N.; Hirao, A., editors. Springer; Japan: 2015. p. 191-305.
137. Caldwell G, Meirim MG, Neuse EW, van Rensburg CEJ. *Appl Organomet Chem.* 1998; 12:793–799.
138. Caldwell G, Meirim M, Neuse E, Beloussow K, Shen WC. *J Inorg Organomet Polym.* 2000; 10:93–101.
139. Johnson M, Kreft E, N'Da D, Neuse E, van Rensburg CJ. *J Inorg Organomet Polym.* 2003; 13:255–267.
140. Johnson M, Neuse E, van Rensburg CJ, Kreft E. *J Inorg Organomet Polym.* 2003; 13:55–67.
141. Meirim M, Neuse E, Caldwell G. *J Inorg Organomet Polym Mater.* 1998; 8:225–236.
142. Greenwald RB, Conover CD, Choe YH. *Crit Rev Ther Drug Carrier Syst.* 2000; 17:62.
143. Neuse E, Meirim M, N'Da D, Caldwell G. *J Inorg Organomet Polym.* 1999; 9:221–230.
144. Neuse EW. *Macromol Symp.* 2001; 172:127–138.
145. Gul A, Akhter Z, Siddiq M, Sarfraz S, Mirza B. *Macromolecules.* 2013; 46:2800–2807.
146. Gul A, Sarfraz S, Akhter Z, Siddiq M, Kalsoom S, Perveen F, Ansari FL, Mirza B. *J Organomet Chem.* 2015; 779:91–99.

147. Wei H, Quan CY, Chang C, Zhang XZ, Zhuo RX. *J Phys Chem B*. 2010; 114:5309–5314. [PubMed: 20369878]
148. Yan Y, Zhang J, Qiao Y, Ganewatta M, Tang C. *Macromolecules*. 2013; 46:8816–8823.
149. Helena Garcia M, Morais TS, Florindo P, Piedade MFM, Moreno V, Ciudad C, Noe V. *J Inorg Biochem*. 2009; 103:354–361. [PubMed: 19128838]
150. Valente A, Garcia MH, Marques F, Miao Y, Rousseau C, Zinck P. *J Inorg Biochem*. 2013; 127:79–81. [PubMed: 23896008]
151. Li J, Murakami T, Higuchi M. *J Inorg Organomet Polym Mater*. 2013; 23:119–125.
152. Li J, Futera Z, Li H, Tateyama Y, Higuchi M. *Phys Chem Chem Phys*. 2011; 13:4839–4841. [PubMed: 21327286]
153. Govender P, Antonels NC, Mattsson J, Renfrew AK, Dyson PJ, Moss JR, Therrien B, Smith GS. *J Organomet Chem*. 2009; 694:3470–3476.
154. Govender P, Renfrew AK, Clavel CM, Dyson PJ, Therrien B, Smith GS. *Dalton Trans*. 2011; 40:1158–1167. [PubMed: 21165516]
155. Pitto-Barry A, Barry NPE, Zava O, Deschenaux R, Dyson PJ, Therrien B. *Chem Eur J*. 2011; 17:1966–1971. [PubMed: 21274948]
156. Therrien B, Süß-Fink G, Govindaswamy P, Renfrew AK, Dyson PJ. *Angew Chem Int Ed*. 2008; 47:3773–3776.
157. Pitto-Barry A, Zava O, Dyson PJ, Deschenaux R, Therrien B. *Inorg Chem*. 2012; 51:7119–7124. [PubMed: 22716166]
158. Raja DS, Bhuvanesh NSP, Natarajan K. *Dalton Trans*. 2012; 41:4365–4377. [PubMed: 22354161]
159. Nehru S, Arunachalam S, Arun R, Premkumar K. *J Biomol Struct Dyn*. 2014; 32:1876–1888. [PubMed: 24053452]
160. Vignesh G, Senthilkumar R, Paul P, Periasamy VS, Akbarsha MA, Arunachalam S. *RSC Adv*. 2014; 4:57483–57492.
161. Senthil Kumar R, Periasamy VS, Preethy Paul C, Riyasdeen A, Arunachalam S, Akbarsha MA. *Med Chem Res*. 2011; 20:726–731.
162. Lakshmi Praba J, Arunachalam S, Riyasdeen A, Dhivya R, Vignesh S, Akbarsha MA, James RA. *Spectrochim Acta A*. 2013; 109:23–31.
163. Norihiro, K. *Jpn Patent*. 57102895. 1982.
164. Monge S, Canniccioni B, Graillet A, Robin JJ. *Biomacromolecules*. 2011; 12:1973–1982. [PubMed: 21553908]
165. Maiti S, Banerjee S, Palit SK. *Prog Polym Sci*. 1993; 18:227–261.
166. Stejskal J, Sapurina I, Trchova M. *Prog Polym Sci*. 2010; 35:1420–1481.
167. Carraher CE Jr, Roner MR, Pham N, Moric-Johnson A. *J Macromol Sci A*. 2014; 51:547–556.
168. Carraher CE Jr, Truong NTC, Roner MR, Moric A, Trang NT. *J Chin Adv Mater Soc*. 2013; 1:134–150.
169. Zhang Q, Vakili MR, Li XF, Lavasanifar A, Le XC. *Biomaterials*. 2014; 35:7088–7100. [PubMed: 24840615]
170. Roner M, Carraher C, Shahi K, Ashida Y, Barot G. *BMC Cancer*. 2009; 9:358. [PubMed: 19811643]
171. Ostrovskaya LA, Varfolomeev SD, Voronkov MG, Korman DB, Bluchterova NV, Fomina MM, Rikova VA, Goldberg VM, Abzaeva KA, Zhilitskaya LV, Snegur LV, Simenel AA, Zykova SI. *Russ Chem Bull*. 2014; 63:1211–1217.
172. van Rijt SH, Sadler PJ. *Drug Discov Today*. 2009; 14:1089–1097. [PubMed: 19782150]
173. Kelland L. *Nat Rev Cancer*. 2007; 7:573–584. [PubMed: 17625587]
174. Mbonyana CW, Neuse EW, Perlwitz AG. *Appl Organomet Chem*. 1993; 7:279–288.
175. Schechter B, Caldwell G, Meirim MG, Neuse EW. *Appl Organomet Chem*. 2000; 14:701–708.
176. Caldwell G, Neuse EW, van Rensburg CE. *J Inorg Organomet Polym*. 1997; 7:217–231.
177. N'Da DD, Neuse EW. *J Inorg Organomet Polym Mater*. 2010; 20:468–477.
178. Shen WC, Beloussow K, Meirim MG, Neuse EW, Caldwell G. *J Inorg Organomet Polym Mater*. 2000; 10:51–60.

179. Geetha B, Sodhi A, Singh SM. *Immunopharm Immunot.* 1991; 13:1–10.
180. Smit T, Neuse E, Becker P, Anderson R, van Rensburg C. *Drug Dev Res.* 2006; 66:204–209.
181. Yokoyama M, Okano T, Sakurai Y, Suwa S, Kataoka K. *J Control Release.* 1996; 39:351–356.
182. Nishiyama N, Kato Y, Sugiyama Y, Kataoka K. *Pharm Res.* 2001; 18:1035–1041. [PubMed: 11496942]
183. Cabral H, Nishiyama N, Okazaki S, Koyama H, Kataoka K. *J Control Release.* 2005; 101:223–232. [PubMed: 15588907]
184. Shen W, Luan J, Cao L, Sun J, Yu L, Ding J. *Biomacromolecules.* 2014; 16:105–115. [PubMed: 25435165]
185. Xiao H, Zhou D, Liu S, Zheng Y, Huang Y, Jing X. *Acta Biomater.* 2012; 8:1859–1868. [PubMed: 22281944]
186. Yang Q, Qi R, Cai J, Kang X, Sun S, Xiao H, Jing X, Li W, Wang Z. *RSC Adv.* 2015; 5:83343–83349.
187. Song H, Xiao H, Zheng M, Qi R, Yan L, Jing X. *J Mater Chem B.* 2014; 2:6560–6570.
188. Wang R, Xiao H, Song H, Zhang Y, Hu X, Xie Z, Huang Y, Jing X, Li Y. *J Mater Chem.* 2012; 22:25453–25462.
189. Xiao H, Li W, Qi R, Yan L, Wang R, Liu S, Zheng Y, Xie Z, Huang Y, Jing X. *J Control Release.* 2012; 163:304–314. [PubMed: 22698937]
190. Xiao H, Zhou D, Liu S, Qi R, Zheng Y, Huang Y, Jing X. *Macromol Biosci.* 2012; 12:367–373. [PubMed: 22213516]
191. Dhar S, Lippard SJ. *Proc Natl Acad Sci.* 2009; 106:22199–22204. [PubMed: 20007777]
192. Zhou DF, Xiao HH, Meng FB, Li XY, Li YX, Jing XB, HYB. *Adv Healthcare Mater.* 2013; 2:822–827.
193. Zhou D, He S, Cong Y, Xie Z, Chen X, Jing X, Huang Y. *J Mater Chem B.* 2015; 3:4913–4921.
194. Wang R, Hu X, Wu S, Xiao H, Cai H, Xie Z, Huang Y, Jing X. *Mol Pharm.* 2012; 9:3200–3208. [PubMed: 22954154]
195. Karim KJA, Utama RH, Lu H, Stenzel MH. *Polym Chem.* 2014; 5:6600–6610.
196. Dag A, Jiang Y, Karim KJA, Hart-Smith G, Scarano W, Stenzel MH. *Macromol Rapid Commun.* 2015; 36:890–897. [PubMed: 25790077]
197. Xu J, Fu Q, Ren JM, Bryant G, Qiao GG. *Chem Commun.* 2013; 49:33–35.
198. Fu Q, Xu J, Ladewig K, Henderson TMA, Qiao GG. *Polym Chem.* 2015; 6:35–43.
199. Bontha S, Kabanov AV, Bronich TK. *J Control Release.* 2006; 114:163–174. [PubMed: 16914223]
200. Haxton KJ, Burt HM. *Dalton Trans.* 2008:5872–5875. [PubMed: 19082039]
201. Rieter WJ, Pott KM, Taylor KM, Lin W. *J Am Chem Soc.* 2008; 130:11584–11585. [PubMed: 18686947]
202. Liu D, Poon C, Lu K, He C, Lin W. *Nat Commun.* 2014; 5:4182. [PubMed: 24964370]
203. Sood P, Thurmond KB, Jacob JE, Waller LK, Silva GO, Stewart DR, Nowotnik DP. *Bioconjugate Chem.* 2006; 17:1270–1279.
204. Campone M, Rademaker-Lakhai JM, Bennouna J, Howell SB, Nowotnik DP, Beijnen JH, Schellens JH. *Cancer Chemoth Pharm.* 2007; 60:523–533.
205. Bouma M, Nuijen B, Harms R, Rice JR, Nowotnik DP, Stewart DR, Jansen BAJ, van Zutphen S, Reedijk J, van Steenberghe MJ, Talsma H, Bult A, Beijnen JH. *Drug Dev Ind Pharm.* 2003; 29:981–995. [PubMed: 14606662]
206. Rademaker-Lakhai JM, Terret C, Howell SB, Baud CM, de Boer RF, Pluim D, Beijnen JH, Schellens JH, Droz JP. *Clin Cancer Res.* 2004; 10:3386–3395. [PubMed: 15161693]
207. DEJG, Dolmans J, Fukumura D, Jain RK. *Nat Rev Cancer.* 2003; 3:380–387. [PubMed: 12724736]
208. Jeong YH, Yoon HJ, Jang WD. *Polym J.* 2012; 44:512–521.
209. Agostinis P, Berg K, Cengel KA, Foster TH, Girotti AW, Gollnick SO, Hahn SM, Hamblin MR, Juzeniene A, Kessel D, Korbelik M, Moan J, Mroz P, Nowis D, Piette J, Wilson BC, Golab J. *CA Cancer J Clin.* 2011; 61:250–281. [PubMed: 21617154]

210. Agostinis P, Berg K, Cengel KA, Foster TH, Girotti AW, Gollnick SO, Hahn SM, Hamblin MR, Juzeniene A, Kessel D. *CA Cancer J Clin.* 2011; 61:250–281. [PubMed: 21617154]
211. Spyropoulos-Antonakakis N, Sarantopoulou E, Trohopoulos P, Stefi A, Kollia Z, Gavriil V, Bourkoula A, Petrou P, Kakabakos S, Semashko V, Nizamutdinov A, Cefalas AC. *Nanoscale Res Lett.* 2015; 10:1–19. [PubMed: 25977644]
212. Zhang JX, Zhou JW, Chan CF, Lau TCK, Kwong DWJ, Tam HL, Mak NK, Wong KL, Wong WK. *Bioconjugate Chem.* 2012; 23:1623–1638.
213. Gianferrara T, Bergamo A, Bratsos I, Milani B, Spagnul C, Sava G, Alessio E. *J Med Chem.* 2010; 53:4678–4690. [PubMed: 20491441]
214. Ravanat JL, Cadet J, Araki K, Toma HE, Medeiros MHG, Mascio PD. *J Photochem Photobiol A.* 1998; 68:698–702.
215. Schmitt F, Govindaswamy P, Süß-Fink G, Ang WH, Dyson PJ, Juillerat-Jeanneret L, Therrien B. *J Med Chem.* 2008; 51:1811–1816. [PubMed: 18298056]
216. Rani-Beeram S, Meyer K, McCrate A, Hong Y, Nielsen M, Swavey S. *Inorg Chem.* 2008; 47:11278–11283. [PubMed: 18980373]
217. Lu Y, Xue F, Yang H, Shi M, Yan Y, Qin L, Zhou Z, Yang S. *J Phys Chem C.* 2015; 119:573–579.
218. Kim J, Yoon HJ, Kim S, Wang K, Ishii T, Kim YR, Jang WD. *J Mater Chem.* 2009; 19:4627–4631.
219. Mauriello-Jimenez C, Croissant J, Maynadier M, Cattoen X, Wong Chi Man M, Vergnaud J, Chaleix V, Sol V, Garcia M, Gary-Bobo M, Raehm L, Durand J-O. *J Mater Chem B.* 2015; 3:3681–3684.
220. Nishiyama N, Nakagishi Y, Morimoto Y, Lai PS, Miyazaki K, Urano K, Horie S, Kumagai M, Fukushima S, Cheng Y, Jang WD, Kikuchi M, Kataoka K. *J Control Release.* 2009; 133:245–251. [PubMed: 19000725]
221. Herlambang S, Kumagai M, Nomoto T, Horie S, Fukushima S, Oba M, Miyazaki K, Morimoto Y, Nishiyama N, Kataoka K. *J Control Release.* 2011; 155:449–457. [PubMed: 21704092]
222. Jang WD, Nakagishi Y, Nishiyama N, Kawauchi S, Morimoto Y, Kikuchi M, Kataoka K. *J Control Release.* 2006; 113:73–79. [PubMed: 16701915]
223. Schmitt J, Heitz V, Sour A, Bolze F, Ftouni H, Nicoud JF, Flamigni L, Ventura B. *Angew Chem Int Ed.* 2015; 54:169–173.
224. Achelle S, Couleaud P, Baldeck P, Teulade-Fichou MP, Maillard P. *Eur J Org Chem.* 2011; 2011:1271–1279.
225. Liu CB, Liu GZ, Liu N, Zhang YU-m, He J, Rusckowski M, Hnatowich DJ. *Nucl Med Biol.* 2003; 30:207–214. [PubMed: 12623121]
226. Hrubý M, Šubr V, Kučka J, Kozempel J, Lebeda O, Sikora A. *Appl Radiat Isot.* 2005; 63:423–431. [PubMed: 15996473]
227. Jayakrishnan, A.; Latha, M. *Controlled and Novel Drug Delivery.* New Delhi: CBS publishers; 1997. p. 236-255.
228. Mumper RJ, Ryo UY, Jay M. *J Nucl Med.* 1991; 32:2139–2143. [PubMed: 1941151]
229. Nijssen F, Rook D, Brandt C, Meijer R, Dullens H, Zonnenberg B, de Klerk J, van Rijk P, Hennink W, van het Schip F. *Euro J Nucl Med.* 2001; 28:743–749.
230. Sinha VR, Goyal V, Trehan A. *Die Pharmazie.* 2004; 59:419–426. [PubMed: 15248454]
231. Tassano MR, Audicio PF, Gambini JP, Fernandez M, Damian JP, Moreno M, Chabalgoity JA, Alonso O, Benech JC, Cabral P. *Bioorg Med Chem Lett.* 2011; 21:5598–5601. [PubMed: 21778055]
232. Visentin R, Pasut G, Veronese FM, Mazzi U. *Bioconjugate Chem.* 2004; 15:1046–1054.
233. Areses P, Agüeros MT, Quincoces G, Collantes M, Richter JÁ, López-Sánchez LM, Sánchez-Martínez M, Irache J, Peñuelas I. *Mol Imaging Biol.* 2011; 13:1215–1223. [PubMed: 21161691]
234. Callahan RJ, Bogdanov A, Fischman AJ, Brady TJ, Weissleder R. *Am J Roentgenol.* 1998; 171:137–143. [PubMed: 9648777]
235. Morais M, Campello MPC, Xavier C, Heemskerk J, Correia JDG, Lahoutte T, Cavelliers V, Hernot S, Santos I. *Bioconjugate Chem.* 2014; 25:1963–1970.

236. Xu X, Zhang Y, Wang X, Guo X, Zhang X, Qi Y, Shen YM. *Bioorg Med Chem*. 2011; 19:1643–1648. [PubMed: 21310621]
237. Mitra A, Mulholland J, Nan A, McNeill E, Ghandehari H, Line BR. *J Control Release*. 2005; 102:191–201. [PubMed: 15653145]
238. Mang'era K, Liu G, Yi W, Zhang Y, Liu N, Gupta S, Rusckowski M, Hnatowich D. *Euro J Nucl Med*. 2001; 28:1682–1689.
239. Smith CJ, Gali H, Sieckman GL, Higginbotham C, Volkert WA, Hoffman TJ. *Bioconjugate Chem*. 2003; 14:93–102.
240. Kim EM, Jeong HJ, Heo YJ, Moon HB, Bom HS, Kim CG. *J Korean Med Sci*. 2004; 19:647–651. [PubMed: 15483337]
241. Salamone A, Carraher C, Stewart J, Miao S, Peterson J, Francis AM. *Polym Mater Sci Eng*. 1999; 81:147.
242. Salamone A, Carraher C, Carraher S, Stewart H, Miao S, Cowen C. *Polym Mater Sci Eng*. 2000; 82:79.
243. Carraher, C., Jr; Haky, J.; Rivalta, A. *Functional Condensation Polymers*. Carraher, C., Jr; Swift, G., editors. Springer; US: 2002. p. 55-62.
244. Carraher, CE., Jr; Currell, B.; Pittman, C., Jr; Sheats, J.; Zeldin, M. *Inorganic and Metal-Containing Polymeric Materials*. Springer Science & Business Media; 2012.
245. Carraher CE Jr, Stewart H, Reckleben L, Williams M, Soldani W, Bernstein D. *Polym Mater Sci Eng*. 1989; 61:437.
246. Astruc D, Ornelas C, Ruiz J. *Acc Chem Res*. 2008; 41:841–856. [PubMed: 18624394]
247. Astruc D. *Nat Chem*. 2012; 4:255–267. [PubMed: 22437709]
248. Deng H, Shen W, Gao Z. *Sensors Actuat B-Chem*. 2012; 168:238–242.
249. Xiao F, Gu M, Liang Y, Dong M, Zhao Z, Zhi D. *J Organomet Chem*. 2014; 772–773:122–130.
250. Xiao F, Liang Y, Li S, Gu M, Yue L. *J Electroanal Chem*. 2014; 733:77–84.
251. Palomera N, Vera JL, Meléndez E, Ramirez-Vick JE, Tomar MS, Arya SK, Singh SP. *J Electroanal Chem*. 2011; 658:33–37.
252. Erden PE, Kaçar C, Öztürk F, Kılıç E. *Talanta*. 2015; 134:488–495. [PubMed: 25618698]
253. Jiménez A, Armada MPG, Losada J, Villena C, Alonso B, Casado CM. *Sensors Actuat B-Chem*. 2014; 190:111–119.
254. Yuan L, Wei W, Liu S. *Biosens Bioelectron*. 2012; 38:79–85. [PubMed: 22766469]
255. Conghaile PÓ, Pöller S, MacAodha D, Schuhmann W, Leech D. *Biosens Bioelectron*. 2013; 43:30–37. [PubMed: 23274194]
256. Antiochia R, Vinci G, Gorton L. *Food Chem*. 2013; 140:742–747. [PubMed: 23692761]
257. Deng H, Teo AKL, Gao Z. *Sensors Actuat B-Chem*. 2014; 191:522–528.
258. Zhao Q, Huang C, Li F. *Chem Soc Rev*. 2011; 40:2508–2524. [PubMed: 21253643]
259. Lo KK-W, Choi AW-T, Law WH-T. *Dalton Trans*. 2012; 41:6021–6047. [PubMed: 22241514]
260. Lo KK-W, Li SP-Y, Zhang KY. *New J Chem*. 2011; 35:265–287.
261. Baggaley E, Weinstein JA, Williams JAG. *Coord Chem Rev*. 2012; 256:1762–1785.
262. Ma Y, Liu S, Yang H, Wu Y, Sun H, Wang J, Zhao Q, Li F, Huang W. *J Mater Chem*. 2013; 1:319–329.
263. Yang T, Liu Q, Pu S, Dong Z, Huang C, Li F. *Nano Res*. 2012; 5:494–503.
264. Zhou Z, Li D, Yang H, Zhu Y, Yang S. *Dalton Trans*. 2011; 40:11941–11944. [PubMed: 21976130]
265. Zhao Q, Zhou X, Cao T, Zhang KY, Yang L, Liu S, Liang H, Yang H, Li F, Huang W. *Chem Sci*. 2015; 6:1825–1831.
266. Dagorne S, Normand M, Kirillov E, Carpentier JF. *Coord Chem Rev*. 2013; 257:1869–1886.
267. Ma HY, Darmawan ET, Zhang M, Zhang L, Bryers JD. *J Control Release*. 2013; 172:1035–1044. [PubMed: 24140747]
268. Panthani MG, Akhavan V, Goodfellow B, Schmidtke JP, Dunn L, Dodabalapur A, Barbara PF, Korgel BA. *J Am Chem Soc*. 2008; 130:16770–16777. [PubMed: 19049468]

269. Nichols B, Qin ZT, Yang J, Vera DR, Devaraj NK. *Chem Commun.* 2014; 50:5215–5217.
270. Patil RR, Yu JH, Banerjee SR, Ren Y, Leong D, Jiang X, Pomper M, Tsui B, Kraitchman DL, Mao HQ. *Mol Ther.* 2011; 19:1626–1635. [PubMed: 21750533]
271. Ye F, Ke T, Jeong E-K, Wang X, Sun Y, Johnson M, Lu Z-R. *Mol Pharm.* 2006; 3:507–515. [PubMed: 17009849]
272. Kim B, Schmieder AH, Stacy AJ, Williams TA, Pan D. *J Am Chem Soc.* 2012; 134:10377–10380. [PubMed: 22693958]
273. Caravan P, Ellison JJ, McMurry TJ, Lauffer RB. *Chem Rev.* 1999; 99:2293–2352. [PubMed: 11749483]
274. Lu Z-R, Wang X, Parker DL, Goodrich KC, Buswell HR. *Bioconjugate Chem.* 2003; 14:715–719.
275. Mohs AM, Wang X, Goodrich KC, Zong Y, Parker DL, Lu Z-R. *Bioconjugate Chem.* 2004; 15:1424–1430.
276. Zong Y, Wang X, Goodrich KC, Mohs AM, Parker DL, Lu ZR. *Magnet Reson Med.* 2005; 53:835–842.
277. Kaneshiro TL, Jeong E-K, Morrell G, Parker DL, Lu Z-R. *Biomacromolecules.* 2008; 9:2742–2748. [PubMed: 18771313]
278. Wu X, Jeong E-K, Emerson L, Hoffman J, Parker DL, Lu Z-R. *Mol Pharm.* 2009; 7:41–48. [PubMed: 19958031]
279. Vaidya A, Sun Y, Ke T, Jeong EK, Lu ZR. *Magnet Reson Med.* 2006; 56:761–767.
280. Wen X, Jackson EF, Price RE, Kim EE, Wu Q, Wallace S, Charnsangavej C, Gelovani JG, Li C. *Bioconjugate Chem.* 2004; 15:1408–1415.
281. Zhang G, Zhang R, Wen X, Li L, Li C. *Biomacromolecules.* 2008; 9:36–42. [PubMed: 18047289]
282. Kim KS, Park W, Hu J, Bae YH, Na K. *Biomaterials.* 2014; 35:337–343. [PubMed: 24139764]
283. Nwe K, Bryant LH Jr, Brechbiel MW. *Bioconjugate Chem.* 2010; 21:1014–1017.
284. Nwe K, Xu H, Regino CAS, Bernardo M, Ileva L, Riffle L, Wong KJ, Brechbiel MW. *Bioconjugate Chem.* 2009; 20:1412–1418.
285. Wiener E, Auteri F, Chen J, Brechbiel M, Gansow O, Schneider D, Belford R, Clarkson R, Lauterbur P. *J Am Chem Soc.* 1996; 118:7774–7782.
286. Bryant LH, Brechbiel MW, Wu C, Bulte JW, Herynek V, Frank JA. *J Magn Reson Imaging.* 1999; 9:348–352. [PubMed: 10077036]
287. Cheng Z, Thorek DL, Tsourkas A. *Angew Chem Int Ed.* 2010; 49:346–350.
288. Cohen SM, Xu J, Radkov E, Raymond KN, Botta M, Barge A, Aime S. *Inorg Chem.* 2000; 39:5747–5756. [PubMed: 11151375]
289. Floyd WC III, Klemm PJ, Smiles DE, Kohlgruber AC, Pierre VC, Mynar JL, Fréchet JM, Raymond KN. *J Am Chem Soc.* 2011; 133:2390–2393. [PubMed: 21294571]
290. Pierre VC, Botta M, Raymond KN. *J Am Chem Soc.* 2005; 127:504–505. [PubMed: 15643857]
291. Laus S, Sour A, Ruloff R, Toth E, Merbach AE. *Chem Eur J.* 2005; 11:3064–3076. [PubMed: 15776490]
292. Rudovský J, Botta M, Hermann P, Hardcastle KI, Lukeš I, Aime S. *Bioconjugate Chem.* 2006; 17:975–987.
293. Kobayashi H, Kawamoto S, Jo S-K, Bryant HL, Brechbiel MW, Star RA. *Bioconjugate Chem.* 2003; 14:388–394.
294. Langereis S, De Lussanet QG, Van Genderen MH, Backes WH, Meijer E. *Macromolecules.* 2004; 37:3084–3091.
295. Liao Z, Wang H, Wang X, Zhao P, Wang S, Su W, Chang J. *Adv Funct Mater.* 2011; 21:1179–1186.
296. Zarabi B, Nan A, Zhuo J, Gullapalli R, Ghandehari H. *Macromol Biosci.* 2008; 8:741–748. [PubMed: 18484565]
297. Wu Y, Carney CE, Denton M, Hart E, Zhao P, Streblow DN, Sherry AD, Woods M. *Org Biomol Chem.* 2010; 8:5333–5338. [PubMed: 20848030]
298. Bryson JM, Fichter KM, Chu W-J, Lee J-H, Li J, Madsen LA, McLendon PM, Reineke TM. *Proc Natl Acad Sci USA.* 2009; 106:16913–16918. [PubMed: 19805101]

299. Olson ES, Jiang T, Aguilera TA, Nguyen QT, Ellies LG, Scadeng M, Tsien RY. Proc Natl Acad Sci USA. 2010; 107:4311–4316. [PubMed: 20160077]
300. Nguyen QT, Olson ES, Aguilera TA, Jiang T, Scadeng M, Ellies LG, Tsien RY. Proc Natl Acad Sci USA. 2010; 107:4317–4322. [PubMed: 20160097]

## Biographies



Dr. Yi Yan received his B.S. from College of Chemistry, Jilin University and Ph.D. from the State Key Laboratory of Supramolecular Structure and Materials, Jilin University under the supervision of Prof. Lixin Wu. Then, he moved to Canada to pursue his postdoctoral research at Queen's University with Prof. Anne Petitjean from August 2011 to October 2012. From November 2012 to April 2015, he was a postdoctoral scholar at the University of South Carolina with Prof. Chuanbing Tang. Since May 2015, he has been a full professor in Department of Applied Chemistry, School of Science at Northwestern Polytechnical University, P. R. China. His research is focused on supramolecular chemistry, controlled polymerization, metal-containing polymers and inorganic-organic hybrids.



Dr. Jiuyang Zhang received his B. S. from Nanjing University (2010). He joined Prof. Chuanbing Tang's group and obtained his Ph.D. (2014) from University of South Carolina-Columbia. He is now working in Prof. Frank Bates' group as a postdoctoral associate. His current work focuses on sustainable thermoplastics with advanced architectures.



Dr. Lixia Ren received her B.S. from Hebei University in 2004 and Ph. D. from Institute of Chemistry Chinese Academy of Science under the supervision of Prof. Yongming Chen in 2009. She did her postdoctoral research at University of South Carolina with Prof. Chuanbing Tang from 2009 to 2011. Currently she is an associate professor at Tianjin



University, China. She is interested in controlled polymerization of topological polymers, supramolecular polymers, metal-containing polymers and polymer-based biomaterials.



Prof. Chuanbing Tang received B.S. from Nanjing University and Ph.D. from Carnegie Mellon University with Profs. Krzysztof Matyjaszewski and Tomasz Kowalewski. He was a postdoctoral scholar at the University of California Santa Barbara with Profs. Edward J. Kramer and Craig J. Hawker. Since August 2009, he has been an Assistant Professor, Associate Professor and College of Arts and Sciences Distinguished Professor in Department of Chemistry and Biochemistry at the University of South Carolina. His research interests focus on organic polymer synthesis, sustainable polymers from biomass, metal-containing polymers, dielectric polymers, and polymers for biomedical applications.

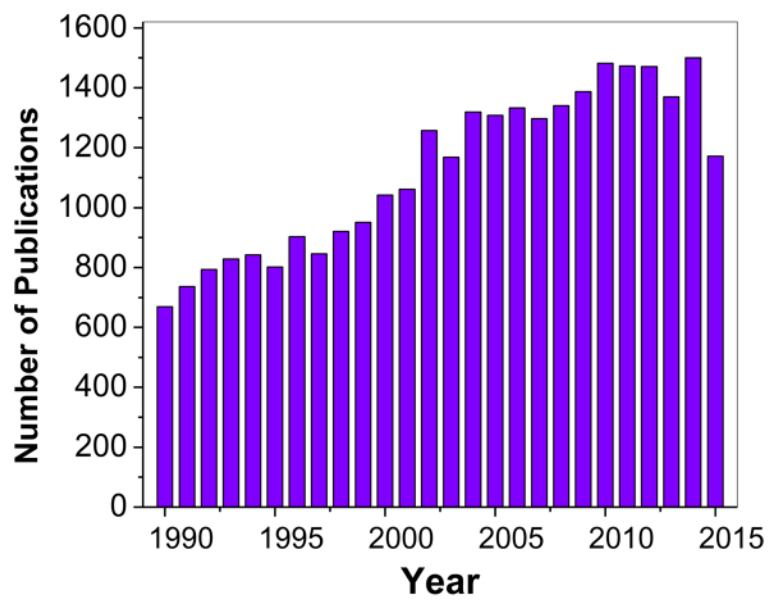


**Fig. 1.** Publications containing “organometallic polymers” from 1990 to 2015 based on SciFinder search.

H																	He																												
Li	Be											B	C	N	O	F	Ne																												
Na	Mg											Al	Si	P	S	Cl	Ar																												
K	Ca	Sc	Ti	V	Cr	Mn	Fe	Co	Ni	Cu	Zn	Ga	Ge	As	Se	Br	Kr																												
Rb	Sr	Y	Zr	Nb	Mo	Tc	Ru	Rh	Pd	Ag	Cd	In	Sn	Sb	Te	I	Xe																												
Cs	Ba	La	Hf	Ta	W	Re	Os	Ir	Pt	Au	Hg	Tl	Pb	Bi	Po	At	Rn																												
Fr	Ra	Ac	Rf	Db	Sg	Bh	Hs	Mt	Ds	Rg	Cn																																		
			<table border="1"> <tbody> <tr> <td>Ce</td> <td>Pr</td> <td>Nd</td> <td>Pm</td> <td>Sm</td> <td>Eu</td> <td>Gd</td> <td>Tb</td> <td>Dy</td> <td>Ho</td> <td>Er</td> <td>Tm</td> <td>Yb</td> <td>Lu</td> </tr> <tr> <td>Th</td> <td>Pa</td> <td>U</td> <td>Np</td> <td>Pu</td> <td>Am</td> <td>Cm</td> <td>Bk</td> <td>Cf</td> <td>Es</td> <td>Fm</td> <td>Md</td> <td>No</td> <td>Lr</td> </tr> </tbody> </table>															Ce	Pr	Nd	Pm	Sm	Eu	Gd	Tb	Dy	Ho	Er	Tm	Yb	Lu	Th	Pa	U	Np	Pu	Am	Cm	Bk	Cf	Es	Fm	Md	No	Lr
Ce	Pr	Nd	Pm	Sm	Eu	Gd	Tb	Dy	Ho	Er	Tm	Yb	Lu																																
Th	Pa	U	Np	Pu	Am	Cm	Bk	Cf	Es	Fm	Md	No	Lr																																

**Fig. 2.** Metals in periodic tables used in polymeric systems for biomedical applications and covered by this review article.

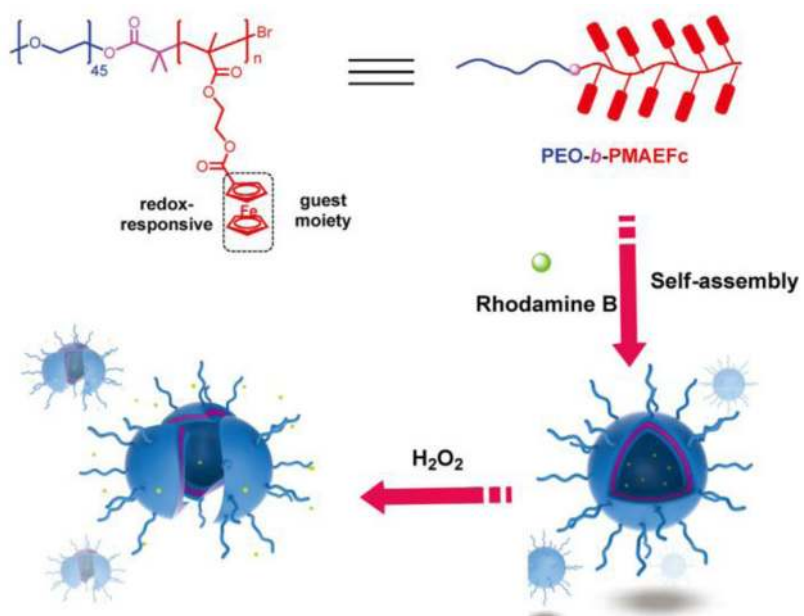


**Fig. 3.** Self-assembly of ferrocene-containing block copolymer PEG-*b*-PMAEFc, and redox-responsive release of a model molecule (Rhodamine B). Adapted with permission from Ref. 67. Copyright © 2014, Royal Society of Chemistry.

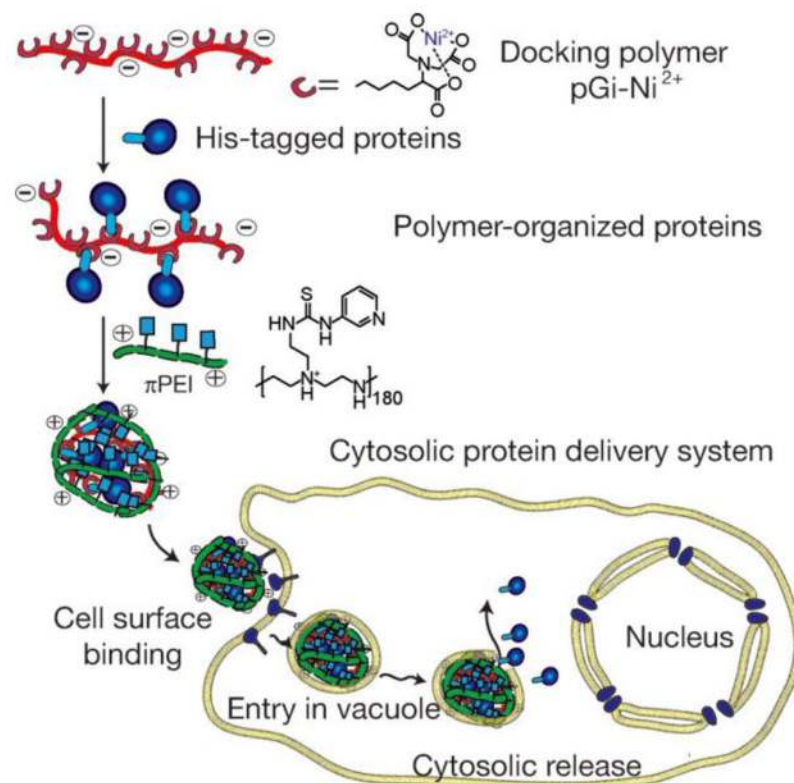


**Fig. 4.** Illustration of the Ni-containing protein delivery system. Adapted with permission from Ref. 70. Copyright © 2015 WILEY-VCH Verlag GmbH & Co. KGaA, Weinheim.

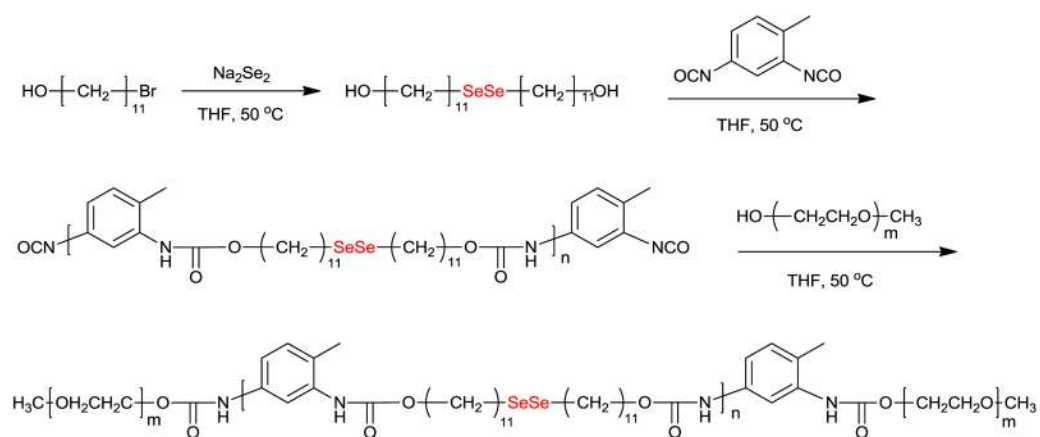


**Fig. 5.** Synthesis of the diselenide-containing main-chain polymers (PEG-PUSESe-PEG).

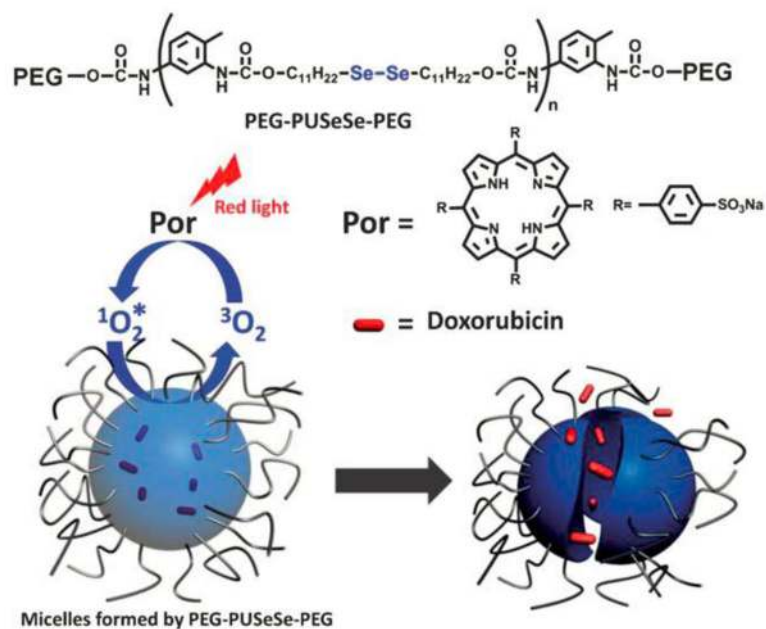


**Fig. 6.** Drug release from diselenide-containing block copolymer micelles under red light. Adapted with permission from Ref. 75. Copyright © 2012, Royal Society of Chemistry.

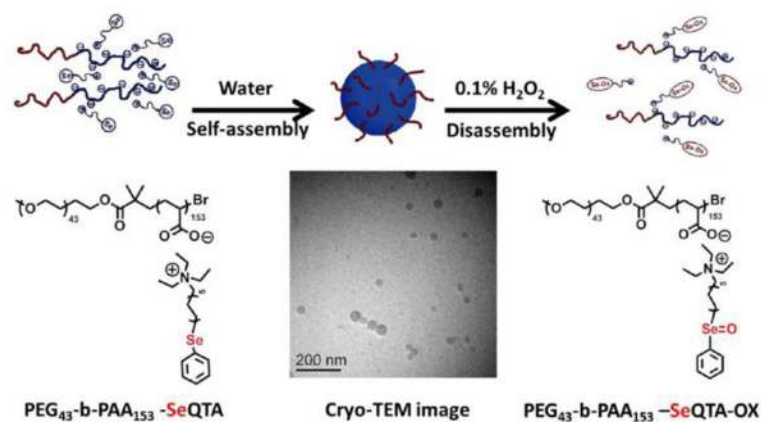


**Fig. 7.** Oxidation-responsive micelles based on a side-chain selenium-containing polymeric supra-amphiphile formed through the electrostatic interaction. Adapted with permission from Ref. 79. Copyright © 2010, American Chemical Society.



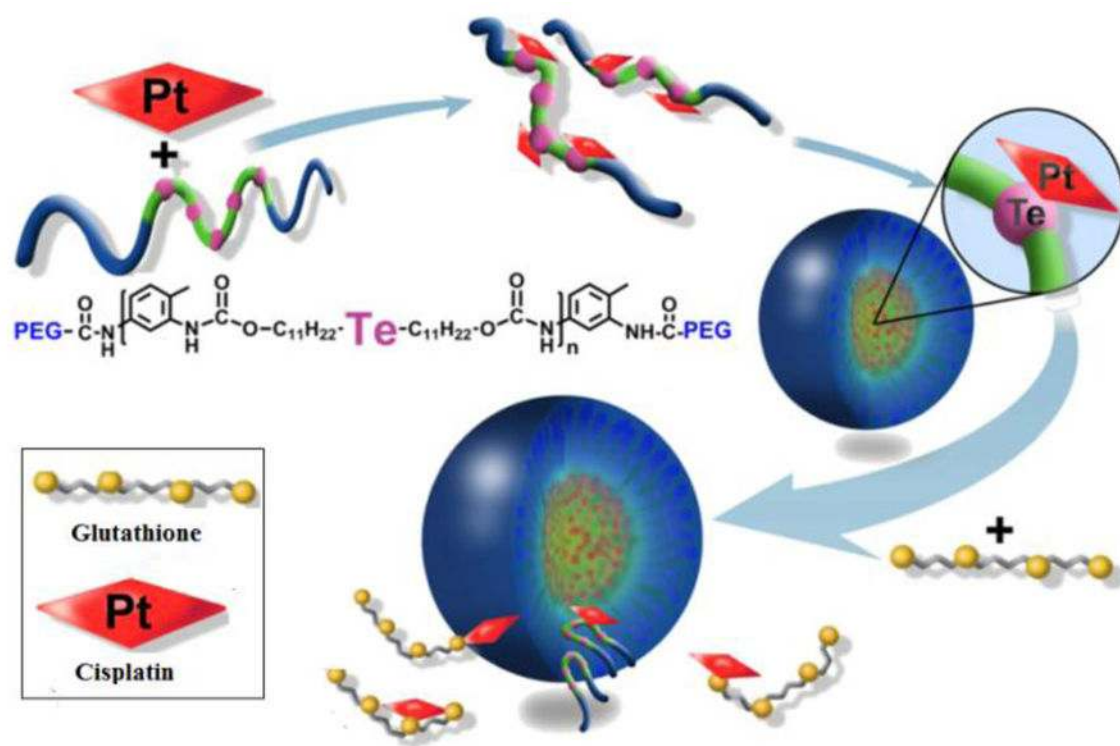


**Fig. 8.** Structure of tellurium-containing polymer, PEG-PUTe-PEG, and the mechanism of association with cisplatin and release *via* glutathione. Adapted with permission from Ref. 81. Copyright © 2014, American Chemical Society.

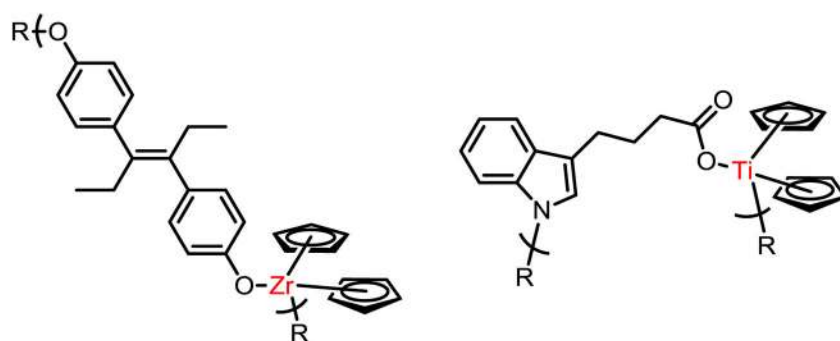


**Fig. 9.**  
Chemical structures of Zr- and Ti-containing polymers with antiviral activity.

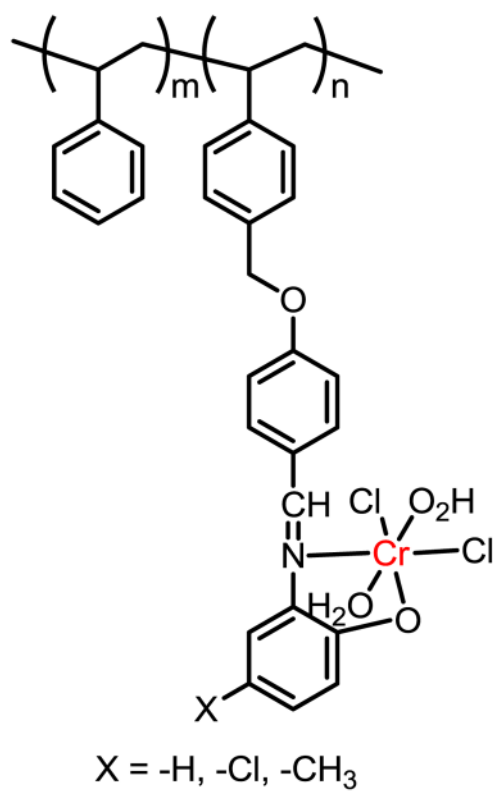


**Fig. 10.**  
Chemical structure of Cr-containing polymers with antibacterial activity.

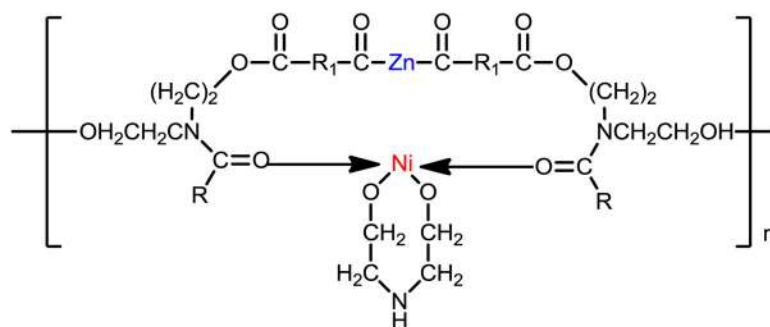


**Fig. 11.** Chemical structure of Ni-Zn-bimetallic sunflower oil based polymers with antifungal property.

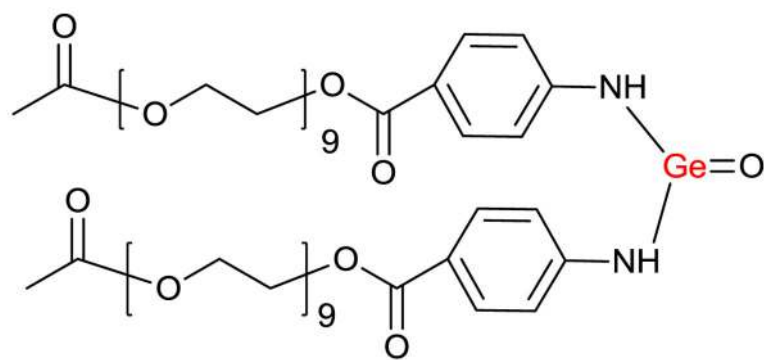


**Fig. 12.**  
Chemical structure of Ge-containing PEO surfactant with antibacterial activity.

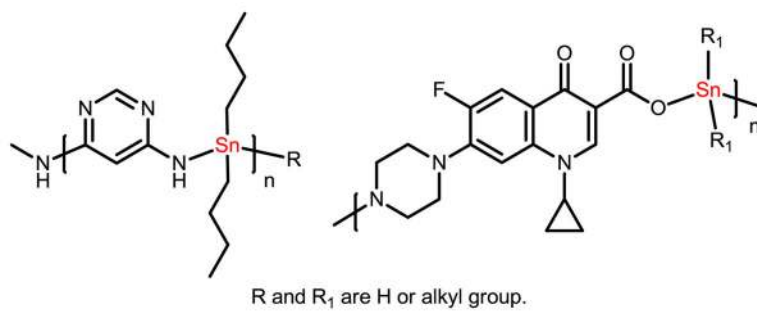


**Fig. 13.**  
Chemical structures of Sn-containing polymers with antibacterial activity.

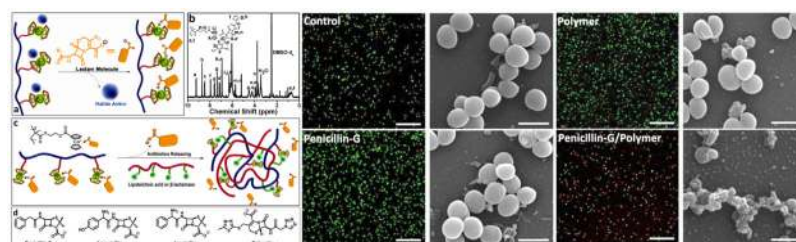


**Fig. 14.**

(a) Formation of ion-pairs between  $\beta$ -lactam antibiotics and cationic cobaltocenium-containing polymers. (b)  $^1\text{H}$  NMR spectrum for ion-pairs of nitrocefin and cationic cobaltocenium-containing polymers. (c) Antibiotic release from antibiotic–metallopolymer ionpairs *via* lipoteichoic acid or  $\beta$ -lactamases. (d) Four  $\beta$ -lactam antibiotics are used for this study. CSLM images (left column) and corresponding SEM images (right column) of HA-MRSA cells incubated respectively in the presence of control solution,  $5.6\ \mu\text{M}$  penicillinG ( $2\ \mu\text{g}/\text{mL}$ ),  $1\ \mu\text{M}$   $\text{Cl}^-$ -paired cationic cobaltocenium-containing polymers ( $12.5\ \mu\text{g}/\text{mL}$ ), and penicillin-G–metallopolymer bioconjugate ( $5.6\ \mu\text{M}$  penicillin-G and  $1\ \mu\text{M}$  metallopolymers). CSLM imaging employed BacLight live/dead stain (green indicates live cells, red indicates dead cells). Scale bars in confocal images,  $50\ \mu\text{m}$ ; scale bar in SEM images,  $1\ \mu\text{m}$ . Adapted with permission from Ref. 122. Copyright © 2014, American Chemical Society.

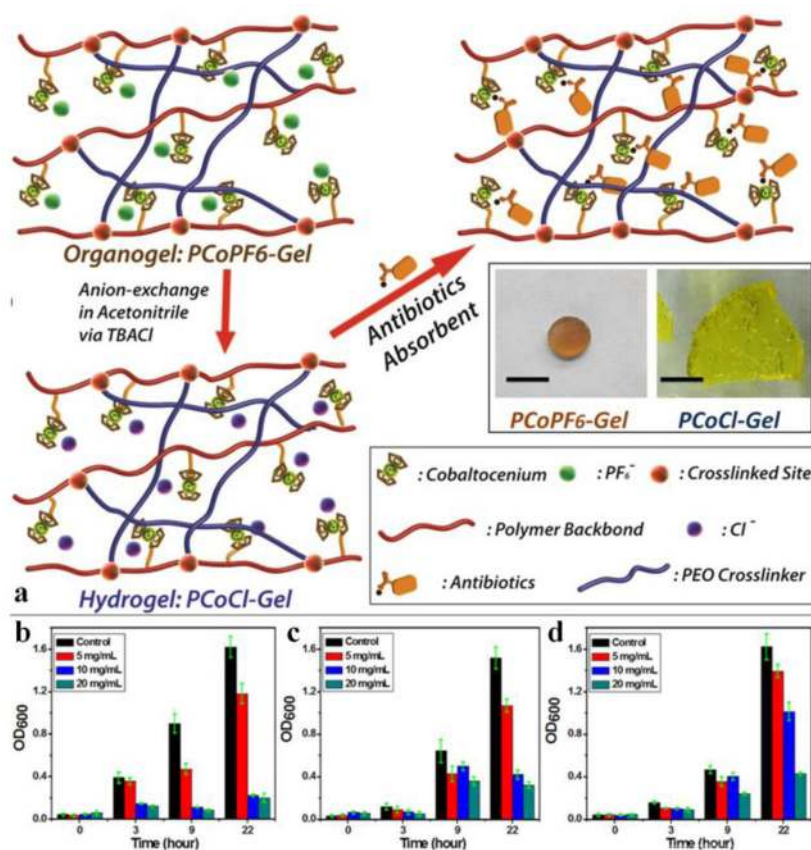


**Fig. 15.**

(a) Illustration of anion-paired cobaltocenium-containing organogels and hydrogels. Inserted: optical images of representative gels (Scale Bar: 13cm). Inhibition of cobaltocenium-containing hydrogels (PCoCl-Gel) was observed against (b) Gram-negative *E. coli*; (c) Gram-positive *S. aureus*; and (d) HA-MRSA under different concentrations by standard solution micro-broth measurement. Adapted with permission from Ref. 123. Copyright © 2015, Rights Managed by Nature Publishing Group.



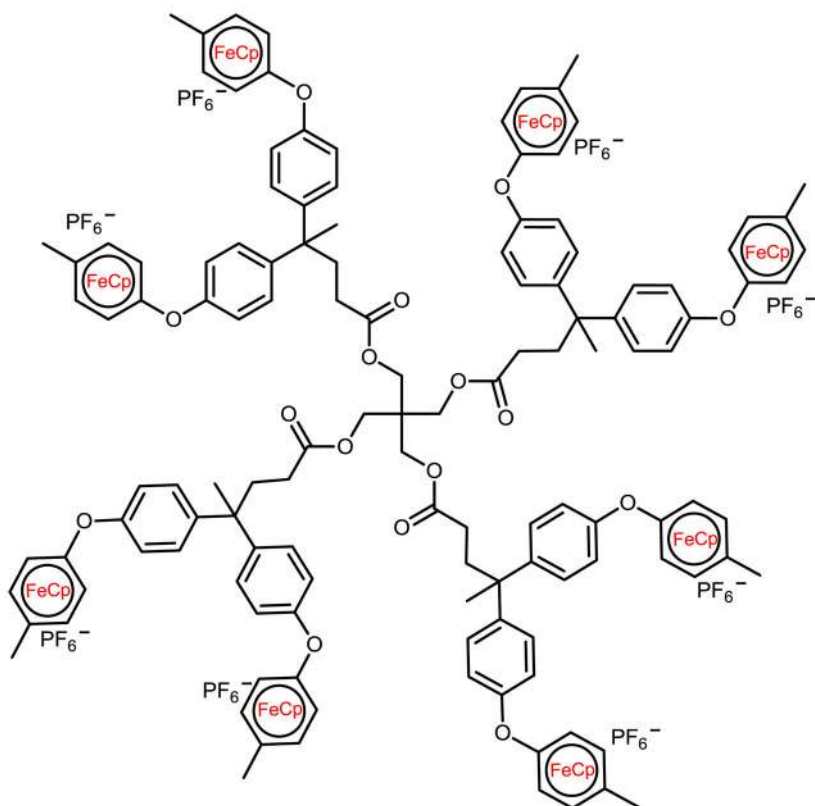


**Fig. 16.**  
Chemical structure of Fe-containing dendrimer with antibacterial activity.



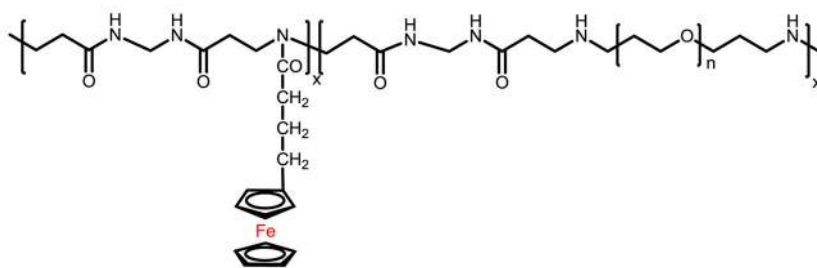


**Fig. 18.**  
Chemical structure of ferrocene-containing polymers reported by the Neuse group.

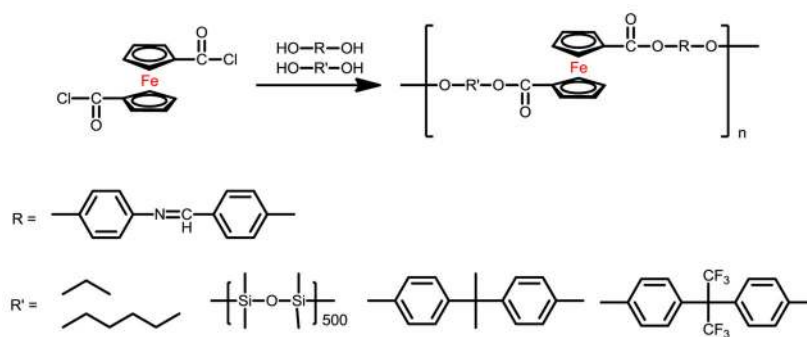


**Fig. 19.** Chemical structure of main-chain ferrocene-containing polymers reported by the Mirza group.

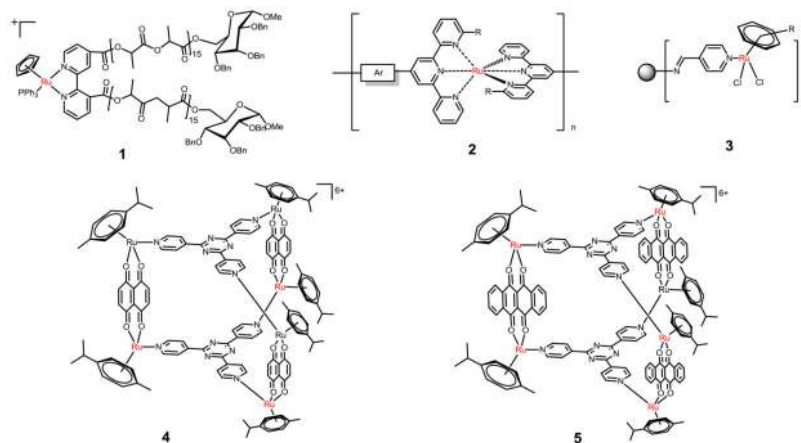


**Fig. 20.** Chemical structures of representative Ru-containing polymers with anticancer activity (Ref. 149, 151, 152, 153).

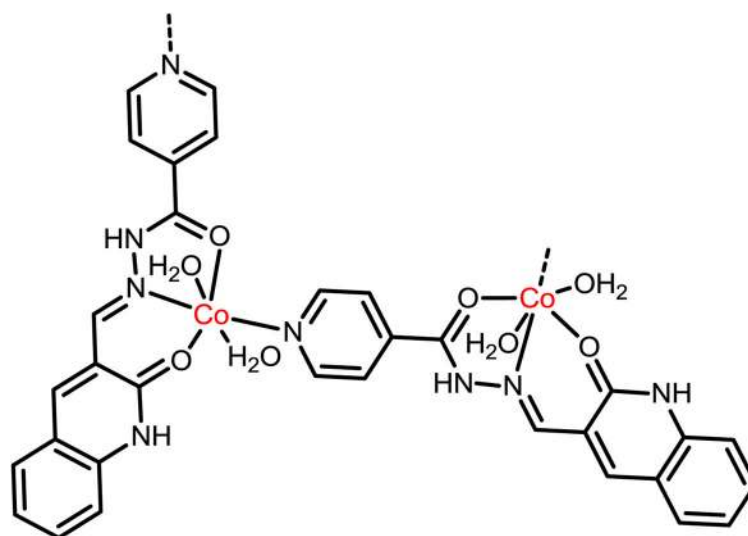


**Fig. 21.**  
Chemical structure of Co-containing coordination polymer with anticancer activity.

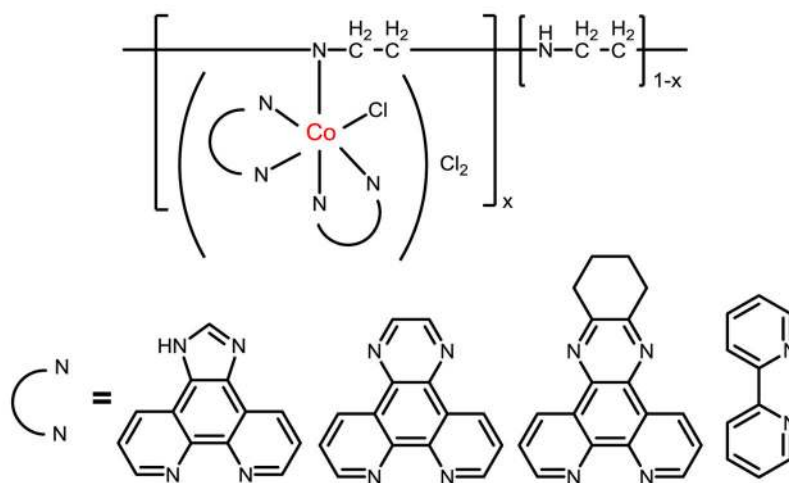
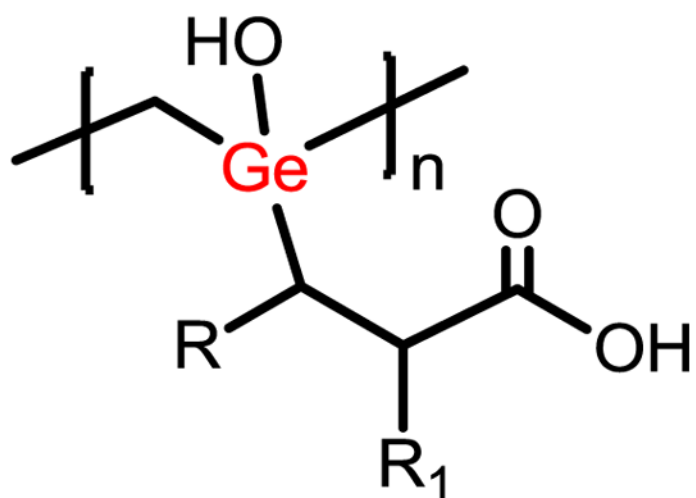


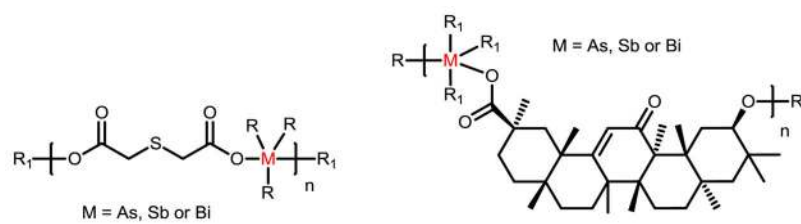
**Fig. 22.** Chemical structures of side-chain Co-containing polymers with anticancer properties.



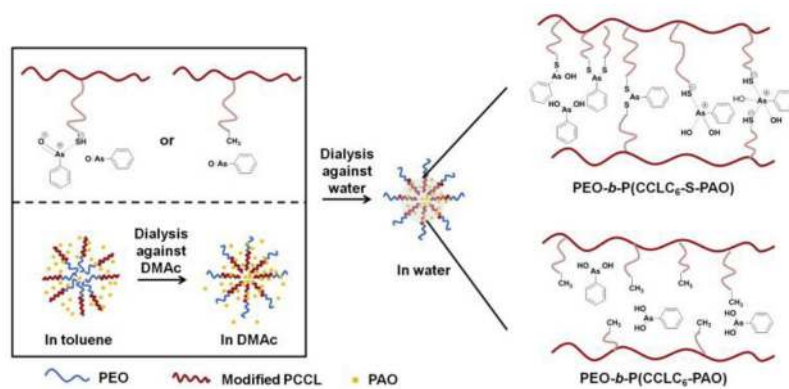
R and R<sub>1</sub> are H or alky group.

**Fig. 23.**  
Chemical structure of Ge-containing polymer with anticancer activity.

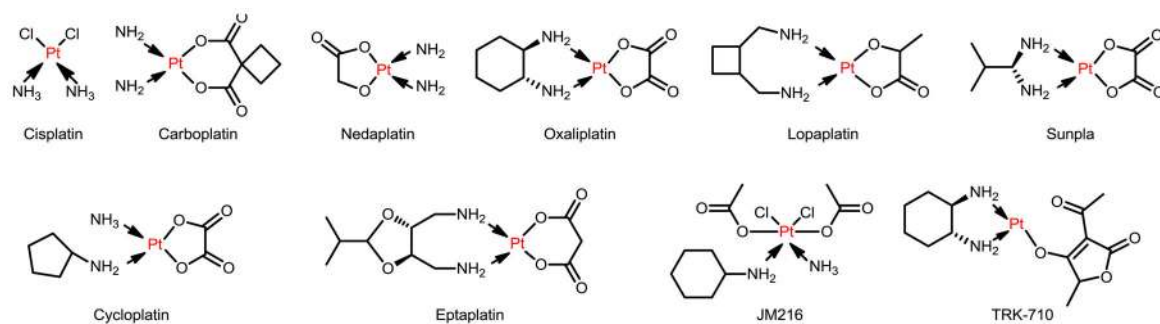




**Fig. 24.** Chemical structures of hybrid polymers from Group VA with thiodiglycolic acid and glycyrrhetic acid.

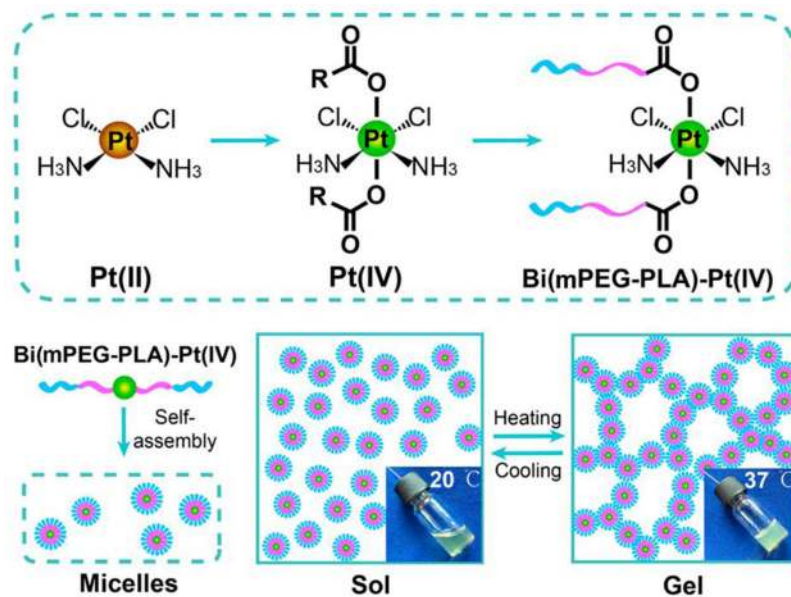


**Fig. 25.** Encapsulation of PAO into PEO-*b*-P(CCLC<sub>6</sub>-SH) and PEO-*b*-P(CCLC<sub>6</sub>) micelles. Adapted with permission from Ref. 169. Copyright © 2014 Elsevier Ltd. All rights reserved.

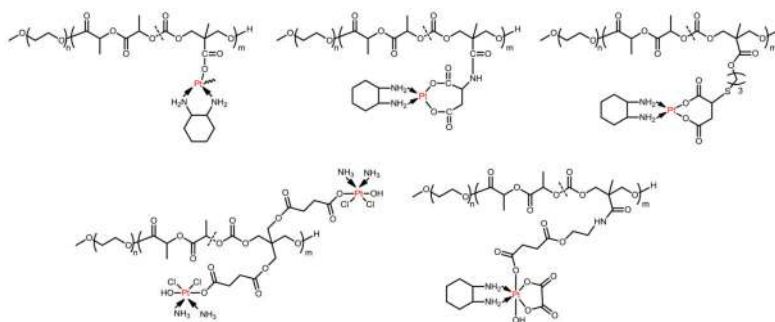
**Fig. 26.**

Chemical structures of small molecular Pt-containing anticancer drugs. The compounds in the first row are commercial available, those in the second row are in phase I or phase II clinical state.





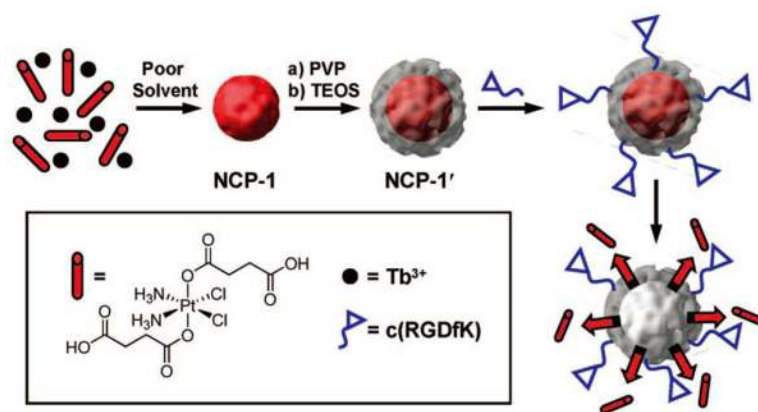
**Fig. 28.** Molecular design of the unique polymer–Pt(IV) conjugate and corresponding thermogel. Adapted with permission from Ref. 184. Copyright © 2015, American Chemical Society.



**Fig. 29.**  
Chemical structures of anticancer Pt-containing polymers developed by the Jing and Huang group (Ref. 185–191).

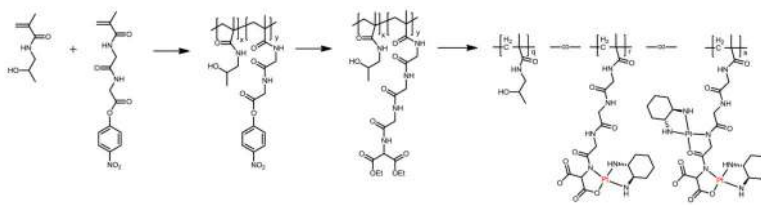


**Fig. 30.** Chemistry of constructing cross-linked polymer vesicles and their drug conjugation with cisplatin. Adapted with permission from Ref. 197. Copyright © 2012, Royal Society of Chemistry.

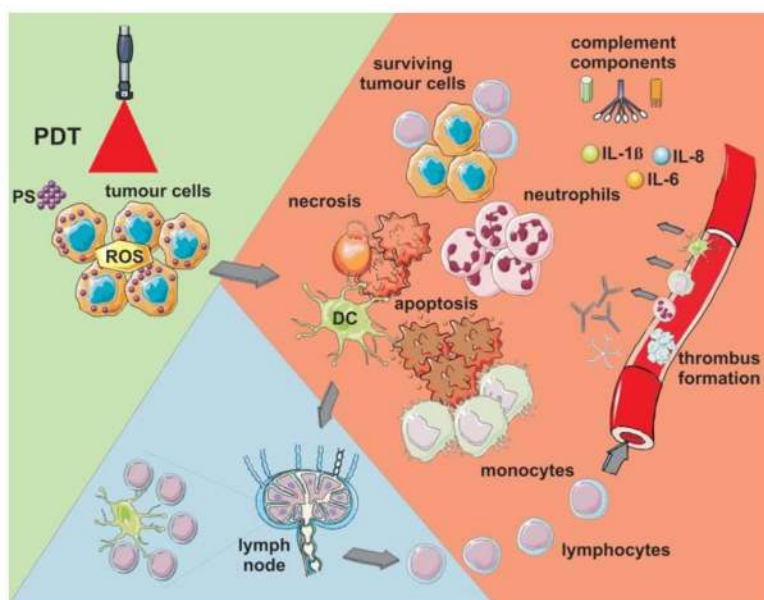


**Fig. 31.** Formation of Pt-containing nanoscale coordination polymers. Adapted with permission from Ref. 201. Copyright © 2008, American Chemical Society.

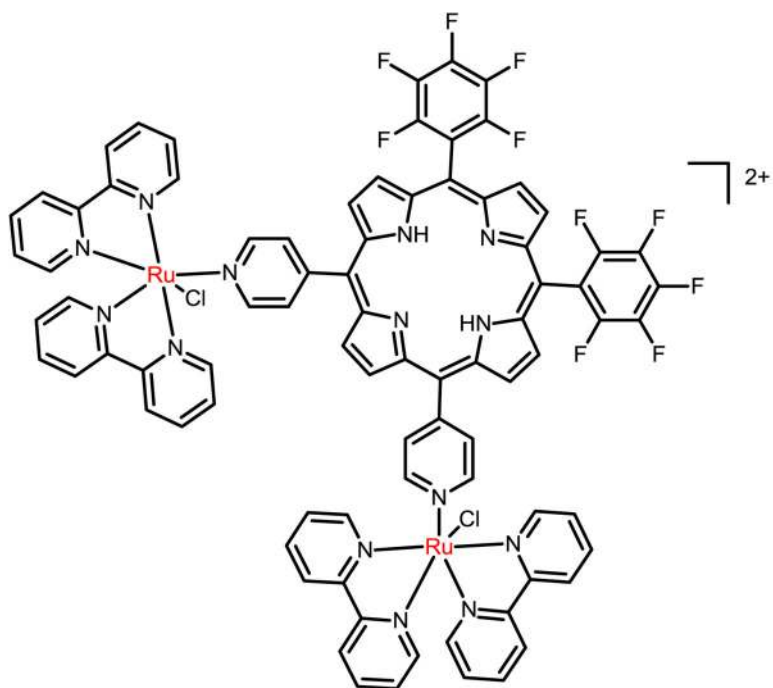




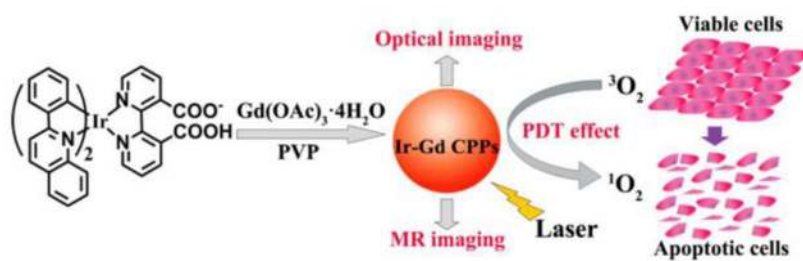
**Fig. 32.**  
Synthetic approach of Pt-containing anticancer drug AP5346.



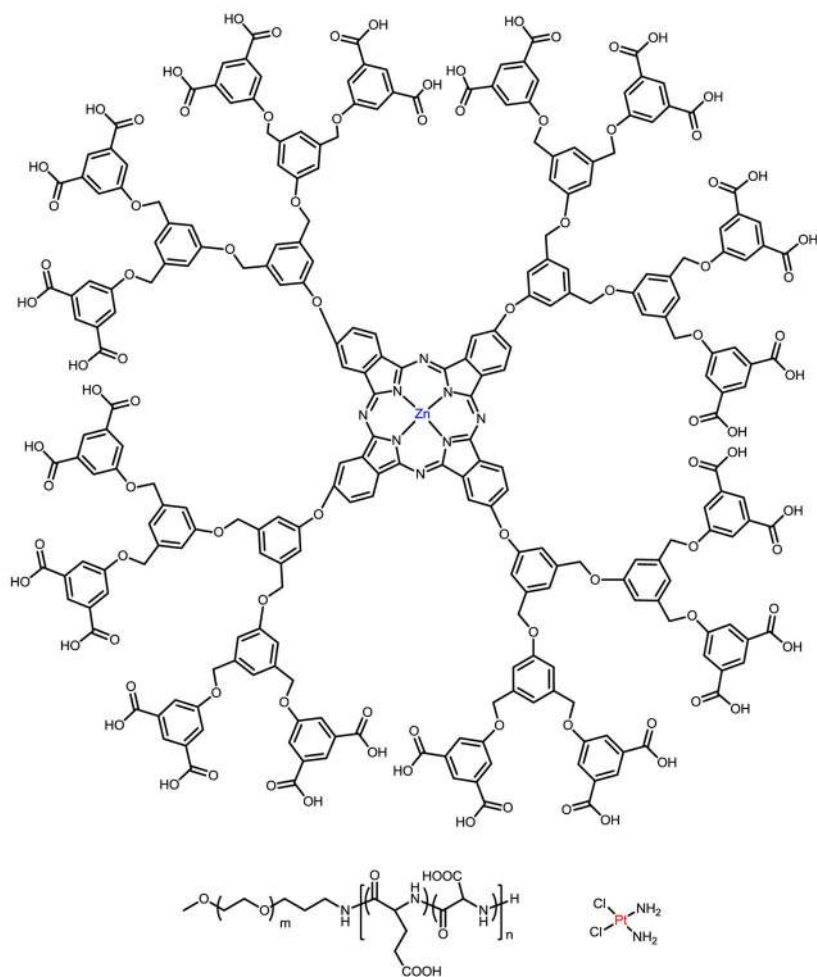
**Fig. 33.** PDT-induced effects. Light-mediated excitation of photosensitizer-loaded tumor cells leads to the production of reactive oxygen species (ROS) within these cells, leading to cell death (predominantly apoptotic and necrotic). Adapted with permission from Ref. 210. Copyright © 2011 American Cancer Society, Inc.



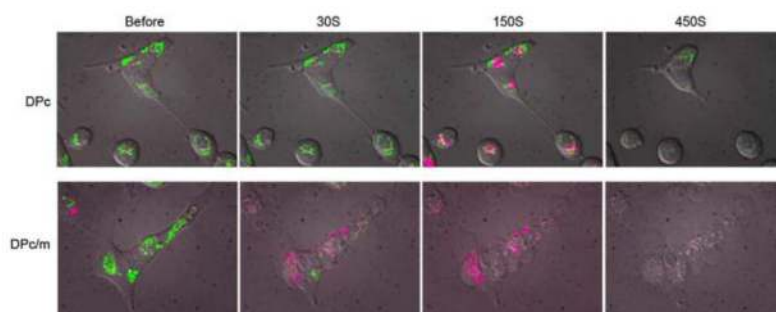
**Fig. 34.**  
Chemical structure of a Ru-containing PDT agent.



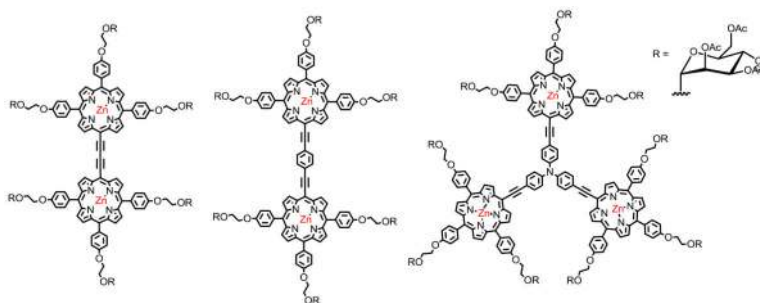
**Fig. 35.** Synthesis and theranostic applications of Ir–Gd coordination polymer particles. Adapted with permission from Ref. 217. Copyright © 2015, American Chemical Society.



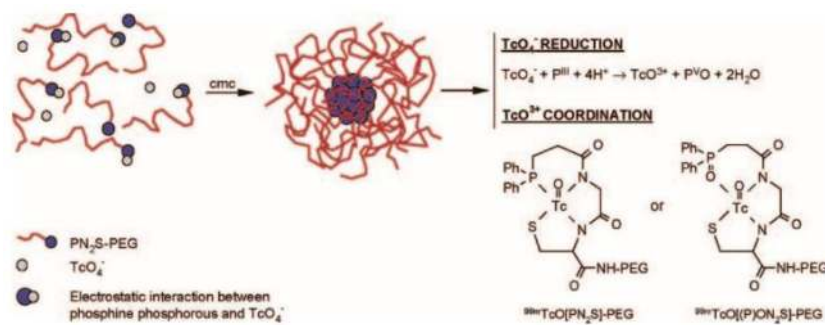
**Fig. 36.**  
Chemical structure of the dendrimer-metal complex reported by the Jang group.



**Fig. 37.** Time-dependent morphological changes of the DPc- and DPc/m-treated A549 cells during photoirradiation. Adapted with permission from Ref. 220. Copyright © 2008 Elsevier B.V. All rights reserved.

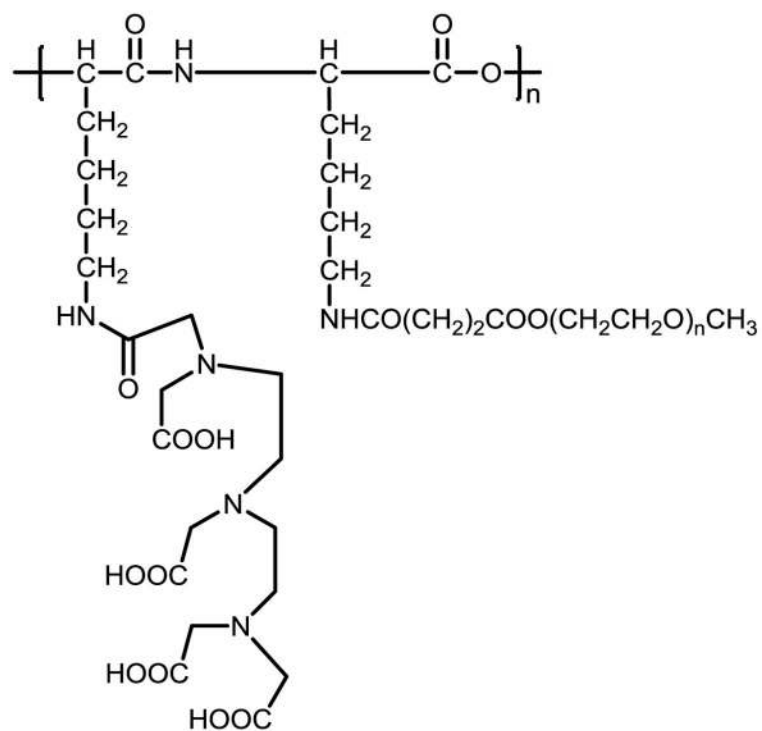


**Fig. 38.**  
Chemical structures of conjugated zinc porphyrin oligomers.

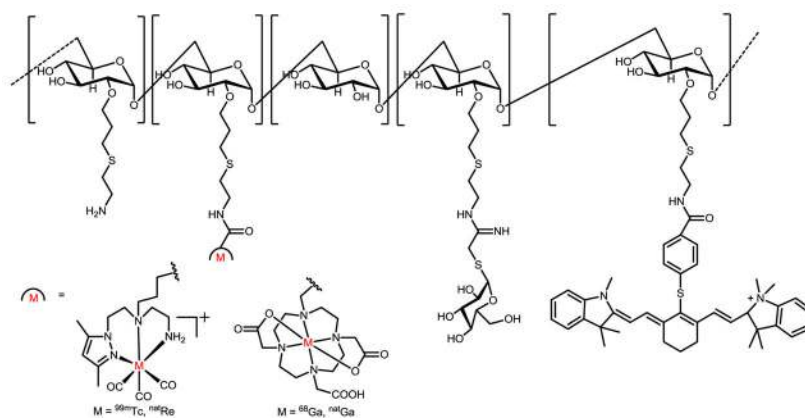


**Fig. 39.** Illustration of direct labeling of PEGylated  $\text{PN}_2\text{S}$  ligands. A drawing of the mechanism of  $^{99\text{m}}\text{Tc}$  reduction-coordination mediated by  $\text{PN}_2\text{S-PEG}$  micelle aggregation with the two possible coordination species is shown. Adapted with permission from Ref. 232. Copyright © 2004, American Chemical Society.

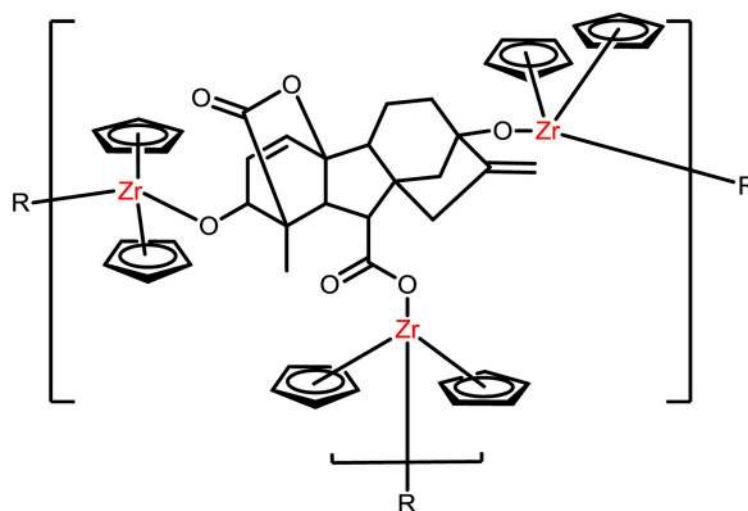




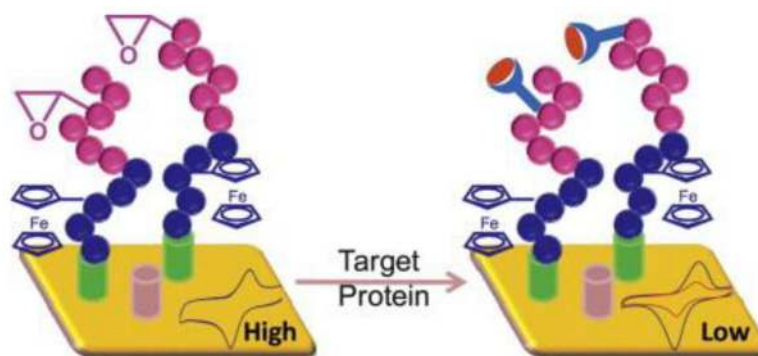
**Fig. 40.** Chemical structure DTPA-terminated poly-*L*-lysine which can be used to chelate  $^{99\text{m}}\text{Tc}$ .



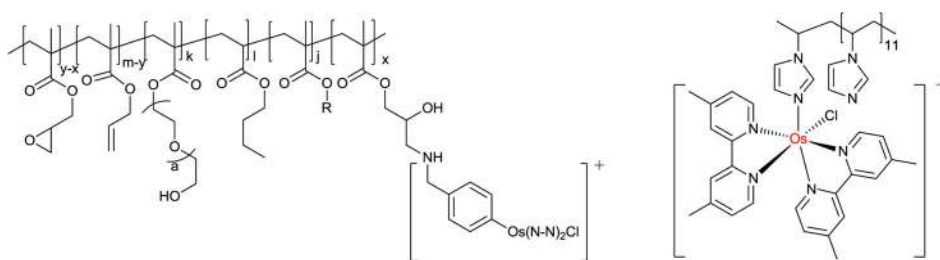
**Fig. 41.** Chemical structure of multifunctional imaging agent for sentinel lymph node based on the modification of dextran with radionuclide ( $^{99\text{m}}\text{Tc}$  or  $^{68}\text{Ga}$ ) and a near-infrared (NIR) reporter.



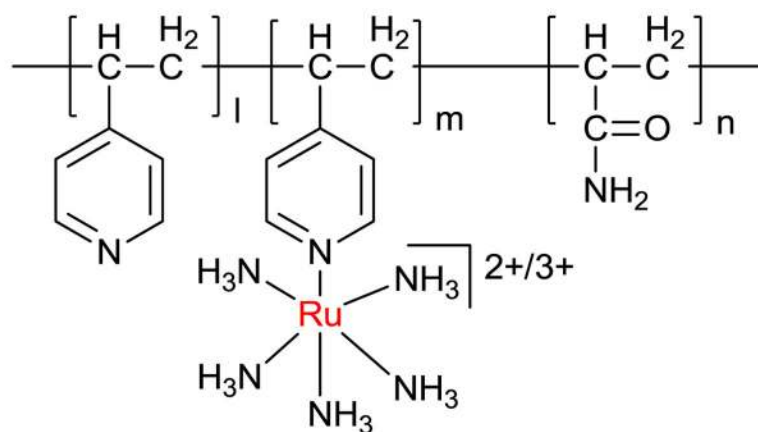
**Fig. 42.**  
Chemical structure of Zr-gibberellic acid-containing crosslinked polymer for biocide.



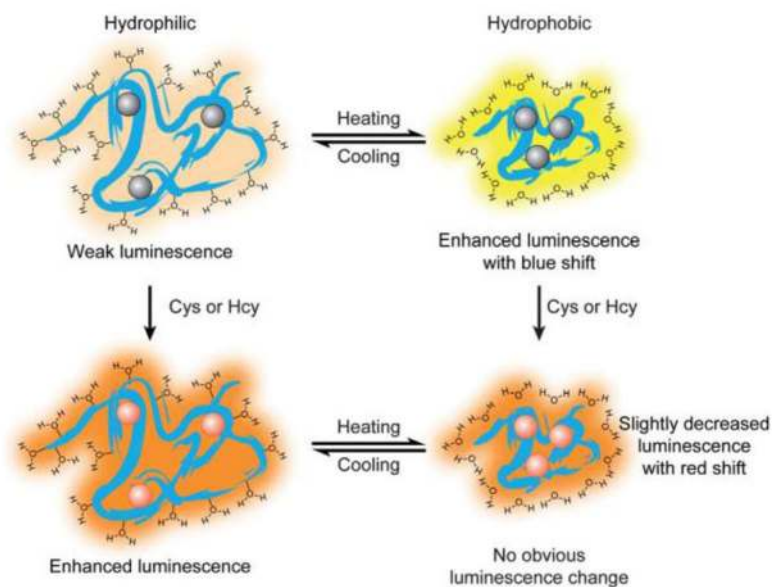
**Fig. 43.** Schematic illustration of ferrocene-based sensor. Adapted with permission from Ref. 254. Copyright © 2012 Elsevier B.V. All rights reserved.



**Fig. 44.**  
Chemical structure of Os-containing polymers used in biosensors.

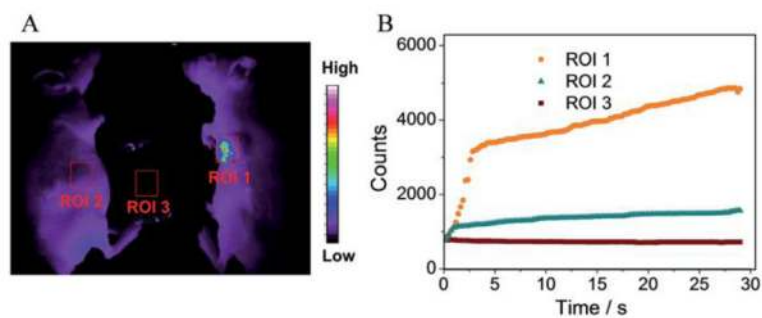


**Fig. 45.**  
Chemical structure of Ru-containing polymer used in biosensor.



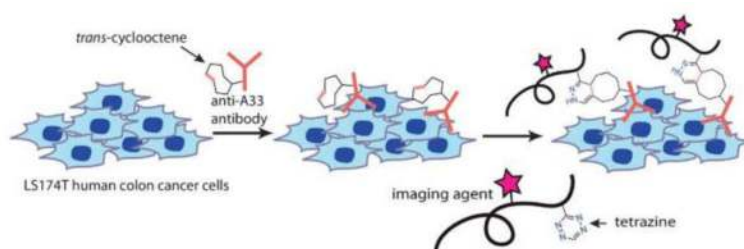
**Fig. 46.**

Illustration of the conformation of Ir-containing polymers in aqueous solution as a dual phosphorescent sensor for Cys/Hcy and temperature. Adapted with permission from Ref. 262. Copyright © 2012, Royal Society of Chemistry.



**Fig. 47.** (A) *In vivo* luminescence imaging of a tumor-bearing mouse (ROI 1) and the control nude mouse (ROI 2) after injection of the FPPdots. (B) The change in luminescence intensity of the marked regions (ROI 1, ROI 2 and ROI 3). Adapted from Ref. 265 with permission from The Royal Society of Chemistry.





**Fig. 48.** Gallium-containing dextran as bioimaging agent for tumor cells. Adapted from Ref. 269 with permission from The Royal Society of Chemistry.

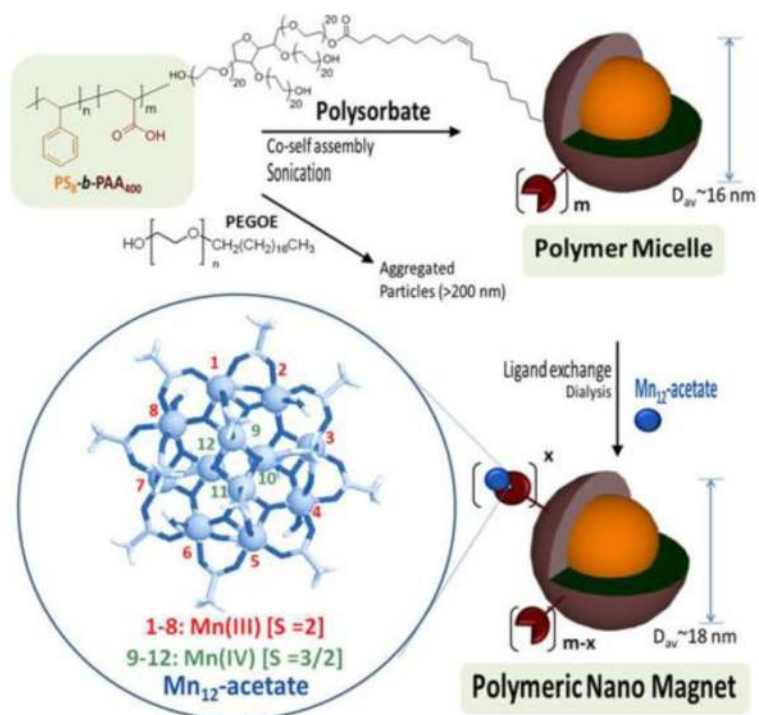


**Fig. 49.** Synthesis and characterization of Poly-SMM. Adapted with permission from Ref. 272. Copyright © 2012, American Chemical Society.

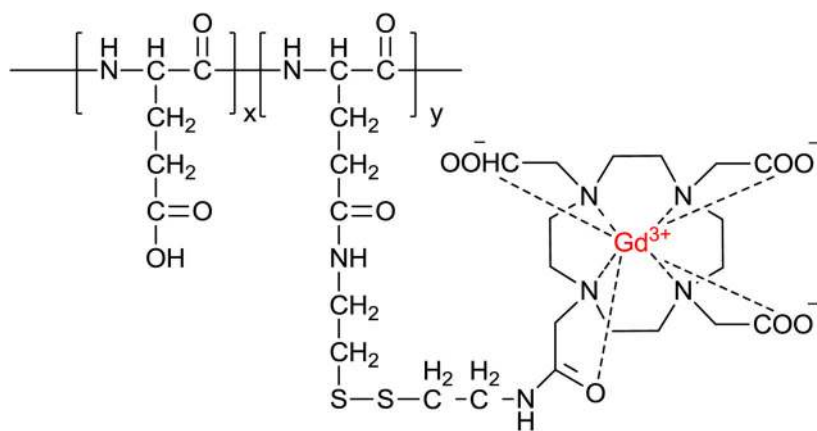


**Fig. 50.**  
Chemical structure of Gd-containing polymer with cystamine as the cleavable spacer.

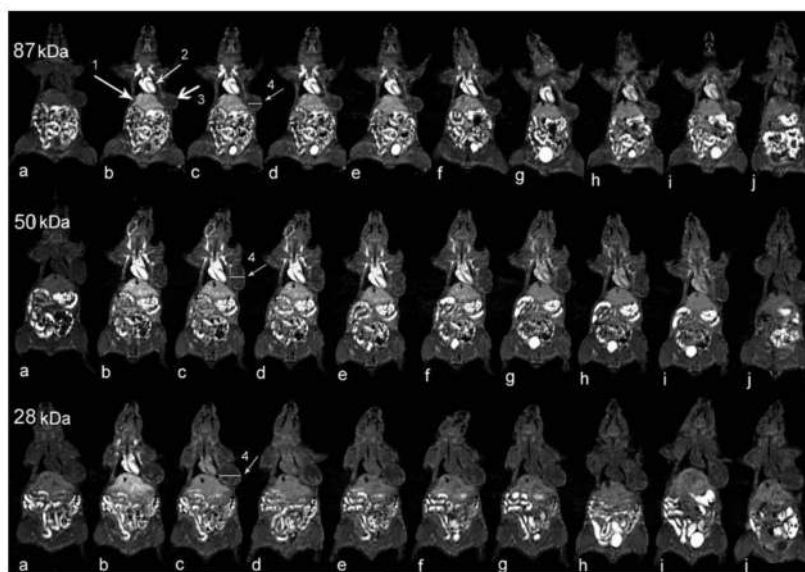


**Fig. 51.** Coronal MR images of tumor bearing mice (a) before and at (b) 1, (c) 11, (d) 20, (e) 30, (f) 60, (g) 120, (h) 180, and (i) 240 min and (j) 24 h after injection of PGA-1,6-hexanediamine-(Gd-DO3A) conjugates of different molecular weights. Adapted with permission from Ref. 276. Copyright © 2006, American Chemical Society.

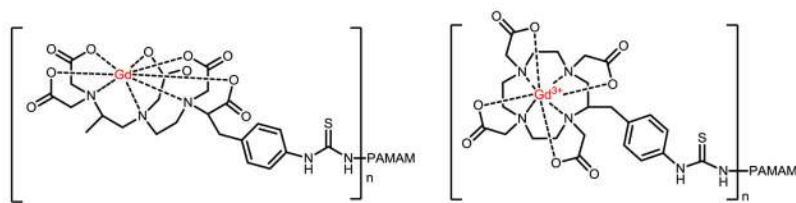


**Fig. 52.**  
Chemical structures of Gd-containing dendrimers for MRI.

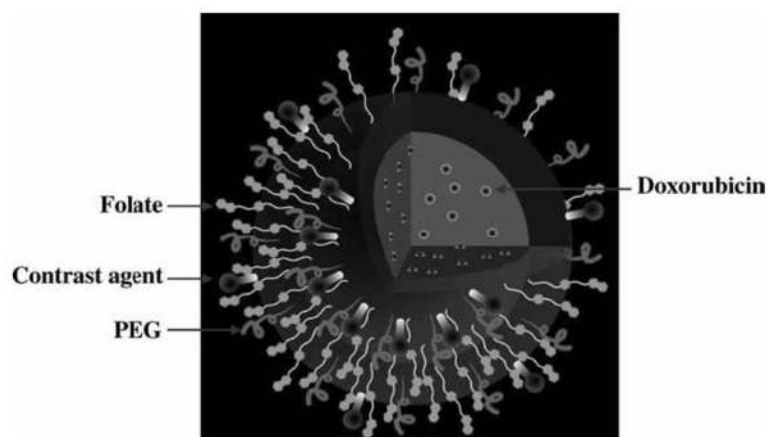


**Fig. 53.** Schematic representation of a multifunctional core-shell nanoparticle system (PLGA/PFPL) composed of a PLGA core and a paramagnetic folate-coated PEGylated liposome shell for MRI and drug delivery for targeted therapy. Adapted with permission from Ref. 295. Copyright © 2011 WILEY-VCH Verlag GmbH & Co. KGaA, Weinheim.

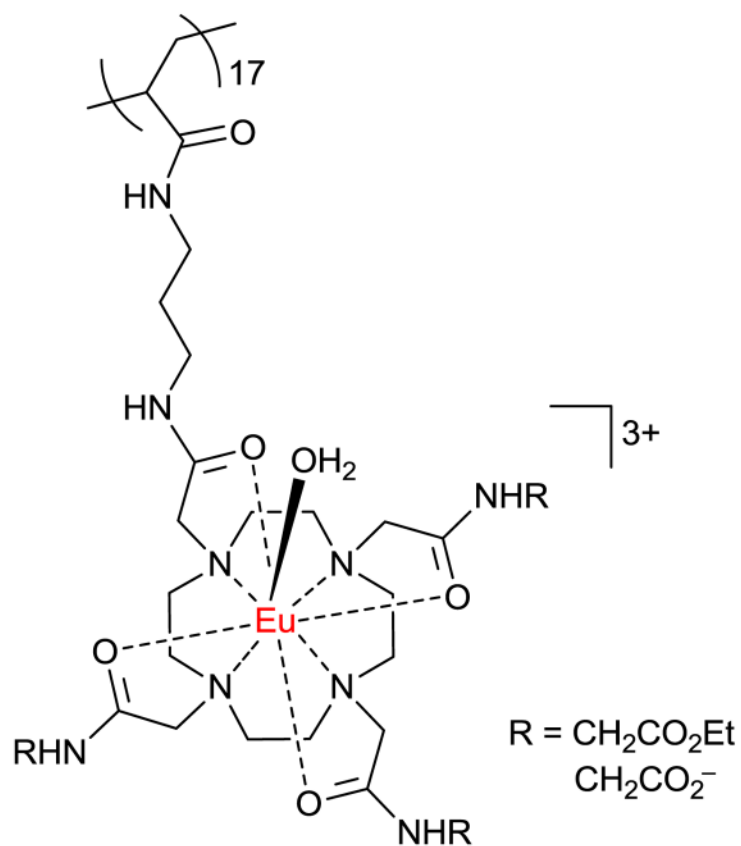


**Fig. 54.**  
Chemical structure of Eu-containing polymers for MRI.

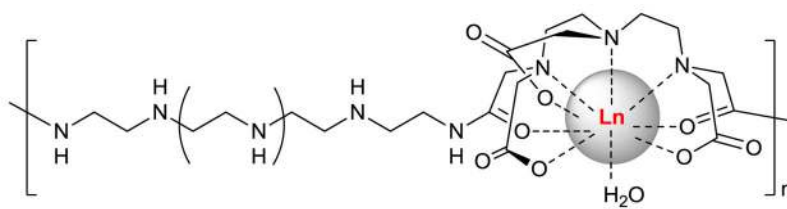


**Fig. 55.**  
Chemical structure of Ln-containing polymers for MRI.



**Table 1**

IC<sub>50</sub> values (ng/mL) for the tested cell lines upon treatment with glycyrrhetic acid (GA) and metal-containing polymers. The values given in parentheses are the standard deviations. (Ph<sub>3</sub> indicated triphenyl metal-containing dihalide used to form polymers. Me is methyl group). Adapted with permission from Ref. 168. Copyright © 2013 Taylor & Francis.

Compound	WI-38	NIH/3T3	AsPC-1	PANC-1
Ph <sub>3</sub> Sb/GA	130(10)	2800(22)	1900(23)	1700(8)
Ph <sub>3</sub> Bi/GA	170(15)	1800(14)	>32,000	3800(9)
Ph <sub>3</sub> As/GA	220(12)	5400(29)	>32,000	2500(9)
Me <sub>3</sub> Sb/GA	>32,000	>32,000	3800(19)	>32,000
Cisplatin	15(10)	1200(19)	1400(150)	340(12)